

UC San Diego

UC San Diego Electronic Theses and Dissertations

Title

Dielectrophoresis for biomarker isolation from biological samples

Permalink

<https://escholarship.org/uc/item/3q40b7b3>

Author

Sonnenberg, Avery Renault

Publication Date

2013

Peer reviewed|Thesis/dissertation

UNIVERSITY OF CALIFORNIA, SAN DIEGO

**DIELECTROPHORESIS FOR BIOMARKER ISOLATION FROM
BIOLOGICAL SAMPLES**

A dissertation submitted in partial satisfaction of the requirements for
the degree Doctor of Philosophy

in

Bioengineering

by

Avery Renault Sonnenberg

Committee in charge:

Professor Michael J. Heller, Chair
Professor Sadik Esener
Professor Xiaohua Huang
Professor Thomas Kipps
Professor John Watson

2013

Copyright
Avery Renault Sonnenberg, 2013
All rights reserved.

The Dissertation of Avery Renault Sonnenberg is approved, and it is acceptable in quality and form for publication on microfilm and electronically:

Chair

University of California, San Diego

2013

DEDICATION

For Michael Heller, my wise mentor.

TABLE OF CONTENTS

SIGNATURE PAGE	iii
DEDICATION	iv
TABLE OF CONTENTS	v
LIST OF FIGURES	ix
LIST OF TABLES	xi
ACKNOWLEDGEMENTS	xii
VITA	xv
ABSTRACT OF THE DISSERTATION	xvii
CHAPTER ONE: Introduction	1
1.1 Background.....	2
1.1.1 Cancer Biomarkers.....	2
1.1.2 DNA as a cancer biomarker	2
1.1.3 Cell-free circulating DNA.....	3
1.1.4 Monitoring of drug delivery nanoparticles	6
1.1.5 Sample Preparation	6
1.2 DEP Theory	8
1.3 Scope of the dissertation.....	14
CHAPTER TWO: Dielectrophoretic (DEP) Isolation of DNA and Nanoparticles from Blood	17
2.1 Introduction.....	18
2.2 Methods	20
2.2.1 DEP Device and Methods.....	20
2.2.2 Buffers, Blood Samples, and Conductivity Measurements	23
2.2.3 Single-Stranded (ss) and Double-Stranded (ds) High Molecular Weight (HMW) DNA and Low Molecular Weight (LMW) DNA.....	25
2.2.4 Micron Size Particles and Nanoparticles	26
2.2.5 Experimental Setup and Measurements.....	27
2.3 Results.....	28

2.3.1	DEP Separation and Detection of ss-HMW-DNA and ds-HMW-DNA in Blood	28
2.3.2	DEP with Disrupted Settled Blood	31
2.3.3	DEP with Low Molecular Weight DNA in Buffer	31
2.3.4	Post Staining DNA after DEP.....	33
2.3.5	DEP Detection Level for Nanoparticles in Blood.....	34
2.4	Discussion.....	36
CHAPTER THREE: Dielectrophoretic Isolation and Detection of CFC-DNA Nanoparticle Biomarkers and Virus from Blood		
	Biomarkers and Virus from Blood	39
3.1	Introduction.....	40
3.2	Methods	42
3.2.1	DEP Devices and Methods	42
3.2.2	Experimental Setup and Imaging.....	42
3.2.3	Whole Blood Samples from CLL Patients.....	45
3.2.4	Virus Preparation	45
3.2.5	Mitochondria Preparation	46
3.2.6	Buffers, Blood Samples, and Conductivity Measurements	46
3.3	Results.....	47
3.3.1	DEP Separation and Detection of CFC-DNA from CLL Patient Blood Samples	48
3.3.2	DEP Isolation and Detection of T7 (<i>mCherry</i>) Bacteriophage from Blood ..	51
3.3.3	DEP Isolation and Detection of Mitochondria from Biological Buffer.....	52
3.3.4	Isolation and Detection of HMW-DNA from Serum Using New DEP Microarray Devices.....	53
3.4	Discussion.....	56
CHAPTER FOUR: Isolation and Detection of Cell Free Circulating DNA Directly from Chronic Lymphocytic Leukemia Patient Blood		
	Chronic Lymphocytic Leukemia Patient Blood	58
4.1	Introduction.....	59
4.2	Materials and methods	61
4.2.1	Sample Acquisition.....	61

4.2.2	Qiagen DNA extraction from plasma	62
4.2.3	DNA extraction on Dielectrophoresis Devices	62
4.2.4	DNA Quantification.....	64
4.2.5	PCR analysis	65
4.3	Results.....	65
4.3.1	DEP Isolation of CFC-DNA from Blood.....	65
4.3.2	CFC-DNA sample preparation procedures.....	66
4.3.3	On-chip fluorescent detection of CFC-DNA	68
4.3.4	DNA concentration in eluted samples	70
4.3.5	Gel Analysis of PCR results	71
4.3.6	Sequencing analysis of PCR product.....	73
4.4	Discussion.....	75
CHAPTER FIVE: New Electrokinetic Devices and Methods for High Conductance and		
	High Voltage Dielectrophoresis (DEP)	80
5.1	Invention	81
5.2	Novelty.....	82
5.3	Existing Art.....	82
5.4	Method of Operation.....	83
5.4.1	Previous Device Design.....	83
5.4.2	Basic design of earlier three chambered multi-pore electrokinetic DEP devices for the separation of DNA/Nanoparticles from blood and other high conductance samples.....	86
5.4.3	Description of New Devices, Designs and Concepts for even simpler two chambered and single pore electrokinetic DEP devices for the rapid separation of cells, CFC-DNA /RNA or nanoparticles from blood and other high conductance samples.	89
5.5	Stage of development of the invention	93
5.6	Potential commercial applications of the invention.....	94
CHAPTER SIX: Summary and future work.....		
6.1	Summary and conclusions	97

6.2	Limitations	99
6.2.1	Limitations of current DEP device	99
6.2.2	Limitations of comparison to Qiagen extraction kit	100
6.2.3	Limitations of biomarkers and rate of adoption.....	101
6.3	Future Work	102
6.3.1	Integration of DEP array with on-chip downstream analysis	102
6.3.2	Use of DEP to collect other types of biomarkers.....	103
6.3.3	DEP theory for nanoscale entities in high conductance.....	108
6.3.4	Manipulation of dielectric properties of medium or target.....	109
	REFERENCES	111

LIST OF FIGURES

Figure 1.1: Detection of genetically and epigenetically altered DNA in blood.....	4
Figure 1.2: Elevation of cell-free DNA in miscellaneous malignancies	5
Figure 1.3: Sample preparation.....	7
Figure 1.4: Positive DEP.....	9
Figure 1.5: Negative DEP	10
Figure 1.6: Single Shell Model	12
Figure 1.7: Clausius-Mossotti Factor is a function of frequency.....	13
Figure 2.1: DEP microarray device and scheme for DEP separation of DNA and nanoparticles from blood	21
Figure 2.2: DEP separation of DNA from blood samples	30
Figure 2.3: DEP of fluorescent low molecular weight DNA.....	32
Figure 2.4: Post staining of DNA after DEP.....	34
Figure 2.5: Detection levels for nanoparticles in buffy coat blood.....	35
Figure 3.1: DEP Force Vector Diagram	44
Figure 3.2: DEP Isolation and Fluorescent Detection of CFC-DNA in Blood Samples from CLL Patients.....	50
Figure 3.3: DEP Separation of T7 (mCherry) Bacteriophage in Blood.....	52
Figure 3.4: DEP of Fluorescent Stained Mitochondria.....	53
Figure 3.5: Detection of hmw-DNA in Serum Using New DEP Microarray Devices.	55
Figure 4.1: DEP microarray device and scheme for isolation of CFC-DNA from blood .	63
Figure 4.2: Comparison of process times and steps for the three different DNA sample preparation methods.....	68

Figure 4.3: Fluorescent detection of CFC-DNA in CLL patient and normal blood samples	70
Figure 4.4: Concentration of CFC-DNA in the DEP and Qiagen eluted samples	72
Figure 5.1: Original concept/scheme for the DEP separation of DNA/Nanoparticles from blood and other high conductance samples	85
Figure 5.2: Seamless Sample to Answer Diagnostics.....	86
Figure 5.3: Multiple chamber high conductance DEP Device	89
Figure 5.4: Top view of multiple chamber high conductance DEP device	89
Figure 5.5: Basic Diagram of the new Single Pore Two Chamber DEP Device.....	91
Figure 5.6: Results for using a two chamber single pore device	92
Figure 5.7: Basic design diagram for a very novel and simple Pipette Tip DEP Device which can be constructed from commonly used materials	93
Figure 5.8: PCR results from cfc-DNA extracted from CLL cancer blood samples.....	94
Figure 6.1: DEP separation of E. coli at high and low frequency	101
Figure 6.2: On-chip PCR	101
Figure 6.3: Fluorescent extracellular vesicles trapped on a DEP Device	106
Figure 6.4: Shows the DEP separation of red fluorescent E. coli.....	108

LIST OF TABLES

Table 2.1: DEP targets, buffers, and electrical conductivities for each experiment.....	24
Table 4.1: IGVH PCR band intensities for DEP blood and Qiagen plasma.....	73
Table 4.2: IGVH PCR band intensities for Normal samples	74
Table 4.3: Sanger sequencing results for PCR product from samples isolated from blood with DEP.....	75

ACKNOWLEDGEMENTS

I would like to acknowledge and thank the many parties that made this work possible. My labmates have been very supportive of this project, often dedicating time and expertise that was critical for its success. Dr. Jennifer Marciniak deserves a special thank you, as she taught me many laboratory techniques as a new graduate student and was involved in at least some way in almost all of this work. I would also like to thank Dr. Raj Krishnan for his work in this area which provided the justification for its pursuit as my thesis topic. I would like to thank James McCanna for stimulating and insightful conversations leading to a greater theoretical understanding of the phenomena we have observed and Tsukasa Takahashi for his help in experimental fixture design and fabrication. Elaine Skowronski and Sareh Manouchehri deserve recognition for their hard work contributing to the material in Chapter 4 and for their dedication to continuing and expanding upon this work in their own projects. A very special “Thank you” to Dr. Thomas Kipps and all of the members of his lab, especially Dr. Laura Rassenti, Dr. Emanuela Ghia, and Dr. George Widhopf, for providing critical access to CLL samples and associated expertise. The study in Chapter 4 would not have been possible without their long-term dedication and support. I would also like to thank Dr. Clark Chen and Dr. Bob Carter for their offering of valuable clinical samples as well as, Dr. Johnny Akers, Dr. David Gonda, and Justin Scheer for their help evaluating these samples with DEP devices. I would like to thank Biological Dynamics for providing support and microarray devices and access to their facilities and Raj Krishnan, David Charlot, and Gene Tu for their valuable input into experimental design and device operation. Robert Turner and

Rana Haddad were also very helpful at Biological Dynamics ensuring that the prototype DEP systems were up and running for the work in Chapter 4. This thesis would also not have been possible without the support and continued involvement of my thesis committee: Dr. Michael Heller (Chair), Dr. Sadik Esener, Dr. Xiaohua Huang, Dr. John Watson, and Dr. Thomas Kipps.

I would like to thank my mother, father, and brothers for supporting my decision to move across the country and my new Arizona family for making me feel welcome out west. Finally, I want to thank my amazing wife, Sonya, for her love, support, and patience, which are somehow always available in direct proportion to my exhaustion.

This research was supported in part by the National Institutes of Health National Cancer Institute NanoTumor Center Grant through grant number U54-CA119335. Other funding sources include Biological Dynamics and a contract with the Defense Threat Reduction Agency (DTRA). I would like to thank the HHMI for the Med-into-Grad Fellowship that I held as a graduate student.

Chapter 1 is, in part, published as the following two manuscripts: Avery Sonnenberg, Jennifer Y. Marciniak, Alexander P. Hsiao, Rajaram Krishnan, Michael J. Heller. *Dielectrophoretic (DEP) Isolation of DNA and Nanoparticles from Blood*. Electrophoresis. 2012, 33(16), 2482-90 and Avery Sonnenberg, Jennifer Y. Marciniak, James McCanna, Rajaram Krishnan, Laura Rassenti, Thomas J. Kipps and Michael J. Heller. *Dielectrophoretic Isolation and Detection of CFC-DNA Nanoparticulate Biomarkers and Virus from Blood*. Electrophoresis. 2013, 34(7), 1076-84.

Chapter 2, in part, is published as the following manuscript: Avery Sonnenberg, Jennifer Y. Marciniak, Alexander P. Hsiao, Rajaram Krishnan, Michael J. Heller. Dielectrophoretic (DEP) Isolation of DNA and Nanoparticles from Blood. *Electrophoresis*. 2012, 33(16), 2482-90

Chapter 3, in part, is a reprint of the following manuscript: Avery Sonnenberg, Jennifer Y. Marciniak, James McCanna, Rajaram Krishnan, Laura Rassenti, Thomas J. Kipps and Michael J. Heller. *Dielectrophoretic Isolation and Detection of CFC-DNA Nanoparticulate Biomarkers and Virus from Blood*. *Electrophoresis*. 2013, 34(7), 1076-84.

Chapter 4, in part, is in preparation for submission for publication as: Avery Sonnenberg, Jennifer Marciniak, Laura Rassenti, Emanuela Ghia, Elaine Skowronski, James McCanna, Sareh Manouchehri, George Widhopf, Thomas Kipps, and Michael Heller. *Isolation and Detection of Circulating Cell Free DNA Directly from Chronic Lymphocytic Leukemia Patient Blood*.

Chapter 5 is a reprint of the following provisional patent application: Michael Heller, Rajaram Krishnan, Avery Sonnenberg. *New Electrokinetic Devices and Methods for High Conductance and High Voltage Dielectrophoresis (DEP)*. Patent Pending. Provisional Patent # 61/413,306.

The dissertation author was the primary author on all manuscripts.

VITA

- 2007 B.S. in Electrical Engineering, Rochester Institute of Technology
- 2007 M.S. in Electrical Engineering, Rochester Institute of Technology
- 2007-2013 Graduate Student Researcher, University of California, San Diego
- 2013 Ph.D. in Bioengineering, University of California, San Diego

Publications

Avery Sonnenberg, Jennifer Marciniak, Laura Rassenti, Emanuela Ghia, Elaine Skowronski, James McCanna, Sareh Manouchehri, George Widhopf, Thomas Kipps, and Michael Heller. Isolation and Detection of Circulating Cell Free DNA Directly from Chronic Lymphocytic Leukemia Patient Blood (In preparation).

James P. McCanna, Avery Sonnenberg, Michael J. Heller. Low Level Fluorescent Detection of Nanoparticles via Dielectrophoresis. *Biophotonics* 2013 (In review).

Avery Sonnenberg, Jennifer Y. Marciniak, James McCanna, Rajaram Krishnan, Laura Rassenti, Thomas J. Kipps and Michael J. Heller. Dielectrophoretic Isolation and Detection of cfc-DNA Nanoparticulate Biomarkers and Virus from Blood. *Electrophoresis*. 2013. (doi:10.1002/elps.201200444).

Avery Sonnenberg, Jennifer Y. Marciniak, Alexander P. Hsiao, Rajaram Krishnan, Michael J. Heller. Dielectrophoretic (DEP) Isolation of DNA and Nanoparticles from Blood. *Electrophoresis*. 2012, 33(16), 2482-90

Rajaram Krishnan, Eugene Tu, David Charlot, Lucas Kumosa, William Hanna, James McCanna, Jerry Lu, Avery Sonnenberg, Michael Heller. An AC Electrokinetic Device for the rapid separation and detection of cancer related DNA nanoparticulate biomarkers. Biomedical Circuits and Systems Conference (BioCAS), 2011 IEEE, pp.373-376.

Michael Heller, Rajaram Krishnan, Avery Sonnenberg. New Electrokinetic Devices and Methods for High Conductance and High Voltage Dielectrophoresis (DEP). Patent Pending. Provisional Patent # 61/413,306.

Michael Heller, Raj Krishnan, Avery Sonnenberg. Rapid detection of cancer-DNA biomarkers and nanoparticles. Biomedical Optics & Medical Imaging. SPIE Newsroom. 2010.

Fields of study

Major Field: Bioengineering

Professor Michael J. Heller

ABSTRACT OF THE DISSERTATION

**DIELECTROPHORESIS FOR BIOMARKER ISOLATION FROM
BIOLOGICAL SAMPLES**

by

Avery Renault Sonnenberg

Doctor of Philosophy in Bioengineering

University of California, San Diego, 2013

Professor Michael J. Heller, Chair

Cell-free circulating (CFC) DNA is now considered an important biomarker for early detection of cancer, residual disease, monitoring chemotherapy and other aspects of cancer management. The isolation of CFC-DNA from plasma as a “liquid biopsy” may begin replacing more invasive tissue biopsies as a means to detect and analyze cancer mutations. Unfortunately, conventional techniques for the isolation of CFC-DNA from plasma require a relatively time consuming and complex process which would rule out their use for point of care diagnostic applications. This work demonstrated the rapid

isolation and detection of both single-stranded and double-stranded HMW-DNA and 40 nm nanoparticles directly from whole blood and buffy coat blood samples. We then went on to show the rapid isolation and detection of SYBR Green stained CFC-DNA from 20 μ L whole blood samples from Chronic Lymphocytic Leukemia (CLL) patients, as well as isolation of cell-free mitochondria and virus from high conductivity buffers. To investigate the potentially clinical utility of this technology, we isolated CFC-DNA from fresh blood samples of fifteen CLL patients and three healthy individuals. CFC-DNA from 25 μ L (a drop) of blood was separated and concentrated into DEP high-field regions in about three minutes and held while blood cells, proteins and other biomolecules were removed by a fluidic wash. Concentrated CFC-DNA was detected by fluorescence and then eluted for PCR and DNA sequencing. The complete process, blood to CFC-DNA for PCR, spanned less than 10 minutes. Eluted CFC-DNA, from 5 μ l of the original CLL blood sample, was amplified by PCR using IGVH-specific primers to identify the unique IGHV gene expressed by the leukemic B-cell clone. The PCR results obtained by DEP from CLL blood were comparable to results obtained using conventional sample preparation of CFC-DNA starting with one ml of plasma and the sequencing results were accurate for all 15 patient samples. The ability of DEP to provide rapid isolation of CFC-DNA from the equivalent of a drop of blood represents a major step forward in the mission to create viable point of care cancer diagnostics and patient monitoring. This technology is applicable to a wide variety of biomarkers in biological and environmental samples and has broad implications as low-complexity and easily integrated front-end sample processing solution.

CHAPTER ONE:

Introduction

1.1 Background

1.1.1 Cancer Biomarkers

The American Cancer Society predicted that 1,638,910 new cancer cases and 577,190 cancer deaths would occur in 2012, making cancer responsible for 1 in 4 deaths in the United States[1]. Advances in scientific understanding of cancer mechanisms and environmental risk factors, expansion in the number of available treatments, and improved ability and implementation of screening and early detection techniques have all led to a slow decline in the incidence rate and number of deaths resulting from cancer in the United States over the past decade. An area of continued research interest is biomarker discovery and utilization in diagnosis and treatment guidance for all diseases, including cancer. The increased ability to collect genetic[2-6], epigenetic[7-9], proteomic[10-12], and other information is of great value in prediction, detection, diagnosis, and prognosis in cancer[13-15].

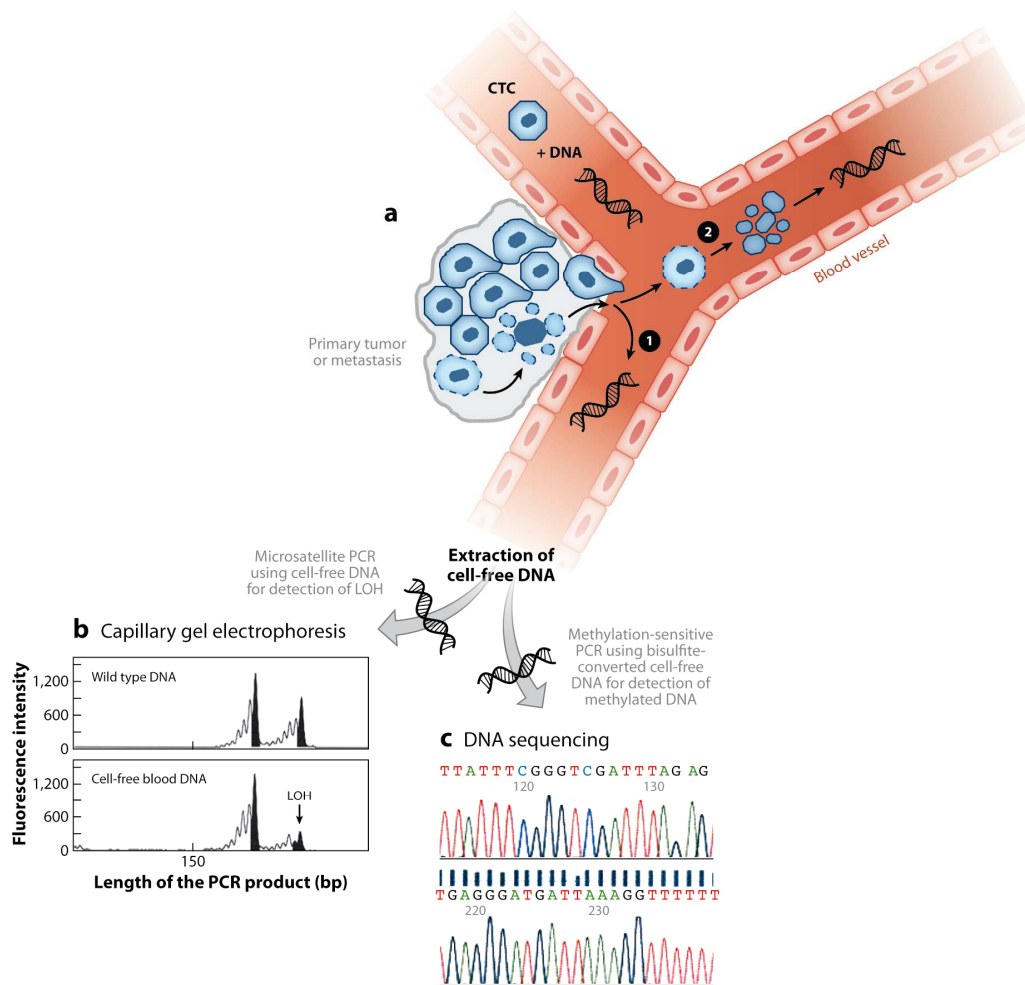
1.1.2 DNA as a cancer biomarker

The uncontrolled cellular division in cancer is made possible by the accumulation of genetic and epigenetic mutations that disrupt the balance between cell growth and cell death mechanisms present in healthy tissues. For this reason, access to the DNA of a tumor cell population can provide a wealth of information about its development and potential for treatment. Mutations have been linked to risk of developing cancer [16, 17], the likely progression path of the disease [16], and its response to various treatments [18, 19]. This information can be accessed via biopsy of the cancerous tissue itself or

through the collection of circulating tumor cells (CTCs) or cell-free circulating (CFC) DNA. As collecting a tissue biopsy is an invasive procedure and circulating tumor cells are rare and complex to isolate, a promising candidate to pursue for expanded use in biomarker collection is CFC-DNA.

1.1.3 Cell-free circulating DNA

In the past decade a considerable amount of information has emerged that demonstrates a close association of cell-free circulating (CFC) DNA with tumor burden and cancer progression [20-22]. Thus, the ability to isolate CFC-DNA biomarkers from blood and other clinical samples is important for early detection of cancer [20-23], residual disease detection [9, 24], and monitoring of chemotherapy [25] as well as many other diagnostic applications. When cancer and other diseases are present, CFC-DNA biomarkers are often found in the blood along with apoptotic DNA fragments. Apoptotic DNA is normally present in the blood at levels from 0 to 100 ng/ml with an average value of about 30 ng/ml [21, 26, 27]. CFC-DNA from cancer can occur in the blood at levels from 0 to over 1000 ng/ml, with an average value of about 180 ng/ml [21, 26, 27]. CFC-DNA fragments are generally of a higher molecular weight than apoptotic DNA, and are released into the blood by cancerous, necrotic and other diseased cells [6, 20, 28]. Figure 1.1 below illustrates the process by which tumor DNA enters the blood stream, either directly from the primary tumor or from apoptotic circulating tumor cells.




 Alix-Panabières C, et al. 2012.
Annu. Rev. Med. 63:199–215

Figure 1.1: Detection of genetically and epigenetically altered DNA in blood. High levels of cell-free tumor DNA circulate in the blood of cancer patients. (a) This tumor DNA found in blood can be released from either (1) the primary tumor or (micro)metastasis, or (2) apoptotic circulating tumor cells (CTCs). This DNA can be extracted from blood, and the genetic and epigenetic alterations can be determined. To detect loss of heterozygosity (LOH) on cell-free DNA, extracted DNA is amplified in a polymerase chain reaction (PCR)-based fluorescence microsatellite analysis using a gene-specific primer set binding to tumor suppressor genes. The fluorescence-labeled PCR products can be separated by capillary gel electrophoresis and detected by a fluorescence laser. In the diagram (b), the abscissa indicates the length of the PCR product; the ordinate gives information on the fluorescence intensity represented as peaks. The upper and lower parts of the diagram show the PCR products derived from wild-type DNA (from leukocytes) and plasma DNA, respectively. As depicted by the two peaks of the amplified wild-type DNA, both alleles are intact, whereas the lower peak of the PCR product derived from the plasma DNA shows LOH (arrow). (c) To detect cell-free methylated DNA, extracted DNA is denatured and treated with sodium bisulfite. In a methylation-sensitive PCR, the modified DNA is amplified with gene-specific primers. Because sodium bisulfite converts unmethylated cytosine residues into uracil, in contrast to methylated cytosine, the methylation pattern can be determined by DNA sequencing. Reprinted with permission from [5].

Tumor DNA, if recovered and analyzed, can provide important information about the tumor that can guide treatment decisions. There is an elevated level of CFC-DNA in many types of cancer, both solid tumor and hematological malignancies. Examples of the levels seen in patients with advanced disease are shown in Figure 1.2.

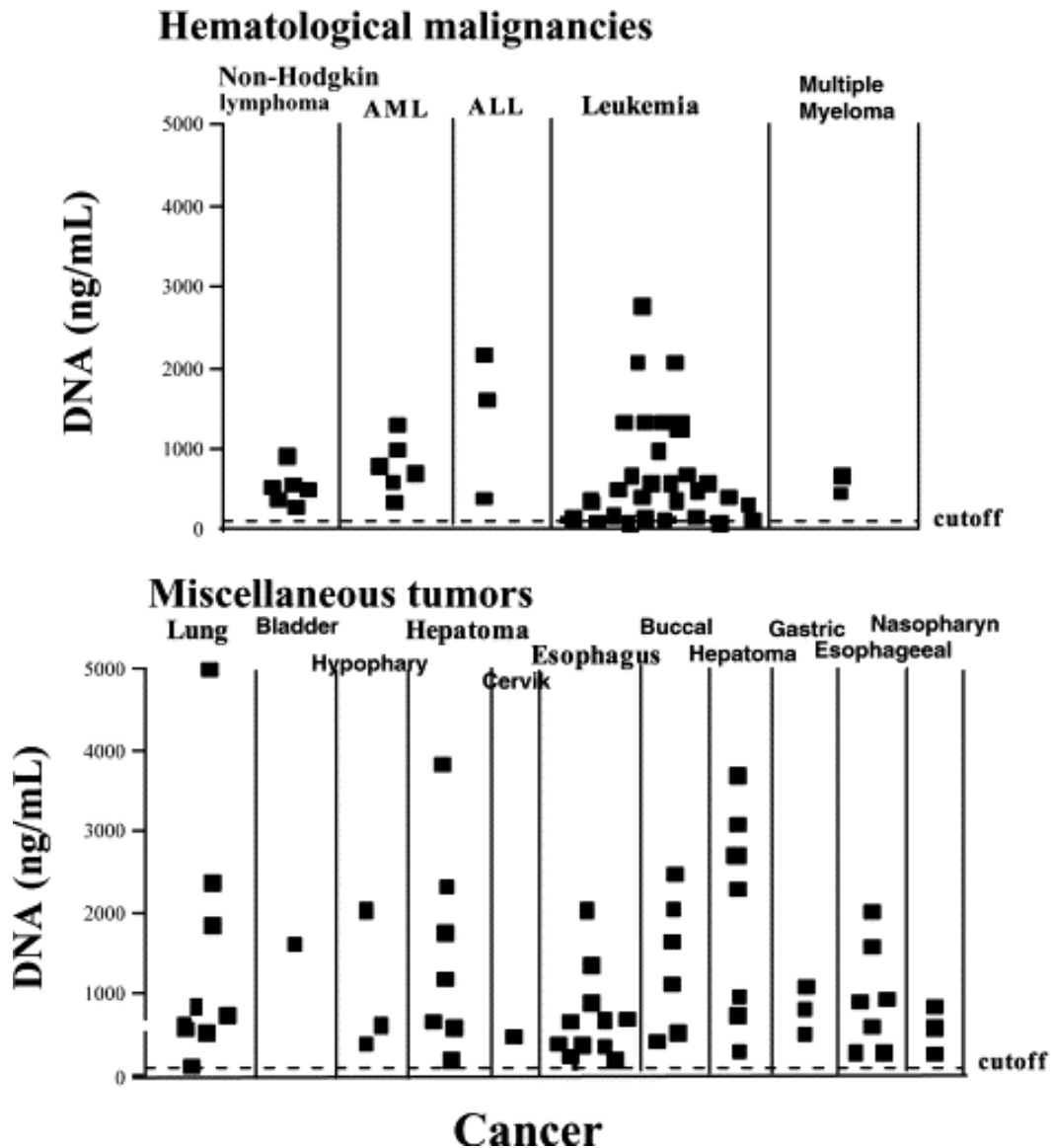


Figure 1.2: Elevation of cell-free DNA in miscellaneous malignancies. Elevated cell-free DNA was found not only in carcinomas but also in hematological malignancies. We tend to select specimens with higher levels of tumor marker or from patients with more advanced diseases. Reprinted with permission from [26].

1.1.4 Monitoring of drug delivery nanoparticles

In addition to the detection of CFC-DNA biomarkers, another important challenge for nanomedicine will be the monitoring of drug delivery nanoparticles [29-32]. A variety of approaches are now being used for encapsulating drug molecules within nanoparticles and nanovesicles which can range in size from 20 nm to 500 nm [33, 34]. While considerable efforts are being carried out on the development of drug delivery nanoparticles, presently there are no viable methods to monitor their concentration in whole blood.

1.1.5 Sample Preparation

At this time, the processes for isolating and purifying HMW/CFC-DNA and nanoparticles directly from blood are complex, time consuming and expensive. The procedures can involve centrifugation, filtration, washing and extraction of the DNA by phenol/chloroform methods, ion exchange binding or other laborious procedures [20, 23, 26-28]. After the extraction process, the DNA can be run on a PAGE gel to determine its size and concentration and/or genotyped using PCR techniques [20, 27, 34]. Additional disadvantages for current protocols include the extended amount of time between blood drawing, cell separation, DNA extraction and final DNA analysis. Delay in processing blood to plasma or serum causes release of DNA molecules by normal cells [20, 27]. The process by which the DNA is isolated also leads to degradation of DNA into smaller fragments due to mechanical shearing [20, 26]. Additionally, sample processing is highly inefficient and up to 65% of the DNA can be lost [6]. Thus, for research and clinical

diagnostic applications it is important to develop a rapid, sensitive and inexpensive method for the isolation and detection of CFC-DNA and drug delivery nanoparticles directly in blood. Figure 1.3 below shows the steps necessary to isolate and lyse peripheral blood mononuclear cells from a whole blood sample. Once the DNA is collected, it is then isolated with the use of a commercial adsorption column kit. The DNA isolation in this procedure is also used to isolate CFC-DNA from plasma, and is the most commonly used method in studies on CFC-DNA.

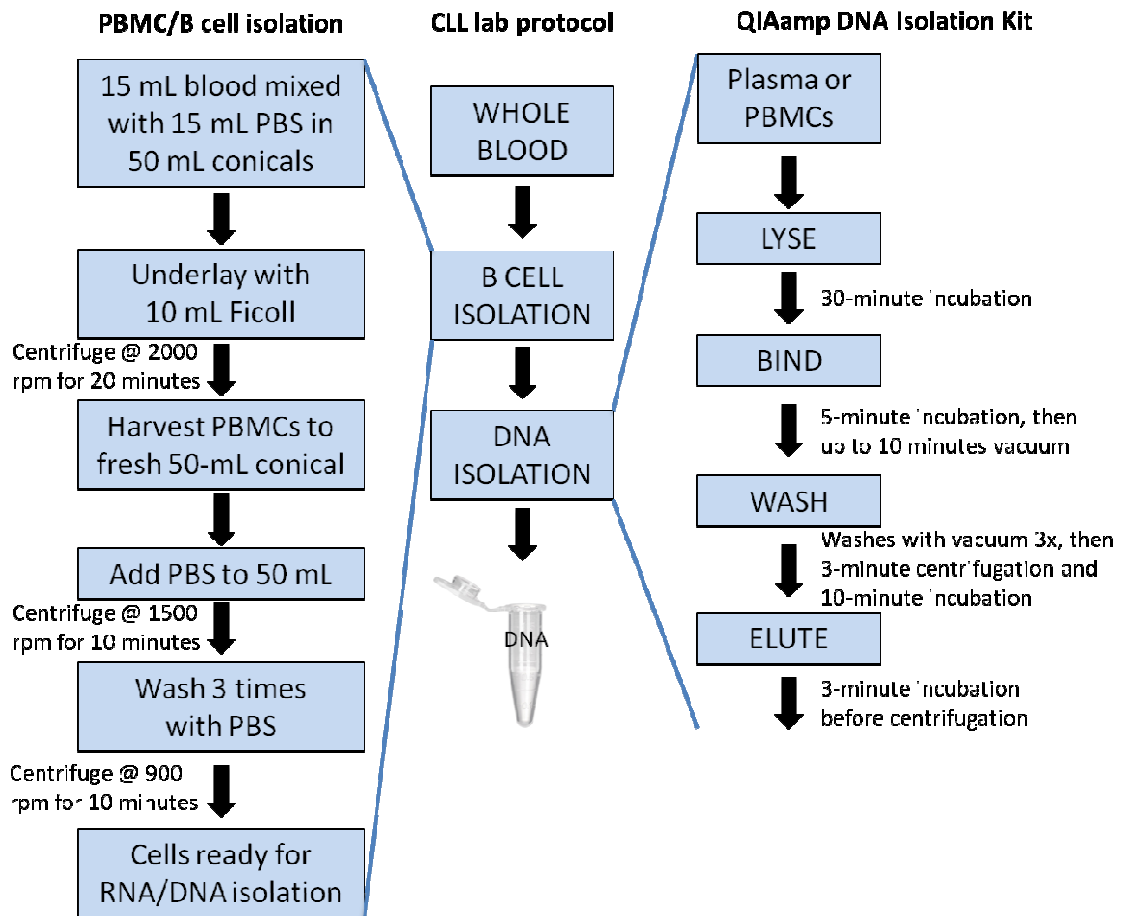


Figure 1.3: Sample preparation. Steps for harvesting, preparing, and extracting DNA from PBMCs. The DNA extraction procedure shown here is also used to isolate CFC-DNA from plasma.

1.2 DEP Theory

Electrokinetic methods such as DC electrophoresis and dielectrophoresis have proven very useful in manipulating biological samples [35-41]. While DC electrophoresis induces movement of an entity based on its net charge and the interaction of that charge with a DC electric field, dielectrophoresis uses an electric field which must be applied asymmetrically by controlling the geometry of the electrodes or the shape of the fluid chamber [42, 43]. When an entity experiences an asymmetric electric field, a dipole forms and is acted upon asymmetrically. The net force experienced due to this electric field is called the dielectrophoretic force and is described by the equation:

$$F_{DEP} = 2\pi r^3 \epsilon_m \operatorname{Re}\{K(\omega)\} \nabla E^2$$

Where r is the effective radius of the entity, ϵ_m is the permittivity of the medium, E is the applied electric field, and $K(\omega)$ is the Clausius-Mossotti Factor (CMF), defined below for spherical entities, which describes the relationship between the entity and the fluid medium in which it is suspended. The complex dielectric constant ϵ^* includes the bulk permittivity $\epsilon_r \epsilon_0$, the conductivity σ , and frequency ω .

$$K(\omega) = \frac{\epsilon_p^* - \epsilon_m^*}{\epsilon_p^* + 2\epsilon_m^*}$$

$$\epsilon^* = \epsilon_r \epsilon_0 + \frac{\sigma}{j\omega}$$

If the real part of the CMF is positive, this indicates that the interaction of the induced dipole and the applied non-uniform electric field will result in a force towards the areas of increasing electric field strength (positive DEP), which is shown below in Figure 1.4, where the particle is more polarizable than the surrounding media.

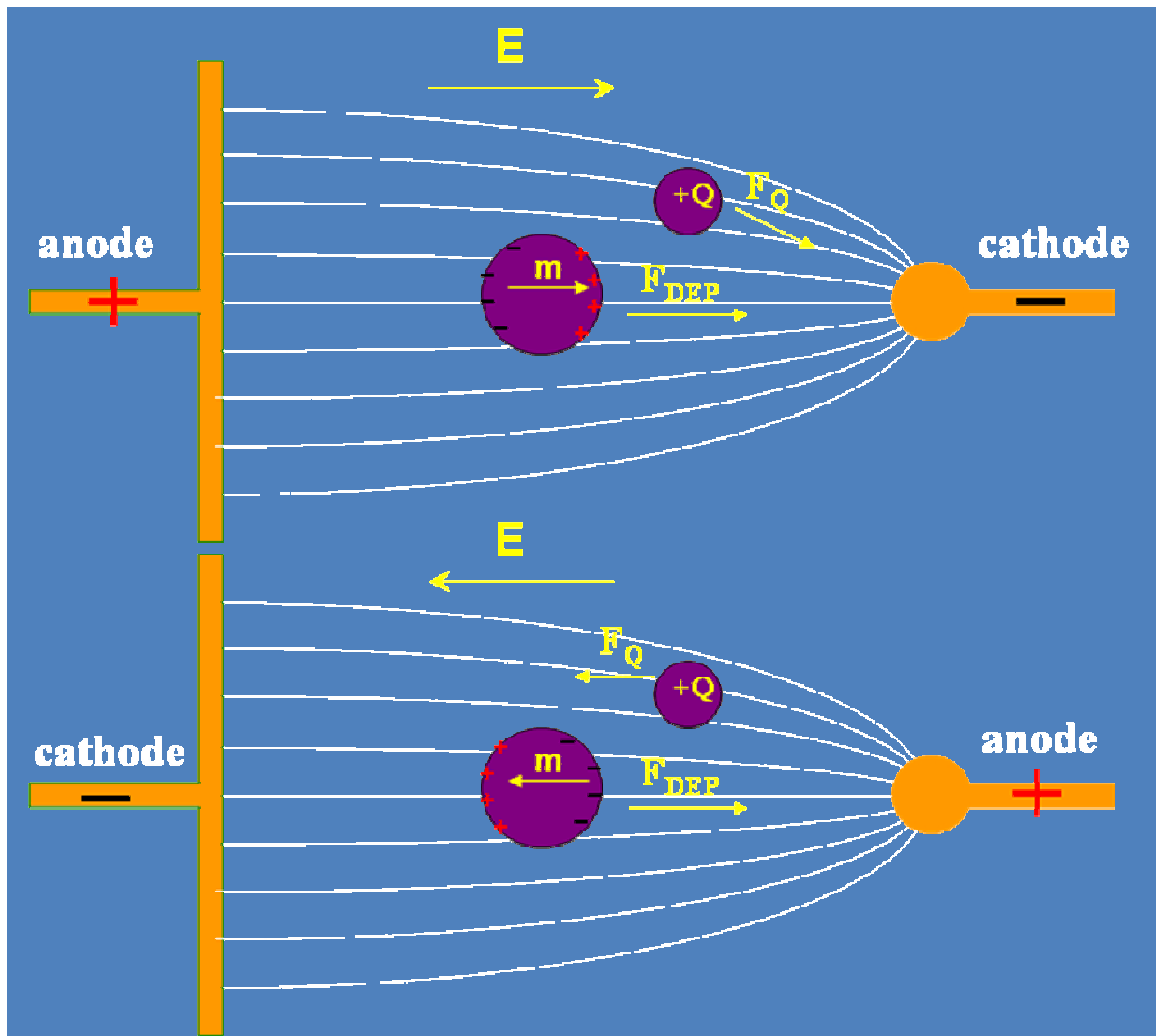


Figure 1.4: Positive DEP. In this example, the particle is more polarizable than the surrounding media at the electric field frequency that is being applied. Although the particle has no net charge, the charges towards the right of the figure experience a larger attractive force than those toward the left of the figure, due to the higher electric field strength caused by the asymmetry in the electric field. This occurs on both phases of the AC field application, and the particle experiences positive DEP (p-DEP), causing it to move towards the area of high electric field strength.

If the real part of the CMF is negative, the entity will experience a force directed away from areas of high field strength (negative DEP), as seen in Figure 1.5, where the particle is less polarizable than the surrounding media.

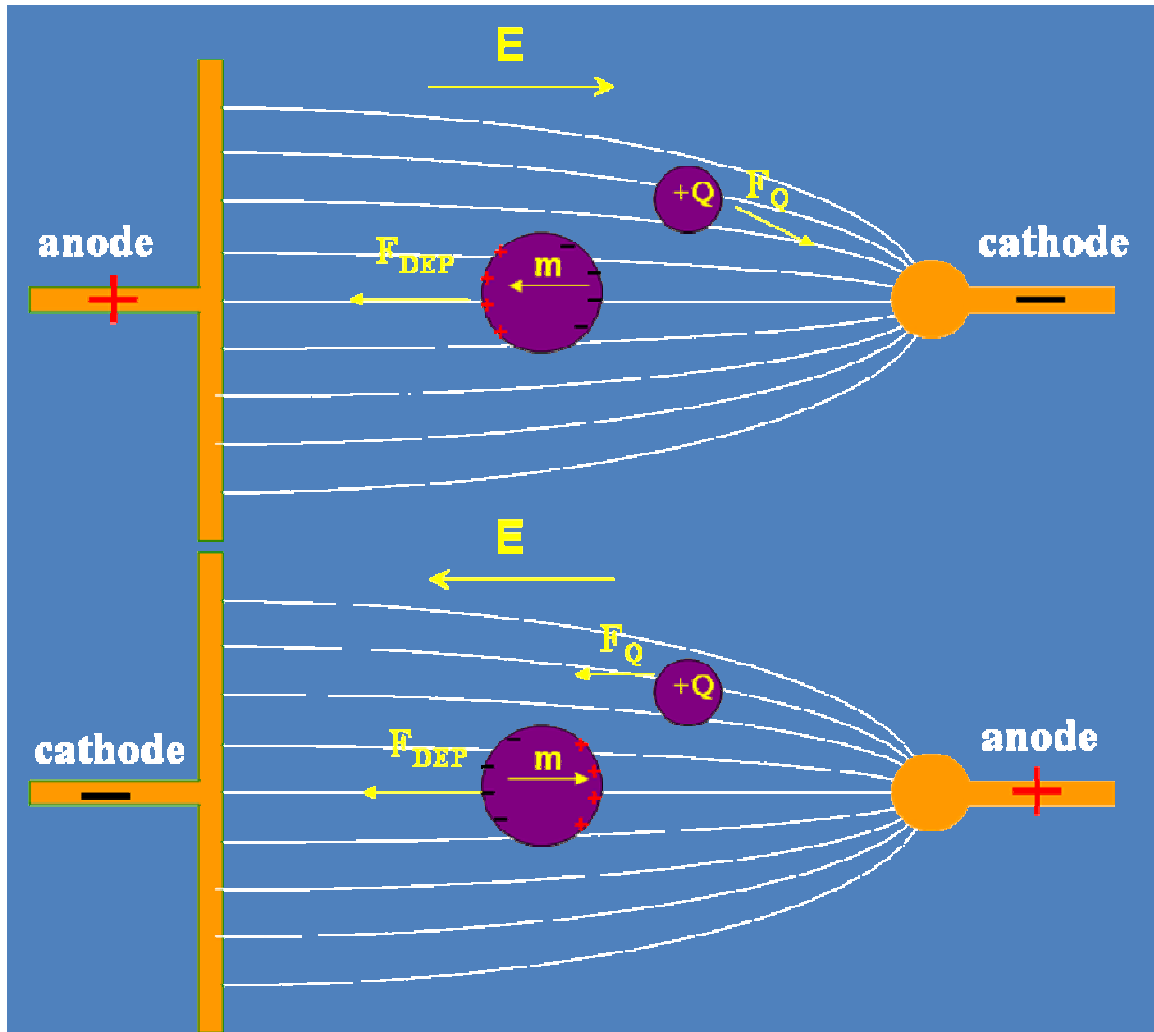


Figure 1.5: Negative DEP. In this example, the particle is less polarizable than the surrounding media at the electric field frequency that is being applied. Although the particle has no net charge, the charges towards the right of the figure experience a larger repulsive force than those toward the left of the figure, due to the higher electric field strength caused by the asymmetry in the electric field. This occurs on both phases of the AC field application, and the particle experiences negative DEP (n-DEP), causing it to move towards the area of low electric field strength. The dipole formation in this figure seems counterintuitive as the counterion cloud surrounding the particle is not pictured. In the case of negative DEP, the media is more polarizable than the particle, resulting in the dipole forming such that both charge centers experience repulsive force as shown above.

If a particle is composed of more than one material, the permittivity and conductivity of each layer must be taken into consideration. The simplest way to do this is to combine the layers into an effective conductivity and permittivity as shown in Figure 1.6 and using the following equation:

$$\epsilon_{p(eff)}^* = \epsilon_2^* \frac{\frac{a_2^3}{a_1^3} + 2 \frac{\epsilon_1^* - \epsilon_2^*}{\epsilon_1^* + 2\epsilon_2^*}}{\frac{a_2^3}{a_1^3} - \frac{\epsilon_1^* - \epsilon_2^*}{\epsilon_1^* + 2\epsilon_2^*}}$$

This results in one effective complex permittivity term that represents the DEP response of a particle made up of a spherical core of radius a_1 , permittivity ϵ_1 , and conductivity σ_1 and an outer shell with inner radius a_1 , outer radius a_2 , permittivity ϵ_2 , and conductivity σ_2 as shown in Figure 1.6 below. For a particle that is made up of more than a single shell around a spherical center, additional layers can be added one at a time using this technique to add layers while moving outward from the center.

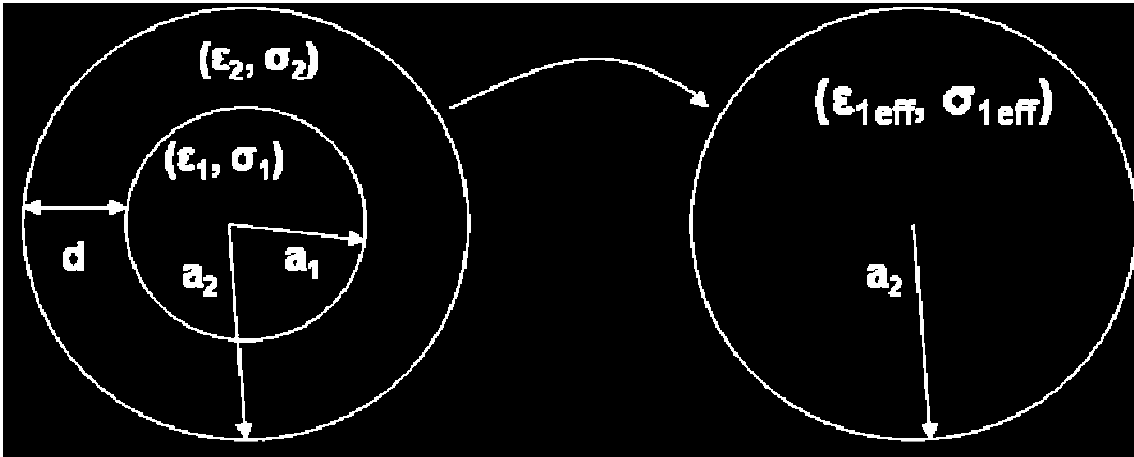


Figure 1.6: Single Shell Model. Successive layers with different dielectric properties can be added, first by combining the innermost two layers, and then adding layers one at a time going outward.

At a given frequency, the sign of the CMF (positive or negative) indicates whether an entity will experience p-DEP or n-DEP. Any transition between a positive and negative CMF is referred to as a crossover frequency. Choosing to apply a non-uniform electric field with a frequency at which one entity has a positive CMF and another has a negative CMF allows the two entities to be separated with DEP[39]. An example of a separation of two cell types is shown below in Figure 1.7. Cell Type A and Cell Type B both have negative CMFs at low frequencies and positive CMFs at higher frequencies (with a second crossover to a negative CMF at very high frequencies). Differences in the dielectric properties of these cells result in a different crossover frequency, where the net DEP force on the cell is zero. To separate the two cells using DEP, an electric field must be applied with a frequency between their crossover frequencies. In this case, the electric field would cause Cell Type A to move toward areas of high electric field strength (positive DEP), while Cell Type B would move away from high field areas (negative DEP). Because the crossover frequencies of these cells are fairly close together, this

separation would be more difficult than some others, as the Clausius-Mossotti factor for Cell Type A would be about 0.2, or 20% of the maximum for a spherical particle, and the CMF for Cell Type B would be about -0.2, or 40% of the maximum for negative DEP on a spherical particle.

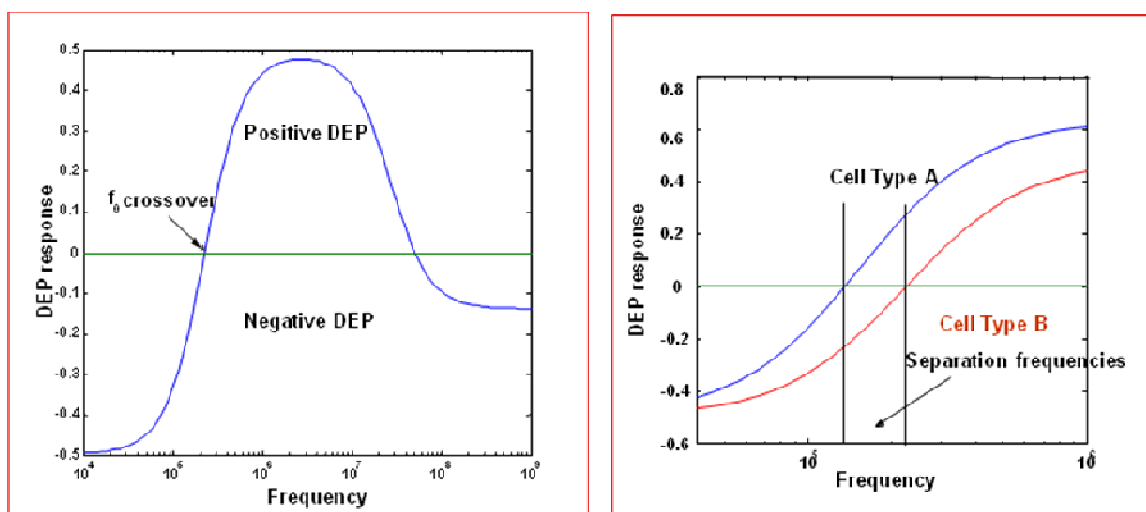


Figure 1.7: Clausius-Mossotti Factor is a function of frequency. The DEP force is proportional to the CMF, which depends on the frequency of the applied electric field. When the CMF transitions between a positive and negative value, the frequency at which the CMF value is zero is called a crossover frequency. Choosing an applied frequency between the crossover frequencies of two particles results in the particle experiencing DEP force in opposing directions. This is the basis for DEP separations of particles.

With regard to nanoparticulate entities such HMW-DNA, mitochondria and virus, the simplified model above for determining the direction and magnitude of DEP force is useful for understanding how the force originates, but does not adequately predict the behavior of particles at low frequencies or when the electric double layer is large, as it is when considering nanoparticles and DNA [44-46]. It has been known for some time that many biological entities experience positive DEP at low frequencies despite the fact that simplifying their multilayer components to an effective bulk conductivity and

permittivity predicts the opposite [47, 48]. To predict the DEP response of particles at low frequency with electric double layers of arbitrary size, a promising method is to numerically solve the Poisson–Nernst–Planck equation [49]. While such analysis is enlightening, it is not absolutely necessary for appreciating the practical clinical significance of the experimental observations detailed in this thesis.

1.3 Scope of the dissertation

This dissertation addresses key questions in the development of dielectrophoresis as a viable technique for collecting analytes from high conductance biological samples. With this work, dielectrophoresis has been established as a method to leverage differences in particle properties to carry out separations of biological entities in their native media by exploiting the differences in their responses to an applied AC electric field in asymmetric field geometries. To our knowledge, this is the first time that DNA and nanoparticles have been directly collected into DEP high-field regions under the high conductivity conditions present in biological buffers such as blood and plasma. The experimental results described herein will inform the direction of future work in DEP collections of analytes of interest from biological solutions, as well as provide guidance on new device design that may allow improved collection efficiency and system integration into high-throughput applications. The ability to conduct conventional downstream analysis techniques such as PCR and DNA sequencing on the material collected with this new method was investigated and the results will impact the area of biomarker collection specifically, and sample preparation in general.

Chapter 1 provides an overview of cell-free circulating DNA as a cancer biomarker, as well as an introduction to the technique of dielectrophoresis.

Chapter 2 describes the usage of a dielectrophoretic device to separate double stranded and single stranded DNA, as well as nanoparticles, from high-conductivity buffer and whole human and rat blood.

Chapter 3 describes the investigation of the hypothesis that this technique can be used to isolate existing DNA that persists in the blood stream of diseased individuals due to a high level of necrotic cell death. Other potential analytes are also investigated, including free mitochondria and virus.

Chapter 4 presents the results obtained from testing the hypothesis that the material isolated from Chronic Lymphocytic Leukemia patient blood samples with a Dielectrophoresis device can be eluted and analyzed to obtain genetic information about the leukemia cell population. Results from multiple downstream analysis techniques answer the question of whether the described dielectrophoresis technique impacts the collected material in a way that would prevent subsequent interrogation of the material.

Chapter 5 describes the invention of an entirely new type of DEP device for use in high conductivity buffers. Some simple example designs are presented, with a description of situations in which this device would have advantages over current devices. Results from a prototype device are also presented.

Chapter 6 provides a summary and conclusion, as well as addresses study limitations and outlines recommendations for future work.

Chapter 1 is, in part, published as the following two manuscripts: Avery Sonnenberg, Jennifer Y. Marciniak, Alexander P. Hsiao, Rajaram Krishnan, Michael J. Heller. *Dielectrophoretic (DEP) Isolation of DNA and Nanoparticles from Blood*. Electrophoresis. 2012, 33(16), 2482-90 and Avery Sonnenberg, Jennifer Y. Marciniak, James McCanna, Rajaram Krishnan, Laura Rassenti, Thomas J. Kipps and Michael J. Heller. *Dielectrophoretic Isolation and Detection of CFC-DNA Nanoparticulate Biomarkers and Virus from Blood*. Electrophoresis. 2013, 34(7), 1076-84.

The author of this dissertation is the primary author of these manuscripts.

CHAPTER TWO:

Dielectrophoretic (DEP) Isolation of DNA and Nanoparticles from Blood

2.1 Introduction

AC electrokinetic methods like dielectrophoresis (DEP) are well-known techniques for achieving effective separations of cells, nanoparticles, and biomolecules [35-41]. However, until recently DEP had remained impractical for general use in high conductance solutions (~ 10 mS/cm) and with complex biological samples such as whole blood [35, 36, 38-40]. For example, earlier DEP work on separating bacteria from blood required a 50-fold dilution of the blood sample ($\sim 7-9$ mS/cm) before the DEP separation process could be carried out [40]. Other DEP separations, including cells [41, 50-52], virus [52], polystyrene nanoparticles [53-57], DNA [58-60] and proteins [61, 62] also required low-conductance conditions (below 1 mS/cm). While some progress has been made on carrying out DEP under high conductance conditions, generally this work has been limited to separations of cells and micron-size entities by negative DEP forces using hybrid DEP devices [50, 63-67]. Recently, we have developed DEP methods that now allow nanoscale entities including HMW-DNA and nanoparticles to be separated under high conductance conditions [68-70]. Using microarrays with platinum microelectrodes over-coated with a thin hydrogel layer [71] allows device operation at up to 20 volts peak-to-peak at 10 kHz DEP in high conductance buffers (~ 10 mS/cm). These robust devices ameliorate many of the adverse or disruptive electrolysis effects including bubbling, heat and convection. Thus, HMW-DNA or nanoparticles experiencing positive DEP (p-DEP) could be concentrated into the DEP high-field regions over the microelectrodes, while micron size or larger particles experiencing negative DEP (n-DEP) were concentrated into the DEP low-field regions between the microelectrodes.

Experiencing positive DEP force means that at the applied frequency (10 kHz), the HMW-DNA or nanoparticles were more polarizable than the surrounding solution and the DEP force moved them towards areas of high electric field strength. At the same frequency, the blood cells experienced negative DEP force because they are less polarizable than the surrounding solution and thus repelled from areas of high field strength. The polarizability of any entity depends on the solution in which it is suspended as well as the frequency of the applied electric field, a relationship described by the Clausius-Mossotti Factor (CMF). At a given frequency, the sign of the CMF (positive or negative) indicates whether an entity will experience p-DEP or n-DEP. Any transitions between a positive and negative CMF is referred to as a crossover frequency. Choosing to apply an electric field with a frequency at which one entity has a positive CMF and another has a negative CMF allows the two entities to be separated with DEP [39]. After the DEP separation is completed a simple fluidic wash removes the larger particles (cells) in the low-field regions, while the nanoparticles remain concentrated in the high-field regions. In this study, we now show that DEP can be used for the rapid separation and detection of HMW-DNA and nanoparticles directly from biological samples which have both high complexity and high conductivity, including undiluted whole blood, buffy coat blood and settled whole blood samples. This DEP technique significantly minimizes sample preparation which has been a major limitation to the development of new CFC-DNA based diagnostics and drug delivery nanoparticle monitoring applications.

2.2 Methods

2.2.1 DEP Device and Methods

Microarrays used in the DEP experiments (Figure 2.1A) had 100 platinum microelectrodes (80 micron diameter) enclosed in a microfluidic cartridge which formed a 20 μ l sample chamber covered with a glass window [40, 41, 68-70]. For the DEP experiments in this study a subset of nine microelectrodes were used to form checkerboard AC field geometry (Figure 2.1B). The electrodes in the four corners and the center have one polarity, while the electrodes directly above, below, and to the sides of the center electrode have the opposite polarity. Regarding DEP separations, biological cells suspended in high conductivity buffers are often less polarizable than the buffer. As a result, cells are pushed away from the DEP high-field regions and move into the low-field regions exhibiting what is referred to as negative DEP (n-DEP).

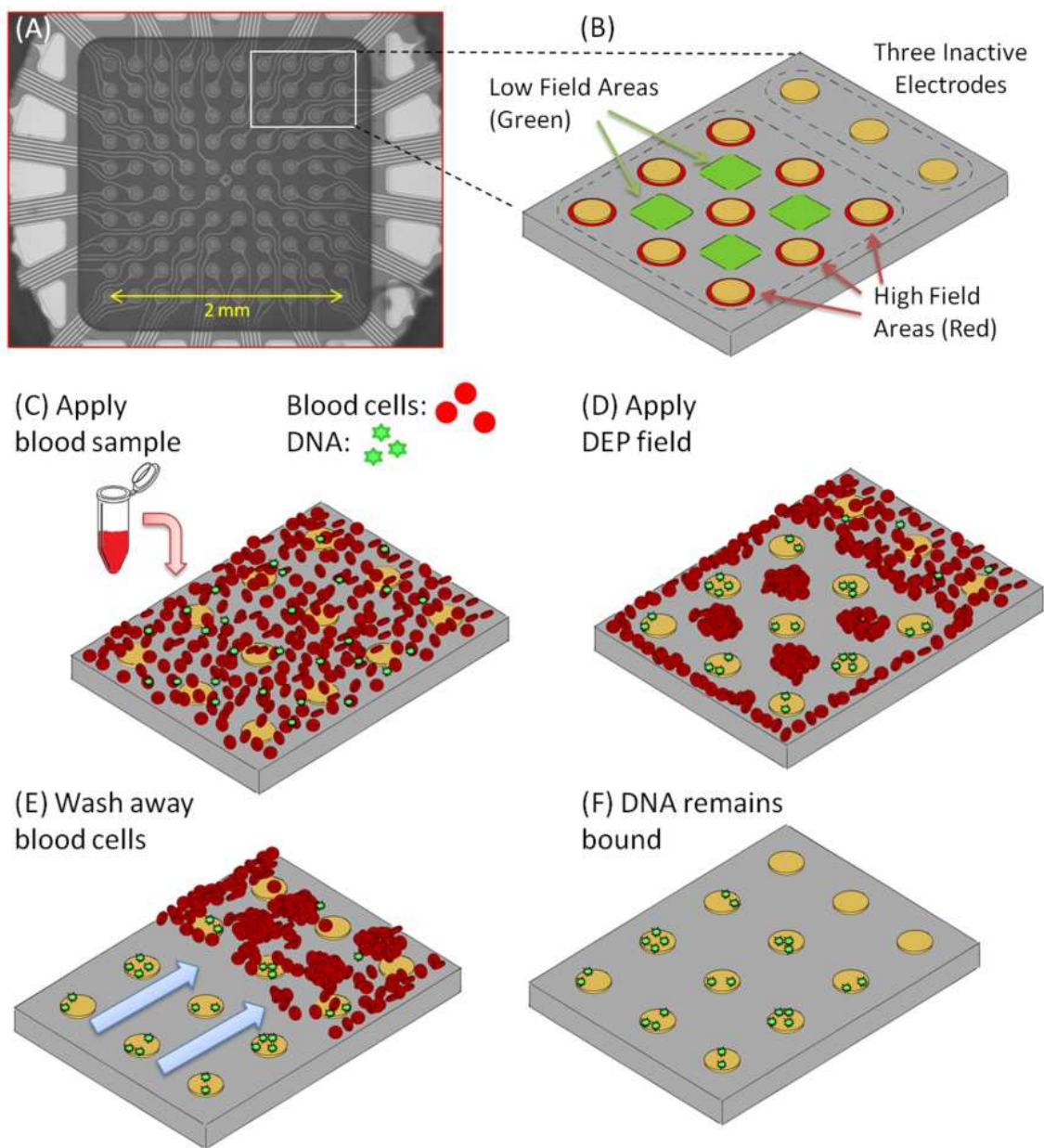


Figure 2.1: DEP microarray device and scheme for DEP separation of DNA and nanoparticles from blood. (A) The microarray device used for this study contained 100 platinum microelectrodes which were 80 microns in diameter. (B) A subset of nine microelectrodes were activated (AC voltage) to form a DEP field geometry which then produces p-DEP high-field regions (red) in or around the microelectrode perimeters, and n-DEP low-field regions (green) in between the microelectrodes. The un-activated microelectrodes serve as control regions where no high or low DEP fields are occurring, and cells or nanoparticles are not collected and concentrated. (C) The microarray with whole blood (red circles) containing fluorescent DNA (green dots). (D) When the DEP field is applied, the fluorescent DNA (green dots) is concentrated in the p-DEP high-field regions on the microelectrodes, while the blood cells (red circles) move into the n-DEP low-field regions between the microelectrodes. (E) A fluidic wash removes the blood cells from the microarray. (F) DNA remains concentrated in the high-field regions.

In all of our DEP experiments carried out at 20 volts peak-to-peak (V_{p-p}) and 10 kHz, blood cells (red and white) exhibit n-DEP, as is expected [72, 73]. Under these same conditions both HMW-DNA and nanoparticles move to the DEP high-field regions exhibiting positive DEP (p-DEP). As previously characterized [72], RBCs under physiological conditions cross from n-DEP to p-DEP in the 20-50 MHz range, and back from p-DEP to n-DEP in the 60-80 MHz range. Any applied AC field with a frequency below the lower crossover frequency will repel RBCs from the high-field regions. To capture HMW-DNA and nanoparticles in the high-field regions, we have observed that lower frequencies result in faster and stronger trapping. The 10 kHz frequency was chosen because going lower than this increases the incidence of bubbling and accelerates electrode corrosion reported in [70]. Similarly, 20 V_{p-p} was the highest voltage we were able to apply while reliably avoiding bubbling and significant corrosion of the electrodes for at least 15 minutes in high conductivity samples.

For the microarray devices used in this study, the p-DEP high-field regions occur around the microelectrode perimeters, and the n-DEP low-field regions occur between the microelectrodes (Figure 2.1B). More detailed explanation for separation of nanoparticles under high conductance conditions are given in our earlier references [68-70]. While DEP devices used in this study utilize an array of circular microelectrodes, many other electrode configurations are possible. For example, other groups have used configurations which include parallel/interdigitated, castellated, oblique, curved, quadrupole and many other electrode types [74, 75].

Figure 2.1 also shows the overall scheme for the DEP separation of HMW-DNA and nanoparticles from blood. Figure 2.1C shows the microarray with whole blood (red circles) containing fluorescent DNA (green dots). Figure 2.1D shows separation of fluorescent DNA (green dots) into the p-DEP high-field regions on the microelectrodes, and blood cells (red circles) moving into the n-DEP low-field regions between the microelectrodes. A fluidic wash removes the blood cells from the microarray (Figure 2.1E), while the DNA remains concentrated (Figure 2.1F). The concentrated fluorescent DNA on the microelectrodes can now be analyzed *in situ* (on the array) by epifluorescent microscopy and/or removed from the array and genotyped by PCR or DNA sequencing.

2.2.2 Buffers, Blood Samples, and Conductivity Measurements

Concentrated 5x Tris Borate EDTA (TBE) buffer solution was obtained from USB Corporation (Cleveland, Ohio), and diluted to 1x. Dulbecco's Phosphate Buffer Saline (1x PBS) solution was obtained from Invitrogen (Carlsbad, CA) and diluted to 0.5x. Human buffy coat blood was obtained from San Diego Blood Bank (San Diego, CA). Whole blood samples were obtained from adult female Sprague Dawley rats. Settled blood for the disrupted blood experiments was collected from an adult male human volunteer in accordance with the policies of the Institutional Review Board of the University of California, San Diego under IRB protocol #070643. The heparinized blood was allowed to settle for 20-30 minutes, at which point 200-400 μ l of supernatant was removed. This supernatant, which is composed mostly of plasma, but still contains a number of red and white blood cells, is referred to as "settled blood" for these

experiments. For preparation of disrupted settled blood, about 10 mg of porous glass microbeads was added to 100 μ l of settled blood which was then agitated by vortexing for 1 minute. This procedure causes disruption of many of the cells; specifically, the white blood cells release high molecular weight DNA (nuclei, nucleosomes, DNA nanoparticulates). The DEP field was applied to the undisrupted and disrupted settled blood samples at 10 kHz and 20 V_{p-p} for 15 minutes. Conductivity measurements were made with an Accumet Research AR-50 Conductivity meter using 2 cell (range: 10-2000 μ S) and 4 cell (range: 1-200 mS) electrodes. Buffer conductivities were: 7.4 mS/cm for human whole blood, 11.5 mS/cm for human plasma, 11.5 mS/cm for human settled blood, 7.6 mS/cm for 0.5x PBS, and 8.6 mS/cm for buffy coat blood. Due to the small volumes available for this work, conductivity of rat whole blood was not measured, but has been reported as 4.4 mS/cm [76]. Whole blood and buffy coat sample conductance values are in the same range as published values [77, 78]. Table 2.1 summarizes the DNA or nanoparticle target, buffer/blood sample, and electrical conductivity used for each DEP experiment.

Table 2.1: DEP targets, buffers, and electrical conductivities for each experiment.

*The value for rat whole blood is a reported value [76] and was not measured for this work.

Target for positive DEP	Fluid Medium	Conductivity	Figure
Single-stranded DNA	Rat whole blood	4.4 mS/cm*	2.2
Double-stranded DNA	Rat whole blood	4.4 mS/cm*	2.2
Cellular Nanoparticulates	Human settled blood	11.5 mS/cm	2.2
Low molecular weight DNA	0.5x PBS	7.6 mS/cm	2.3
High molecular weight DNA	0.5x PBS	7.6 mS/cm	2.4
Polystyrene beads	Human buffy coat blood	8.6 mS/cm	2.5

2.2.3 Single-Stranded (ss) and Double-Stranded (ds) High Molecular Weight (HMW) DNA and Low Molecular Weight (LMW) DNA

The rolling circle amplification (RCA) procedure for preparing the 40-45 kb single stranded (ss) HMW-DNA was described previously [68, 69]. The ss-HMW DNA forms a cluster or ball-like structure due to internal self-hybridization, and is a model for cell-free circulating HMW-DNA nanoparticulates. Samples of the ss-HMW DNA were stained using 1:100 Quant-iT™ OliGreen® (Invitrogen). The stained DNA was visualized using a fluorescence microscope. For the ss-HMW DNA experiments, 12 μl of the stock solution of ss-HMW DNA was added to 24 μl of OliGreen solution. The ss-HMW-DNA solution was then added to 300 μl of rat whole blood for a final DNA concentration of 260 ng/ml. About 150 μl was run through the microarray cartridge for the DEP experiments (actual sample volume in the microarray chamber is 20 μl). The DEP field was applied at 10 kHz and 20 $V_{\text{p-p}}$ for 14 minutes to the nine microelectrodes. The microarray was then washed three times with 0.5x PBS with the DEP field on.

Double-stranded (ds) HMW DNA was obtained from Sigma (St. Louis, MO) as Deoxyribonucleic Acid from *Micrococcus Luteus* (lysodeikticus) Type XI, Highly Polymerized. The ds-HMW-DNA was diluted to 2 $\mu\text{g/ml}$ in 2.5 ml of 1x TBE. For double-stranded DNA DEP experiments, 2 μl of 100x SYBR Green I Dye (Invitrogen) was mixed with 20 μl of ds-HMW DNA, and then the DNA solution was added to 178 μl of whole blood for a final concentration of 200 ng/ μl . The mixture was allowed to sit for 5 minutes, after which it was inserted into the microarray. The DEP field was applied at 10 kHz and 20 $V_{\text{p-p}}$ for 14 minutes to the nine microelectrodes. The microarray was

washed three times with 0.5x PBS with the DEP field on and examined by epifluorescent microscopy. For the DEP experiments involving DNA post-staining, 20 μl of the stock solution of RCA ss-HMW DNA and 1 μl of 10 μm carboxylated microspheres (obtained from Bangs Labs, Fishers, IN) were added to 180 μl of 0.5x PBS. The sample was then put into the microarray and the DEP field (10 kHz, 20 $V_{\text{p-p}}$) was applied for 10 minutes. The microarray was washed with 0.5x PBS and then 200 μl of OliGreen solution was pumped through the microarray at a rate of 40 $\mu\text{l}/\text{min}$ for 5 minutes. After the dye was added, the solution incubated for 5 minutes at room temperature.

Low molecular weight (LMW) DNA oligonucleotide sequences were obtained from Trilink Bio Technologies (San Diego, CA). The single-stranded (ss) 23mer DNA oligonucleotide with a Cy3 fluorescent dye (ex. 550, em. 570) had the sequence 5'-Cy3-ATT CCA TTC GAT TCC ATT CGA TC-3'. For the LMW-DNA experiments the sample was diluted to 150 nM in 300 μl of either 1x TBE or 0.5x PBS, to which 1 μl of the 10 μm microspheres was added. The sample was then put into the microarray and the DEP field (10 kHz, 20 $V_{\text{p-p}}$) was applied for 10-15 minutes. The microarray was then washed with 0.5x PBS and examined by epifluorescent microscopy.

2.2.4 Micron Size Particles and Nanoparticles

1 μl of the stock solution of 10 μm carboxylated polystyrene particles was added to 300 μl of 0.5x PBS along with the high molecular weight (HMW) DNA. Fluorescent polystyrene nanoparticles (FluoSpheres) with NeutrAvidin were purchased from Invitrogen (Carlsbad, CA). The nanoparticles were 0.04 μm (40 nm) in diameter and red

fluorescent (ex. 585, em. 605). For the nanoparticle concentration study, the red fluorescent nanoparticles were serially diluted to the following concentrations: 9.5×10^{11} , 9.5×10^{10} and 9.5×10^9 particles/ml in human buffy coat blood. The DEP field was applied at 10 kHz and 10 V_{p-p} for 20 minutes. For comparison purposes, the number of nanoparticles in an Abraxane nanoparticle drug dosage [79] was calculated by using the recommended dosage of 260 mg/m² combined with an average estimated Body Surface Area of 1.92 m² leading to a value of about 0.5 g of Abraxane per dosage. Since the mean diameter of an Abraxane drug delivery nanoparticle is 130 nm, and estimating a density of ~1 g/ml the number of circulating nanoparticles was calculated to be about 7.5×10^{10} nanoparticles per ml of blood, assuming 6 liters of blood.

2.2.5 Experimental Setup and Measurements

The microarrays were controlled using a custom-made switching system that allows individual control over the voltage applied to each microelectrode. The microelectrodes were set to the desired AC frequency and voltage using an Agilent 33120A Arbitrary Function Generator. The AC frequency used was 10 kHz, at 20 V_{p-p} . The waveform used was sinusoidal. The experiments were visualized using a JenaLumar epifluorescent microscope (Filters: OliGreen-DNA ex. 505 nm, em. 520 nm; red fluorescent nanoparticles ex. 585 nm, em. 605 nm; orange/red fluorescent Cy3 ex. 560, em. long pass 570). Both bright field and fluorescent images were captured using an Optronics 24-bit RGB CCD camera. The image data was processed using a Canopus ADVC-55 video capture card connected to a laptop computer with Adobe Premiere Pro

and Windows Movie Maker. The fluorescence intensity data images were created by inputting fluorescent image frames of the video into MATLAB.

2.3 Results

In our earlier DEP studies we demonstrated the separation of fluorescent HMW-DNA and nanoparticles in high conductance buffers [68-70], as well as provided some preliminary results in blood [80, 81]. Our new work now presents a complete study on the DEP separation of fluorescent 40 nm nanoparticles and a range of HMW-DNA in whole blood, buffy coat blood and settled blood samples. More specifically, this study demonstrates: (1) the DEP separation and detection of both ss-HMW-DNA and ds-HMW-DNA in blood; (2) that DNA from disrupted white blood cells can serve as a model for cell-free circulating (CFC) DNA; (3) that very low molecular weight DNA (< 100 bases) is *not* captured in p-DEP high-field regions; (4) that HMW-DNA separated from blood can be post-stained with fluorescent dyes for subsequent detection; and (5) some lower limits for detecting both HMW-DNA and nanoparticles in blood.

2.3.1 DEP Separation and Detection of ss-HMW-DNA and ds-HMW-DNA in Blood

Disease related CFC-DNA found in blood is generally a heterogeneous mix of DNA nanoparticulates and HMW DNA fragments, as opposed to one particular size DNA fragment. Therefore, it was important to show that the DEP technique is useful for isolating a wide range of HMW-DNAs. The first DEP experiment demonstrates the

isolation and detection of ss-HMW-DNA from whole blood. Figure 2.2a shows the green fluorescent image after the application of the DEP field and washing. No blood cells are left on the array, and intense green fluorescence from the ss-HMW-DNA can be seen concentrated in the p-DEP high-field regions around the nine microelectrodes. It should be pointed out that the fluorescent signal appears significantly higher for the middle microelectrodes of columns 2 and 4, and the upper and lower microelectrodes of column 3, due to greater electric field gradient at these locations. In all cases, the three unactivated microelectrodes in column 1 show no fluorescence.

The next experiment involved the DEP isolation and detection of double-stranded (ds) high molecular weight (>10 kb) DNA. Figure 2.2b shows the green fluorescent image after washing as well as very intense green fluorescence from the ds-HMW-DNA concentrated in the p-DEP high-field regions around the nine microelectrodes. As with the ss-HMW-DNA, fluorescent signal appears significantly higher for the middle microelectrodes of columns 2 and 4, and the upper and lower microelectrodes of column 3, due to greater electric field gradient at these locations. In all cases, the three unactivated microelectrodes in column 1 show no fluorescence. Figure 2.2c is the green fluorescent image after the DEP field is applied to a human whole blood sample to which no DNA has been added. The sample has the same concentration (5x) of SYBR Green I Dye as the sample in Figure 2.2b, and no accumulation of fluorescent material is seen in the p-DEP high-field regions around the nine activated microelectrodes. Figure 2.2d is a COMSOL simulation that confirms that the observed pattern of collection is due to the distribution of the electric field around the electrodes.

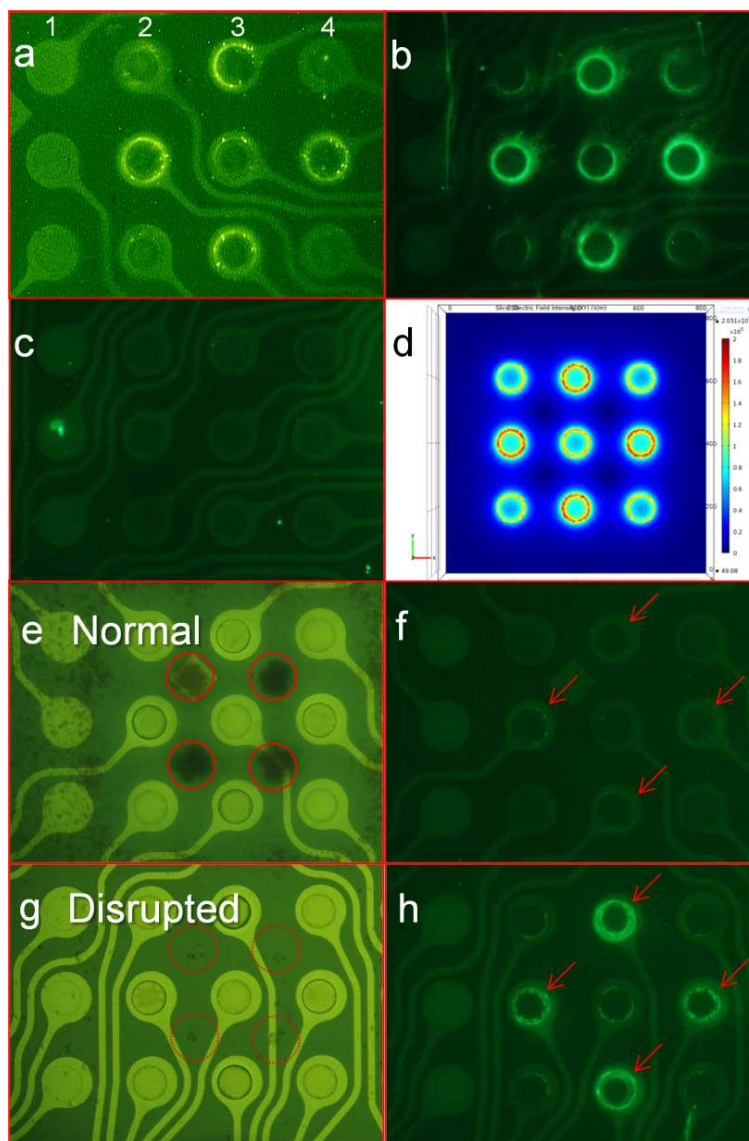


Figure 2.2: DEP separation of DNA from blood samples. The DEP AC voltage (10 kHz , 20 V_{p-p}) was applied to the nine electrodes in columns 2, 3, and 4 of each image, while no voltage was applied to the three electrodes in column 1, which serve as negative controls. (a) Rat whole blood (4.4 mS/cm , reported [76]) containing 260 ng/ml of OliGreen stained ss-HMW-DNA after 14 minutes of DEP and three washes with $0.5\times\text{ PBS}$, showing fluorescent DNA concentrated in the DEP high-field regions. (b) Rat whole blood containing $200\text{ ng}/\mu\text{l}$ of SYBR Green I Dye stained ds-HMW-DNA after 14 minutes of DEP and three washes with $0.5\times\text{ PBS}$, showing fluorescent DNA concentrated in the DEP high-field regions. (c) Human whole blood (7.4 mS/cm) containing SYBR Green I Dye but without any added DNA after 15 minutes of DEP and three washes with $0.5\times\text{ PBS}$, showing no fluorescent DNA concentration. (d) Electric field cross section of checkerboard pattern created with COMSOL Multiphysics (taken $10\text{ }\mu\text{m}$ above the electrode surface). (e) Bright field image of normal settled blood (11.5 mS/cm) with SYBR Green I Dye after 15 minutes of DEP. (f) Green fluorescence image of normal settled blood after 15 minutes, showing no fluorescent DNA concentration. (g) Bright field image of the disrupted settled blood (11.5 mS/cm) with SYBR Green I Dye after 15 minutes of DEP. (h) Green fluorescence image of the disrupted settled blood sample after DEP, showing fluorescent DNA concentrated in the DEP high-field regions.

2.3.2 DEP with Disrupted Settled Blood

The objective for this experiment was to determine if high molecular weight DNA and DNA nanoparticulates (nuclei, nucleosomes, etc.) from disrupted white cells in a settled blood sample could be isolated and detected by DEP. If so, this could serve as a model for analyzing CFC-DNA in blood. Both normal and disrupted settled blood samples with SYBR Green I Dye added were used in these experiments. Settled blood was used in order to allow visualization of the high- and low-field DEP regions during the experiment, which is not possible with whole blood due to the high volume of cells. Figure 2.2e shows repulsion of red blood cells into the n-DEP low-field regions, while little to no fluorescent signal is seen in the p-DEP high-field regions on the microelectrodes in Figure 2.2f. Figure 2.2g shows fewer cells in the low-field regions as most of them have been disrupted during vortexing. Figure 2.2h shows the green fluorescent image of the disrupted sample after DEP, where considerable fluorescent signal is now concentrated in the p-DEP high-field regions around the microelectrodes compared to the normal settled blood (Figure 2.2f), indicating that CFC-DNA has been released from blood cells and collected on the microelectrodes. While the disrupted cells and cell fragments have a different frequency response than that of normal cells, some of the larger fragments still undergo negative DEP at 10 kHz.

2.3.3 DEP with Low Molecular Weight DNA in Buffer

Because cancer related CFC-DNA is generally of much higher molecular weight than non-disease related apoptotic DNA [21, 82], it was important to determine if low

molecular weight DNA is also concentrated in p-DEP high-field regions. To do this, a DEP experiment was carried out using 10 μm polystyrene beads and a fluorescent single-stranded 23-mer oligonucleotide (5'-Cy3- ATT CCA TTC GAT TCC ATT CGA TC-3') in 0.5x PBS. Figures 2.3a and 2.3b show the bright field and red fluorescence images of the microarray before the addition of fluorescent LMW-DNA. A 20 μl sample containing both 10 μm particles and 345 ng/ml of the fluorescent LMW-DNA oligonucleotide in 0.5x PBS was added, seen in Figures 2.3c and 2.3d, and the DEP field was applied for at 10 kHz and 20 $V_{\text{p-p}}$ for 10 minutes.

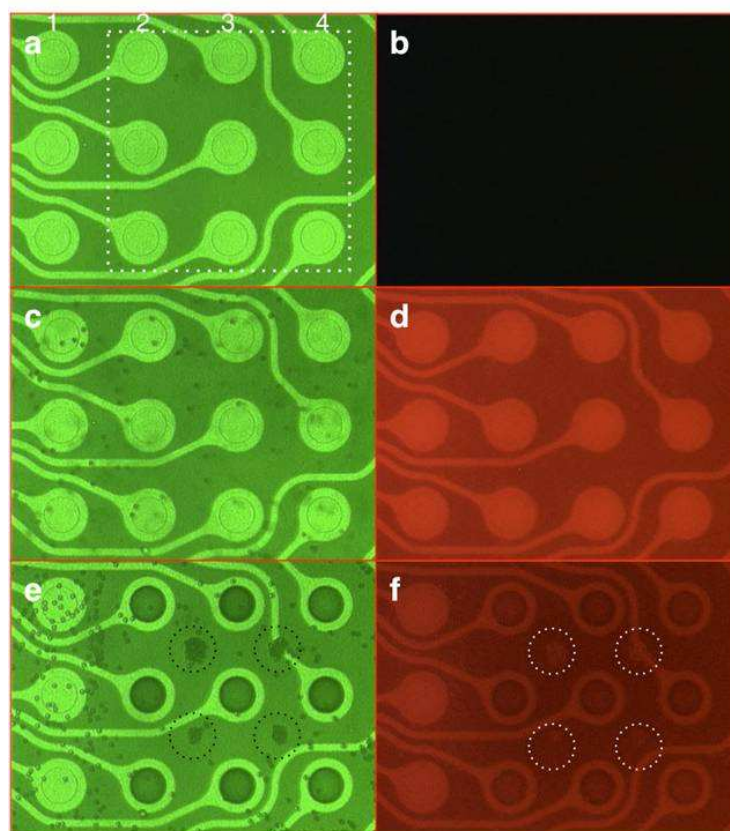


Figure 2.3: DEP of fluorescent low molecular weight (LMW) DNA in buffer (7.6 mS/cm). (a) Bright field and (b) red fluorescence images of the microarray before the sample is added. (c) Bright field and (d) red fluorescence images after a 20 μl sample containing both 10 μm particles and 345 ng/ml of a fluorescent LMW-DNA oligonucleotide in 0.5x PBS was added. (e) Bright field and (f) red fluorescence images after the DEP field was applied at 10 kHz and 20 $V_{\text{p-p}}$ for 10 minutes, showing no fluorescent LMW-DNA being concentrated in the DEP high-field regions.

The 10 μm beads mimic the response of blood cells under these conditions and serve to illustrate the DEP field geometry. Figure 2.3e shows that the 10 μm particles have been concentrated into the n-DEP low-field regions, however Figure 2.3f shows no fluorescent signal appears in the p-DEP high-field regions on or around the microelectrodes. Thus, even at very high concentrations little if any LMW-DNA is collected.

2.3.4 Post Staining DNA after DEP

In principle, it should not be necessary to pre-stain or fluorescently label DNA before the DEP field is applied. Nevertheless, we thought it was important to demonstrate that DNA can first be concentrated into p-DEP high-field regions and then post-stained with fluorescent dyes. For this DEP experiment the sample contained both 10 μm particles and 800 ng/ml of HMW-DNA (unstained) in 0.5x PBS. After the sample is added to the array, a random distribution of the 10 μm particles is seen over the microarray in Figure 2.4a and 2.4b (the 10 μm particles have some intrinsic green fluorescence). The bright field image (Figure 2.4c) and the fluorescent image (Figure 2.4d) show that the 10 μm particles have now been concentrated into the n-DEP low-field regions. However, no green fluorescent signal is observed in the p-DEP high-field regions on or around the microelectrodes. With the DEP field still active, a solution of OliGreen fluorescent dye was then flushed over the microarray. Figure 2.4e shows that some of the 10 μm particles have been removed by the fluidic wash, while Figure 2.4f now shows green fluorescent signal in the p-DEP high-field regions. This clearly

demonstrates that un-stained HMW-DNA captured during the DEP process can be post-stained with a fluorescent dye.

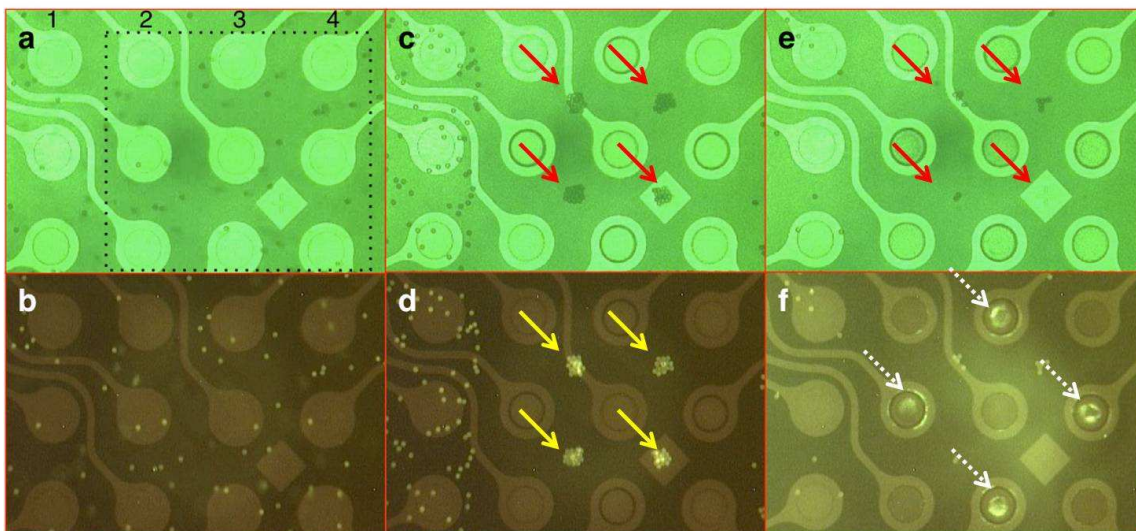


Figure 2.4: Post staining of DNA after DEP. (a) and (b) show the microarray in bright field and green fluorescence after a 20 μl sample containing both 10 μm particles and 800 ng/ml of unstained HMW-DNA in 0.5x PBS (7.6 mS/cm) was added, but before the DEP field has been applied. (c) and (d) show the bright field and green fluorescence images after the DEP field was applied at 10 kHz and 20 V_{p-p} for 10 minutes. The 10 μm particles are now concentrated in the low-field regions. (e) and (f) show the bright field and green fluorescence images after a solution containing OliGreen fluorescent dye was flushed over the microarray at a rate of 40 μl per minute for 5 minutes. The fluorescent stained HMW-DNA is now visible in the DEP high-field regions. The square feature visible in the lower right portion of the images is an alignment mark in the platinum layer.

2.3.5 DEP Detection Level for Nanoparticles in Blood

With regard to using DEP for monitoring the level of drug delivery nanoparticles in blood, DEP experiments were carried out to determine a lower limit for detecting fluorescent nanoparticles directly in whole blood. As previously explained, the dosage for Abraxane drug delivery nanoparticles is approximately 7.5×10^{10} particles/ml blood [79]. Figures 2.5a, 2.5b and 2.5c show the bright field image for the three different concentrations of nanoparticles, where the blood cells can be seen moving away from the

activated microelectrodes into the low-field regions. Figures 2.5d, 2.5e and 2.5f now show the red fluorescent images of the three different concentrations of nanoparticles after DEP and the microarray was washed 3 times with 0.5x PBS.

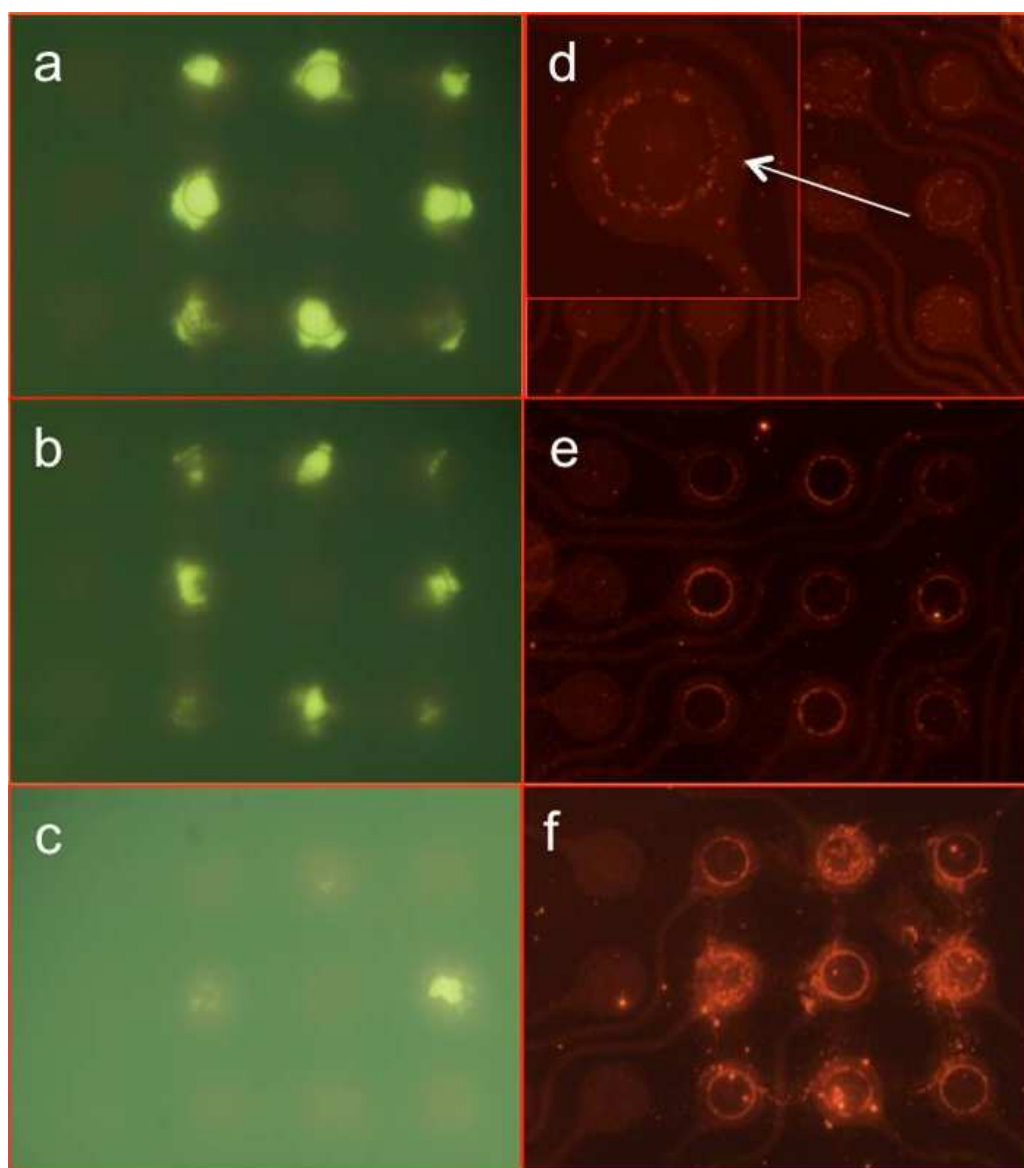


Figure 2.5: Detection levels for nanoparticles in buffy coat blood (8.6 mS/cm). (a), (b) and (c) Bright field images for the three different nanoparticle concentrations at 9.5×10^9 , 9.5×10^{10} and 9.5×10^{11} particles/ml, respectively, where the blood cells are seen moving away from the activated microelectrodes. (d), (e) and (f) Red fluorescent images of the three different concentrations of nanoparticles concentrated in the high-field regions after the microarray was washed with 0.5x PBS. The enlargement of one of the microelectrodes (d) showing the nanoparticles are detectable at the lowest concentration level of 9.5×10^9 particles/ml.

Figure 2.5d shows the fluorescent image (with enlargement) for the lowest concentration (9.5×10^9 particles/ml), with fluorescence from the nanoparticles concentrated in the p-DEP high-field regions around the microelectrodes. Figure 2.5e and 2.5f show increased fluorescent signals due to the high concentrations of nanoparticles. These results demonstrate the intrinsic ability of DEP to detect nanoparticles under high-conductance conditions in blood at dosage levels now used for drug delivery nanoparticles.

2.4 Discussion

This DEP study has demonstrated the rapid isolation and detection of both single-stranded and double-stranded HMW-DNA and 40 nm nanoparticles directly from whole blood and buffy coat blood samples. More specifically, the study shows the separation and concentration of the DNA and nanoparticles into the p-DEP high-field regions while the blood cells are isolated into the n-DEP low-field regions. The high molecular weight DNA fragments and nanoparticles could be easily detected at clinically relevant levels of 260 ng/ml for ss-HMW-DNA and 9.5×10^9 particles/ml for 40 nm nanoparticles. These detection levels are suitable for measuring cancer related CFC-DNA biomarkers [21, 26, 27] and for monitoring drug delivery nanoparticles [79]. Additionally, the DEP results were obtained using relatively small volumes (20 μ l) requiring no sample preparation for whole blood, and only minimal sample processing for settled blood or buffy coat blood. The disrupted blood experiments were not only informative, but could also prove to be an

excellent model for obtaining CFC-DNA, CFC-RNA and other cellular nanoparticulates and organelles (mitochondria, lysosomes, etc.). Thus, our DEP method may be an ideal way to study the true nature of CFC-DNA, as well as that of other potential cellular nanoparticulate biomarkers. Further DEP experiments demonstrated that very low molecular weight DNA appears not to concentrate into the high-field regions. This could be beneficial in that it shows, at least at the DEP AC voltages and frequencies being used, that the process is more selective for high molecular weight DNA and DNA nanoparticulates. Thus, DEP may have a selective advantage for the isolation of cancer and other disease-related CFC-DNA, rather than the lower molecular weight apoptotic DNA normally found in blood. A final advantage for this DEP method is the fact that isolated targets do not have to be labeled. In addition to specific fluorescent or colorimetric stains, numerous other molecular biology techniques including PCR, *in situ* hybridization and immunochemistry detection can be easily carried out in the same sample chamber where isolation of the entities has occurred. It should also be possible to use the DEP process to isolate and prepare DNA for sequencing applications. Taken together, the results of this study support the enormous potential of DEP as a “seamless sample-to-answer” technique for the rapid detection of CFC-DNA and nanoparticles directly from blood and other complex biological samples.

Chapter 2, in part, is published as the following manuscript: Avery Sonnenberg, Jennifer Y. Marciniak, Alexander P. Hsiao, Rajaram Krishnan, Michael J. Heller. Dielectrophoretic (DEP) Isolation of DNA and Nanoparticles from Blood. Electrophoresis. 2012, 33(16), 2482-90

The author of this dissertation is the primary author on this publication.

CHAPTER THREE:

Dielectrophoretic Isolation and Detection of CFC-DNA Nanoparticle Biomarkers and Virus from Blood

3.1 Introduction

The rapid isolation and detection of nanoparticulate biomarkers such as cell free circulating (CFC) DNA directly from blood and other clinical samples is a major challenge for many molecular diagnostic applications. CFC-DNA is now considered an important biomarker for early detection of cancer [20-23], residual disease [9, 24] and for monitoring chemotherapy[25]. In addition to CFC-DNA, challenges also exist for the rapid detection of many other important nanoparticulate biomarkers including exosomes/CFC-RNA [83, 84], mitochondria [85], viral pathogens [86] and drug delivery nanoparticles [30-32, 87].

AC dielectrophoresis (DEP) has been known to provide effective separations of cells, nanoparticles, and biomolecules [35-41]. However, until recently DEP techniques had remained impractical for general use with high conductance solutions (~ 10 mS/cm) and with complex biological samples such as whole blood [38-41]. As examples, DEP work on separating bacteria from blood [37, 40], separations of cells [41, 50, 51], virus [52], polystyrene nanoparticles [53-57], DNA [58-60] and proteins [61, 62] all required sample dilution and low-conductance conditions (below 1 mS/cm). While some progress has been made on carrying out DEP under high conductance conditions, this work has been generally limited to separations of cells and micron-size entities by negative DEP forces using hybrid DEP devices [50, 63-67]. Recently we have developed DEP microarray devices and methods that allow nanoscale entities including high molecular weight (HMW) DNA and nanoparticles to be separated and detected from high conductance buffer solutions [68-70], as well as from whole blood samples [87]. Such

DEP microarrays could be operated at up to 20 volts peak-to-peak (pk-pk) at 10 kHz in buffers and biological samples with conductances of more than 10 mS/cm. Under these DEP conditions, HMW-DNA and nanoparticle entities which are more polarizable than the surrounding media experience positive DEP (p-DEP) and are concentrated into the DEP high-field regions over the microelectrodes, while micron-size or larger particles (blood cells) which are less polarizable experience negative DEP (n-DEP) and are concentrated into the DEP low-field regions between the microelectrodes. The polarizability of these entities depends on the solution in which they are suspended as well as the frequency of the applied non-uniform electric, a relationship which is described by the Clausius-Mossoti Factor (CMF). At a given frequency, the sign of the CMF (positive or negative) indicates whether an entity will experience p-DEP or n-DEP. Any transition between a positive and negative CMF is referred to as a crossover frequency. Choosing to apply an non-uniform electric field with a frequency at which one entity has a positive CMF and another has a negative CMF allows the two entities to be separated with DEP[39]. After the DEP separation is completed, a simple fluidic wash removes the larger particles (cells) in the low-field regions, while the nanoparticles remain concentrated in the high-field regions. Generally, proteins and lower molecular weight biomolecules are not affected by the DEP fields and are also removed by the washing procedure. This study now demonstrates the rapid DEP isolation and fluorescent detection of CFC-DNA from whole blood samples obtained from Chronic Lymphocytic Leukemia (CLL) patients, T7 bacteriophage virus from blood samples and mitochondria

from biological buffer solutions. This study also demonstrates the isolation and detection of low levels of HMW-DNA from serum samples using new DEP microarray devices.

3.2 Methods

3.2.1 DEP Devices and Methods

The devices used to create the asymmetric DEP electric field were the Nanochip 100 site microelectronic arrays (Nanogen) which have 100 individually-addressable platinum microelectrodes, each 80 μm in diameter with a spacing of 200 μm between electrode centers. These microarrays are coated with a 10 μm thick polyacrylamide hydrogel layer. The microarray is contained within a fluidic chamber with a glass cover and has a volume of 20 μL [68-70, 87]. These 100 site microelectrode arrays were used to carry out the CLL, T7 bacteriophage and mitochondria DEP experiments. New prototype DEP microarray devices designed by Biological Dynamics containing 1000 platinum microelectrodes (80 μm diameter) were used to carry out DEP isolation of HMW-DNA from human serum experiments. These microarrays are coated with a 10 μm layer of a polyHEMA hydrogel and have an 80 μL sample volume. In studies with these new DEP devices all 1000 microelectrodes on the microarray were activated.

3.2.2 Experimental Setup and Imaging

The microelectrode arrays were connected to a bank of three-position switches allowing each electrode to be disconnected or connected to the positive or negative

terminal of an Agilent 33120A Arbitrary Function Generator. A subset of nine electrodes in a three by three group was used for each experiment. Electrodes were connected in a “checkerboard” pattern as seen in Figure 3.1A and 3.1B, which results in the DEP force vector field shown in Figure 3.1C which was simulated using COMSOL Multiphysics software (v4.0a). A sinusoidal waveform was used at a frequency of 10 kHz at 20 V peak-to-peak (pk-pk) amplitude. The system was visualized using an Olympus BX41 upright epifluorescent microscope with filters for FITC (520 nm) and Texas Red (650 nm). Both bright field and fluorescent images were captured using an Olympus 16-bit (per channel) 5-megapixel RGB Bayer filter CCD camera.

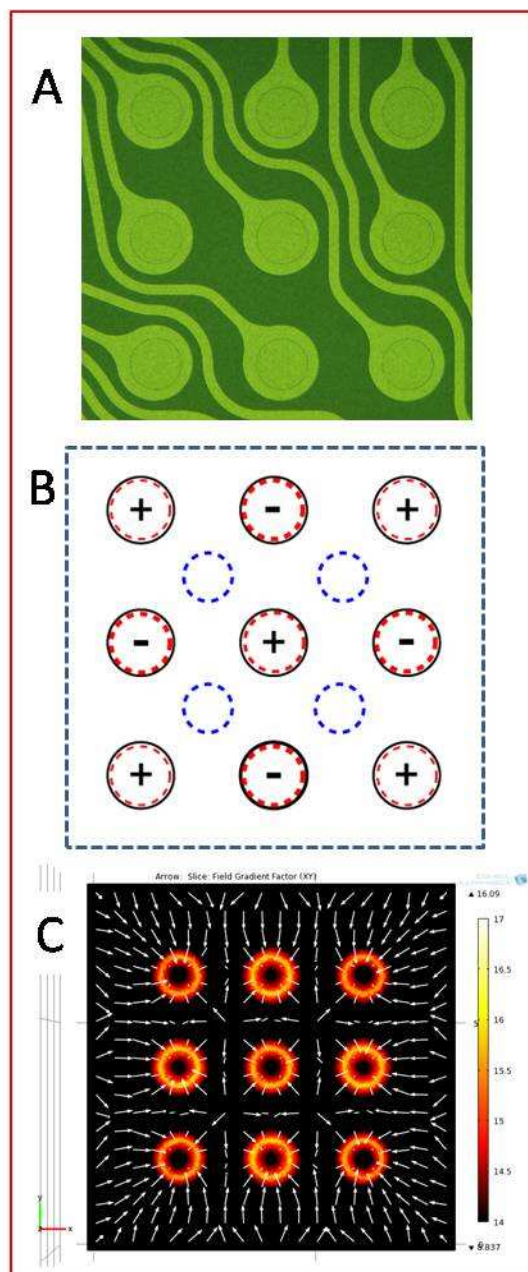


Figure 3.1: DEP Force Vector Diagram. (A) Nine of the 80 μm diameter circular microelectrodes in a 3x3 section of the 100 site microarray used to carry out DEP experiments. (B) The checkerboard pattern used to create the DEP AC field asymmetry, which results in DEP high-field regions on the microelectrodes (red dashed circles) and DEP low-field regions between the microelectrodes (blue dashed circles). (C) The resultant DEP force vector field pattern as modeled with COMSOL Multiphysics (CMF=1, particle diameter=100 nm).

3.2.3 Whole Blood Samples from CLL Patients

Whole blood samples were collected from CLL patients and healthy volunteers in accordance with the policies of the Institutional Review Board of the University of California, San Diego under IRB protocol #070643. The evacuated blood collection tubes contained lithium heparin (Becton Dickinson). SYBR Green I Dye (Invitrogen) was diluted from 10,000x stock to a concentration of 100x in 1x TBE (Fisher Scientific). 10 μL of the 100x SYBR Green I solution was added to 190 μL of blood from each CLL patient or from samples obtained from healthy individuals, for a final dye concentration of 5x. The sample was then allowed to incubate at room temperature for 15 minutes before 20 μL were loaded onto the microarray. The DEP field was applied at 10 kHz and 20 $V_{\text{pk-pk}}$ for 15 minutes. The microarray was washed three times with 0.5x PBS and then fluorescent images were taken.

3.2.4 Virus Preparation

T7 Bacteriophage were grown to express mCherry fluorescent protein using Novagen's T7Select® Phage Display System. The titer of the isolated virus was 10^{10} mL^{-1} , determined by plating dilutions of phage and counting the resulting plaques. 10 μL of the isolated virus solution was added to 190 μL of settled blood and gently mixed before being added to the DEP microelectrode array. The function generator was set to output a 10 kHz sinusoid at 14 $V_{\text{pk-pk}}$. The DEP field was applied for 20 minutes, the microarray was then washed three times with 0.5x PBS and then fluorescent images were taken.

3.2.5 Mitochondria Preparation

Mitochondria from Jurkat cells were first stained using the MitoTracker Red CMXRos (catalog number M-7512) from Invitrogen and then isolated using a Mitochondria Isolation Kit from Sigma (catalog number MITOISO2). Lyophilized dye was dissolved in dimethylsulfoxide (DMSO) to a concentration of 1 mM. Suspension cells were centrifuged (1000 rpm for 10 minutes) and resuspended in 37 °C RPMI 1640 (catalog number: 11875093 from Invitrogen) containing 10% FBS and 500 nM of MitoTracker Red. The cells were then incubated for 45 minutes at 37 °C with 5% CO₂ before repelleting for mitochondria isolation. After the cells were stained, they were centrifuged at 1000xg for 5 minutes (All centrifugation steps were performed at 4 °C). After another wash with PBS and centrifugation, the cell pellet was resuspended in 0.75 mL Lysis Buffer and incubated on ice. After the 5-minute incubation, 1.5 mL of Extraction Buffer was added and then centrifuged at 1000xg for 10 minutes. The supernatant was transferred to a fresh tube and centrifuged at 3500xg for 10 minutes. This supernatant was removed and the remaining pellet was resuspended in 200 µL storage buffer. The field applied was a 10 kHz sinusoid at 50 V_{pk-pk} for 30 minutes.

3.2.6 Buffers, Blood Samples, and Conductivity Measurements

Tris-Borate-EDTA (1x TBE) buffer solution was obtained from Fisher Scientific. Dulbecco's Phosphate Buffer Saline (1x PBS) solution was obtained from Invitrogen (Carlsbad, CA) and diluted to 0.5x. Blood for the controls and disrupted blood experiments was collected from a human adult male volunteer in accordance with the

policies of the Institutional Review Board of the University of California, San Diego under IRB protocol #070643. The collection tubes contained lithium heparin (Becton Dickinson). For “settled blood” experiments, the heparinized blood was allowed to settle for 20-30 minutes and 200-400 μL of supernatant was removed. This supernatant is primarily plasma, but still contains some red and white blood cells. To disrupt settled blood, about 10 mg of porous glass microbeads were added to 100 μL of settled blood, which was then agitated by vortexing for 1 minute. This procedure causes disruption of many of the cells, releasing high molecular weight DNA (nuclei, nucleosomes, DNA nanoparticulates) from white blood cells. The DEP field was applied to the settled blood samples at 10 kHz and $20 V_{\text{pk-pk}}$ for 15 minutes. Conductivity measurements were made with a Horiba B-173 Compact Conductivity Meter. Conductivities were measured to be 7.4 mS/cm for whole blood, 11.5 mS/cm for settled blood, and 1.46 mS/cm for mitochondria storage buffer.

3.3 Results

Our earlier work has demonstrated the ability to use DEP devices and techniques to separate and detect both HMW-DNA and nanoparticles from high conductance buffers [68-70]. More recently, the rapid isolation and detection of HMW-DNA and nanoparticles directly from whole blood samples has been demonstrated at clinically relevant levels [80, 81, 87]. This new study further demonstrates the potential clinical relevance of this DEP technology by now showing: (1) the rapid isolation and detection of SYBR Green stained DNA materials from 20 μL whole blood samples from Chronic

Lymphocytic Leukemia (CLL) patients; (2) the rapid isolation and detection T7 (*mCherry*) bacteriophage from whole human blood; (3) the rapid isolation and detection of human mitochondria from biological storage buffer; and (4) the use of new DEP microarray devices for the rapid isolation and detection of low levels of HMW-DNA (8-16 ng/mL) in serum samples.

3.3.1 DEP Separation and Detection of CFC-DNA from CLL Patient

Blood Samples

Chronic Lymphocytic Leukemia (CLL) has been considered a homogeneous disease of immature, immune-incompetent, minimally self-renewing B cells, which accumulate constantly because of a faulty apoptotic mechanism. CLL is now viewed as originating from antigen-stimulated mature B lymphocytes, which either avoid death through the intercession of external signals or die by apoptosis, only to be replenished by proliferating precursor cells [88]. With regard to CLL disease diagnostics, the Immunoglobulin V_H (IGHV) somatic mutation status has been shown to be of value in predicting outcomes for CLL patients [89-91]. To obtain this information, a typical protocol involves the isolation of peripheral blood mononuclear cells (PBMCs) from a CLL patient, extraction of DNA, PCR amplification of the IGHV region, sizing on an agarose gel, excision and extraction of the amplified band, and sequencing of the resulting DNA. The objective of this study is to determine if DEP can be used to rapidly isolate CLL related CFC-DNA directly from a small blood sample. For these studies, fresh blood samples from CLL patients were obtained from the UCSD Moores Cancer

Center (Dr. Thomas Kipps Lab). Samples were usually run within two to four hours of the blood draw. Figure 3.2 shows results for DEP isolation and fluorescent detection of CFC-DNA from: (A), (B), (C) normal blood samples; (D), (E), (F), (G), (H) five different CLL patient blood samples; and (I) a normal “disrupted” settled blood sample. Normal blood samples, such as shown in Figure 3.2A-3.2C, generally do not show any significant collection of SYBR Green stained fluorescent DNA in the DEP high-field areas. In contrast, all the CLL patient samples (Figures 3.2D-3.2H) show significant amounts of SYBR Green stained DNA in the DEP high-field areas on the nine activated microelectrodes. The normal “disrupted” settled blood sample (Figure 3.2I) also shows significant collection of SYBR Green stained fluorescent DNA in the DEP high-field areas of the nine activated microelectrodes. Since the “disrupted” buffy coat blood represents a good model for HMW/CFC-DNA [87] there is high confidence that the fluorescent stained materials in the three CLL samples is CFC-DNA. Qualitatively, it is estimated from our earlier DEP work [87] and from results shown in Figure 3.5, that these particular CLL samples contain more than 50 ng/mL of CFC-DNA.

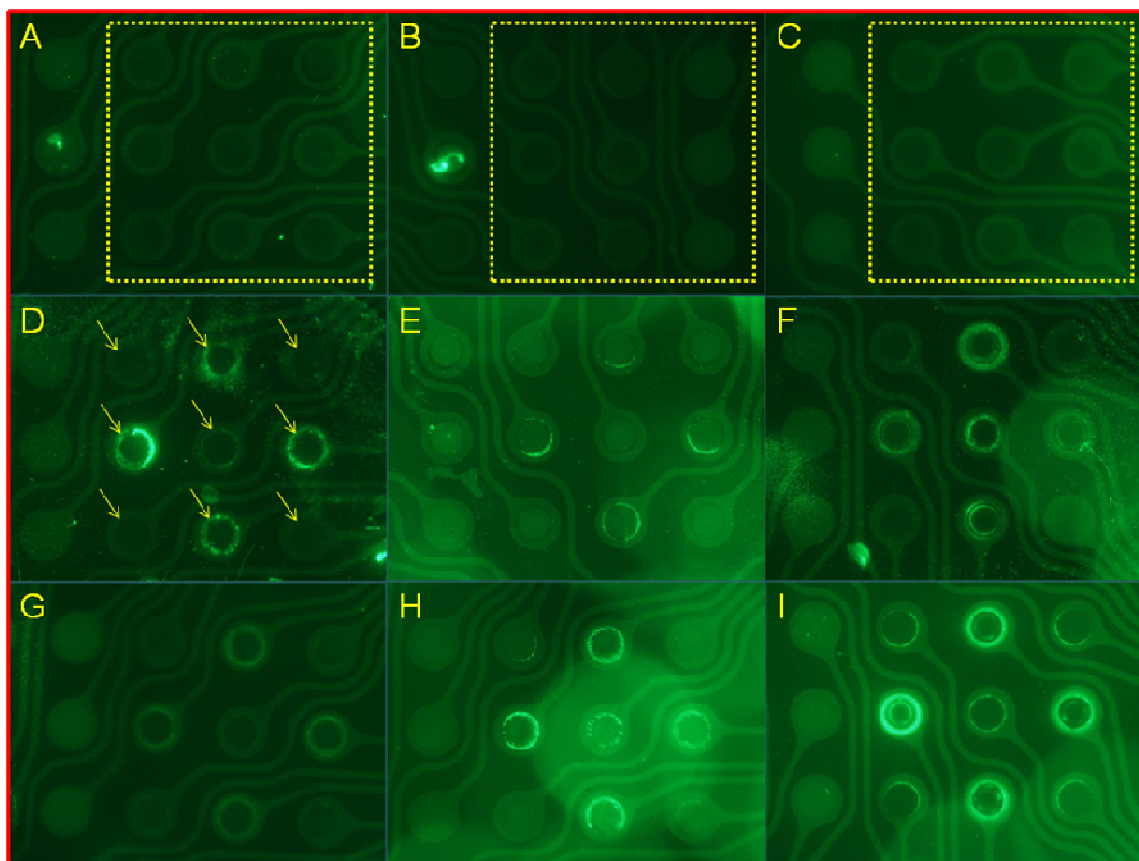


Figure 3.2: DEP Isolation and Fluorescent Detection of CFC-DNA in Blood Samples from CLL Patients. About 20 μL of whole blood was applied to the DEP microarray device. An AC field was then applied at 10 kHz and 20 $V_{\text{pk-pk}}$ to the nine microelectrodes in columns 2, 3, and 4 (yellow dotted area) for 15 minutes. No voltage was applied to the three microelectrodes in column 1 (left side), which serve as a negative control. The DEP microarray was washed three times with 0.5x PBS after which epifluorescent microscope imaging detection was carried out. Figures 2 (A), (B), and (C) show the results for blood samples from three normal (non-CLL) individuals, Figures 2 (D), (E), (F), (G), and (H) show the results for five different CLL patient blood samples, and (I) shows the result for a normal “disrupted” buffy coat blood sample. The normal blood samples (A), (B), and (C) show no significant collection of SYBR Green stained fluorescent DNA in the DEP high-field areas. All five CLL patient samples (D), (E), (F), (G) and (H) show relatively significant amounts of SYBR Green stained DNA in the DEP high-field areas on the nine activated microelectrodes. The normal “disrupted” buffy coat sample (I) also shows significant collection of SYBR Green stained fluorescent DNA in the DEP high-field areas of the nine activated microelectrodes. It should be pointed out that the fluorescent signal often appears significantly higher for the middle microelectrodes of columns 2 and 4, and the upper and lower microelectrodes of column 3, due to greater electric field gradient at these locations. In all cases, the three un-activated microelectrodes in column 1 show no fluorescence.

3.3.2 DEP Isolation and Detection of T7 (*mCherry*) Bacteriophage from Blood

All our previous DEP work has involved the isolation and detection of either HMW-DNA or fluorescent polystyrene nanoparticles from blood and buffer solutions. In order to further investigate the different nanoparticulate entities that can be separated from blood, a fluorescent T7 (*mCherry*) bacteriophage was selected as good (safe) model for virus detection. The T7 bacteriophage is capable of infecting many types of bacteria, including most strains of *Escherichia coli*. The virus has complex structural symmetry, with a spherical protein capsid with an inner diameter of 55 nm and a tail 19 nm in diameter and 28.5 nm long attached to the capsid. The T7 bacteriophage DNA is enclosed within the capsid structure. In this study, DEP isolation and detection was carried out on a 20 μL sample of blood containing fluorescent T7 (*mCherry*) Bacteriophage at a concentration of about 5×10^8 virus/mL. After 20 minutes of applying the AC field at 10 kHz and 14 $V_{\text{pk-pk}}$ and three washes with 0.5x PBS buffer, the fluorescent image in Figure 3.3B shows considerable concentration of the T7 (*mCherry*) Bacteriophage in the DEP high-field areas relative to the (no virus) negative control in Figure 3.3A. While this is only a qualitative example demonstrating the DEP separation of virus directly from blood, the actual number of virus seen on one microelectrode structure is estimated to be about 5×10^5 .

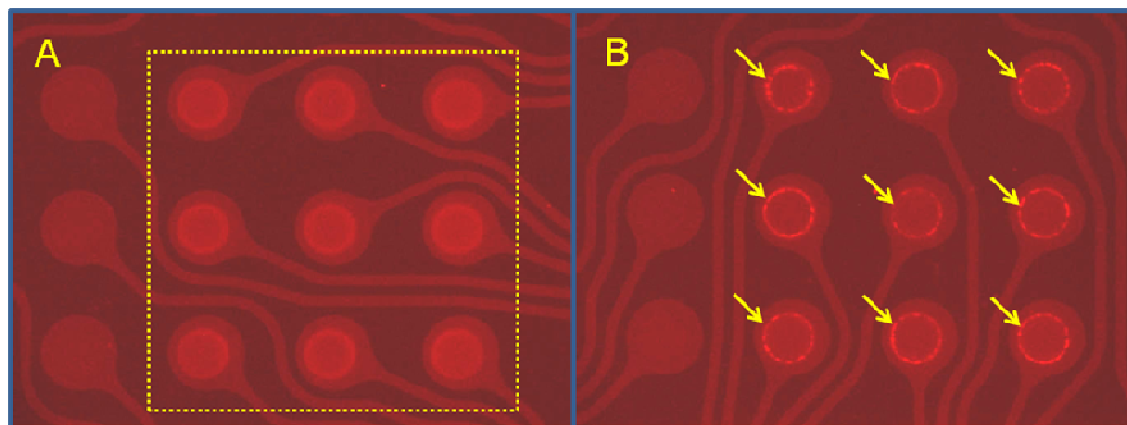


Figure 3.3: DEP Separation of T7 (*mCherry*) Bacteriophage in Blood. 20 μL samples of whole blood without T7 (*mCherry*) Bacteriophage (A), and with T7 (*mCherry*) Bacteriophage (B) were applied to the DEP microarray devices. An AC field was then applied to each sample at 10 kHz and 14 $V_{\text{pk-pk}}$ to the nine microelectrodes in columns 2, 3, and 4 (yellow dotted area) for 20 minutes. No voltage was applied to the three microelectrodes in column 1 (left side), which serve as a negative control. The DEP microarrays were washed three times with 0.5x PBS after which epifluorescent microscope imaging detection was carried out. Figure 3B shows intense red fluorescence from the concentrated T7 (*mCherry*) Bacteriophage in the DEP high-field areas (yellow arrows), relative to the image of the blood sample without T7 (*mCherry*) Bacteriophage (Figure 3.3A).

3.3.3 DEP Isolation and Detection of Mitochondria from Biological

Buffer

Again, all our previous DEP work has been focused on the isolation and detection of HMW-DNA and fluorescent polystyrene nanoparticles from blood and buffer solutions. This study now involves the isolation and detection of human (Jurkat Cell) mitochondria from a biological buffer with a conductance of ~ 1.5 mS/cm. These particular mitochondria are approximately 500-600 nm in size with an outer membrane coat. For this study a 20 μL sample of MitoTracker Red fluorescent stained mitochondria in storage buffer was applied to the DEP microarray device. DEP was carried out at 10 kHz and 50 $V_{\text{pk-pk}}$ for 30 minutes. Figure 3.4B shows intense red fluorescence from the MitoTracker Red fluorescent stained mitochondria which have become highly

concentrated in the DEP high-field areas. This study was meant to be a qualitative example of using DEP to isolate and detect another important cellular nanoparticulate (organelle) which has potential to be a clinical diagnostic biomarker.

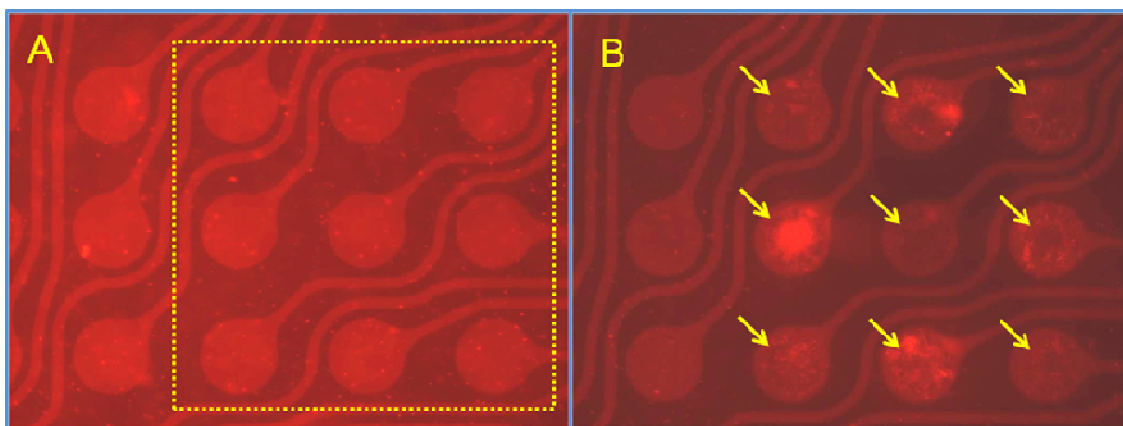


Figure 3.4: DEP of Fluorescent Stained Mitochondria. A 20 μL sample MitoTracker Red fluorescent stained mitochondria in storage buffer was applied to the DEP microarray device. An AC field was then applied to each sample at 10 kHz and 50 $V_{\text{pk-pk}}$ to the nine microelectrodes in columns 2, 3, and 4 (yellow dotted area) for 30 minutes. No voltage was applied to the three microelectrodes in column 1 (left side), which serve as a negative control. The DEP microarrays were washed three times with 0.5x PBS after which epifluorescent microscope imaging detection was carried out. Figure 3.4A shows the microarray before the DEP field was applied, and Figure 3.4B shows the microarray after the DEP field was applied and washed with 0.5x PBS buffer. Figure 3.4B now shows intense red fluorescence from the MitoTracker Red fluorescent stained mitochondria concentrated in the DEP high-field areas (yellow arrows).

3.3.4 Isolation and Detection of HMW-DNA from Serum Using New DEP Microarray Devices

New prototype DEP microarray devices were used to carry out the isolation and detection of HMW-DNA in serum. In these experiments, DEP was carried out on eight samples of a dilution series where the concentration of HMW-DNA in serum ranged from 0 ng/mL to 500 ng/mL. The AC field was applied to each sample at 10 kHz and 7 $V_{\text{pk-pk}}$ for 15 minutes. Figure 3.5A shows that detectable fluorescence was observed in the

DEP high-field areas on the microelectrodes for all the HMW-DNA containing samples, including the very low concentrations of 8 ng/mL and 16 ng/mL. Figure 3.5B shows an enlarged image of the 0 ng/mL negative control, and Figure 3.5C shows the enlarged image for the 250 ng/mL sample. Due to incomplete removal of the silicon dioxide layer, occasionally an electrode will not collect DNA. The ability to detect these low levels of HMW-DNA in human serum (conductance of ~10-11 mS/cm) will be important for future diagnostic applications. For example, cancer related CFC-DNA occurs in the blood at levels from 0 to over 1000 ng/mL, with an average value of about 180 ng/mL [21, 23, 26, 27]. Thus, the ability to detect levels at the 10ng/mL means the technology might be used for early cancer diagnostics.

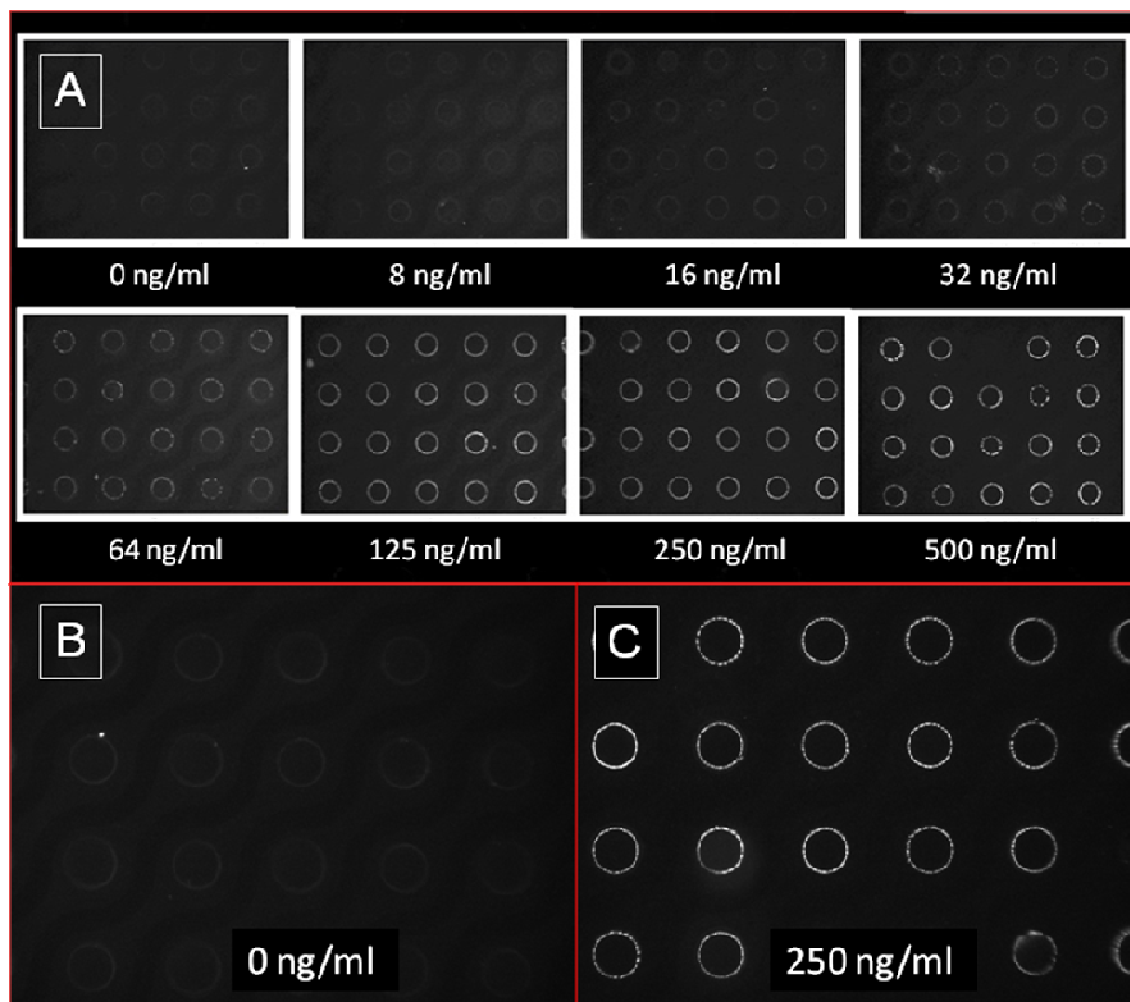


Figure 3.5: Detection of HMW-DNA in Serum Using New DEP Microarray Devices. New prototype DEP microarray devices were used to carry out the isolation and detection of HMW-DNA in serum. In these experiments, DEP was carried out on eight samples of a dilution series where the concentration of HMW-DNA in serum ranged from 0 ng/mL to 500 ng/mL. An AC field was then applied to each sample at 10 kHz and 7 V_{pk-pk} for 15 minutes. The DEP microarrays were washed three times with 0.5x PBS after which epifluorescent microscope imaging detection was carried out. Figure 3.5A shows the results for the series where detectable fluorescence is observed in the DEP high-field areas on the microelectrodes for all HMW-DNA containing samples including the lowest concentrations of 8 ng/mL and 16 ng/mL. Figure 3.5B shows an enlarged image of the 0 ng/mL negative control and Figure 3.5C shows the enlarged image for the 250 ng/mL sample.

3.4 Discussion

The ability to rapidly isolate and detect cancer and other disease related CFC-DNA, cellular nanoparticulates (exosomes, mitochondria, etc.) and virus directly in blood, plasma, serum and biological buffers will be important for many future clinical diagnostic applications. This study demonstrates the potential clinical relevance of this DEP technology by showing the rapid isolation and detection of SYBR Green stained CFC-DNA from 20 μ L whole blood samples from Chronic Lymphocytic Leukemia (CLL) patients. The isolation and detection of T7 (*mCherry*) bacteriophage from whole human blood is an important result that demonstrates that the DEP technology has potential for clinical applications related to virus and other pathogen detection. With regard to other important cellular nanoparticulate (organelle) biomarkers, the rapid isolation and detection of human mitochondria from biological storage buffer shows potential for related clinical and research applications. Finally, the results from the new DEP microarray devices demonstrating the rapid detection of low levels of HMW-DNA in serum samples show promise for early cancer diagnostics. Overall the results of this study support the enormous potential of DEP as a “seamless sample-to-answer” technique for the rapid detection of CFC-DNA and nanoparticulate biomarkers directly from blood and other complex biological samples.

Chapter 3, in part, is a reprint of the following manuscript: Avery Sonnenberg, Jennifer Y. Marciniak, James McCanna, Rajaram Krishnan, Laura Rassenti, Thomas J. Kipps and Michael J. Heller. *Dielectrophoretic Isolation and Detection of CFC-DNA Nanoparticulate Biomarkers and Virus from Blood*. *Electrophoresis*. 2013, 34(7), 1076-84.

The author of this dissertation is the primary author of this manuscript.

CHAPTER FOUR:

Isolation and Detection of Cell Free Circulating DNA Directly from Chronic Lymphocytic Leukemia Patient Blood

4.1 Introduction

Circulating cell-free (CFC) DNA is now considered an important biomarker for early detection of cancer [20-23], residual disease [9, 24], monitoring chemotherapy [25] and other aspects of cancer management. The isolation of CFC-DNA from plasma as a “liquid biopsy” may begin replacing more invasive tissue biopsies as a means to detect and analyze cancer mutations [6, 26-28]. Unfortunately, conventional techniques for the isolation of CFC-DNA from plasma require a relatively time consuming and complex process which would rule out their use for point of care (POC) diagnostic applications. Other limitations of these conventional processes include: (1) the procedures generally require starting with at least one or more milliliters of plasma; (2) obtaining the plasma itself from blood first requires centrifugation and pipetting steps; (3) the large number of manipulations increase the chance for technician errors; (4) the CFC-DNA recovery efficiency decreases as sample size decreases, and as the concentration of CFC-DNA in the sample decreases; (5) CFC-DNA can be degraded by mechanical sheering during the many processing steps; and (6) the time and large number of processing steps add considerable cost to the diagnostic test. In addition to CFC-DNA, other important cancer related biomarkers such as CFC-RNA, exosomes and microvesicles [83, 84] are now also of considerable interest to cancer researchers and clinicians. Procedures for their isolation from plasma also requires relatively long and involved processes.

In the case of hematological cancers such as Chronic Lymphocytic Leukemia (CLL) and Lymphomas, DNA for PCR and sequencing can be obtained directly from the transformed cancer cells [92, 93], as well as from the isolation of CFC-DNA from plasma

[94, 95]. For CLL diagnostics and management, genomic DNA is generally isolated from the peripheral blood mononuclear cells (PBMCs). The PBMCs are usually purified from the CLL patient blood sample by density centrifugation using Ficoll-Hypaque 1077, which is another long and labor intensive process [92]. The specific leukemic B-lymphocyte clone is identified by its unique patient-specific signature of the expressing IGHV gene subgroup [90, 91, 96]. To assess the unique-patient specific-IGHV gene expressed by the CLL B cells, PCR and DNA sequencing are performed on the isolated genomic DNA to determine the mutation status for the expressed IGHV subgroup [92, 93, 97]. Again, like the sample preparation processes for the isolation of CFC-DNA from plasma, obtaining genomic DNA from transformed blood cells is also a very time consuming multi-step process which would not be suitable for point of care (POC) for cancer diagnostics and management.

Promising electrokinetic technologies, in particular dielectrophoresis (DEP) have long been known to provide effective separations of cells, nanoparticles, DNA and other biomolecules [35-41]. However, until recently DEP techniques remained impractical for general use with high conductance solutions (~ 10 mS/cm), which include important clinical samples such as whole blood, plasma and serum [38-41]. In earlier work, sample dilution to low-conductance conditions (below 1 mS/cm) was required before effective DEP separations could be carried out [37, 40, 41, 50-62]. While some progress was made for using DEP under high conductance conditions, these efforts have been generally limited to separations of cells and micron-size entities by negative DEP forces using hybrid electrokinetic devices [50, 63-66]. In general, they still cannot be used with whole

blood samples and more importantly they do not provide efficient isolation of DNA from the sample. Our group has now developed an electrokinetic DEP technology that allows nanoscale entities including high molecular weight (HMW) DNA and nanoparticles to be isolated from high conductance (>10 mS/cm) buffer solutions [68-70], from whole blood samples [87], and most recently CFC-DNA from CLL patient blood samples [98]. In this study, we now show the fluorescent image analyses, PCR and DNA sequencing results for CFC-DNA which was isolated by DEP from 25ul of un-processed CLL patient blood. The PCR and DNA sequencing results for the DEP process are compared to results obtained using conventional sample preparation for isolation of CFC-DNA from one ml of CLL patient plasma, and to “Gold Standard” DNA sequencing results obtained from DNA isolated from the B-lymphocytes of the CLL patients.

4.2 Materials and methods

4.2.1 Sample Acquisition

Blood samples were collected from CLL patients and healthy volunteers (IRB#) in collection tubes containing lithium heparin (BD). For the dielectrophoresis (DEP) experiments, 300 μ L of blood was taken from the top of each undisturbed blood sample within 4-5 hours of collection. The remaining blood was then centrifuged for 10 minutes at 1100 RCF to obtain plasma (Life Technologies Protocols: Plasma and Serum; ProImmune)

4.2.2 Qiagen DNA extraction from plasma

The QIAamp Circulating Nucleic Acid kit was used to extract CFC-DNA from 1 mL of plasma from each of the CLL patients and healthy donors. After addition of a lysing buffer and a 30-minute incubation, the plasma mixture was pulled through a silica binding column with a vacuum manifold, followed by three washing steps on the vacuum manifold. After a 10-minute incubation at 56°C to dry the membrane, the DNA was eluted into the provided elution buffer by centrifugation for 1 minute at 20,000 RCF and stored at 4°C.

4.2.3 DNA extraction on Dielectrophoresis Devices

A 10 x 12 mm silicon die patterned with an interdigitated array of 60 μm diameter platinum microelectrodes on 160 μm center-center pitch was fabricated (Biological Dynamics) as previously described. The array was over-coated with a 200-500 nm thick, porous Poly (2-hydroxyethyl methacrylate) (polyHEMA) hydrogel layer. A 5% polyHEMA solution in ethanol (PolySciences Inc.) was spin-coated at 6000 rpm for 30 seconds using a commercial spin-coater (Brewer Science). The coated chip was then baked at 60°C, in air, for 45 minutes. The chip and its operation are shown below in Figure 4.1.

A printed circuit board (PCB) was attached to the chip using electrically conductive pressure-sensitive adhesive and used to connect the device to a signal generator. The PCB had a center cutout which formed the sides of the fluidic chamber which, when covered with an acrylic window, formed a 25 μL flow cell volume. A

custom-built instrument system (Biological Dynamics, Inc.) provided electronic, optical, and fluidic functions under MATLAB software control.

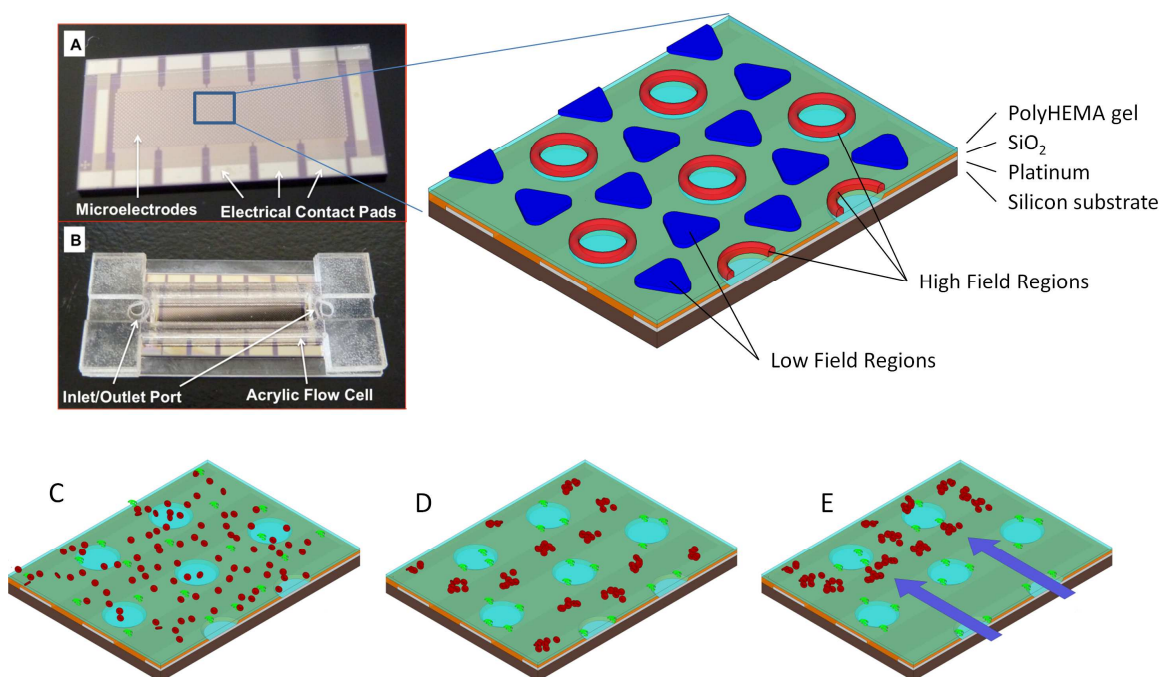


Figure 4.1: DEP microarray device and scheme for isolation of CFC-DNA from blood. (A) shows the DEP microarray device (chip). The enlargement to the right shows the high field regions (positive DEP capture) and low field regions (negative DEP capture). (C) the DEP microarray with whole blood (red circles) containing fluorescent DNA (green dots); (D) application of the AC electric field causing the fluorescent DNA (green dots) to be concentrated in the DEP high-field regions on the microelectrodes, while the blood cells (red circles) move into the DEP low-field regions between the microelectrodes; (E) DEP field turned off and a fluidic wash now removing the blood cells from the microarray and the DNA remaining concentrated in the high-field regions.

Each chip was pre-treated by adding 25 μL of 0.5x PBS (supplier) to the flow cell and applying a 2 V_{RMS} , 5 Hz sinusoidal waveform for 15 seconds to improve the hydrogel porosity. The 0.5x PBS was then removed and 25 μL of blood was added to the flow cell. An 11 Volt peak-to-peak ($V_{\text{p-p}}$), 10 kHz sinusoidal waveform was then applied to the chip for 3 minutes with no fluid flow. The same electric field was maintained while the chip was washed for 5 minutes at 200 $\mu\text{L}/\text{min}$ with 1x TE (supplier). The

electric field was then turned off, allowed captured DNA to diffuse into the 1x TE solution. The 25 μL of fluid was removed within 30 seconds and stored in a microcentrifuge tube. For each CLL patient and healthy donor, this process was repeated 4 times, each time on a new microelectrode device. The 25 μL of eluted sample from each of the 4 runs was combined into a single microcentrifuge tube (100 μL total volume) and stored at 4°C.

In order to visualize collection on the microelectrode array, aliquots of the CLL and healthy donor samples were stained with SYBR Green I fluorescent double-stranded DNA dye (Life Technologies, Carlsbad, CA). 1.5 μL of 100x SYBR Green I was added to 28.5 μL of blood and allowed to incubate at room temperature for 5 minutes. 25 μL of this solution was added to the device and run as described above. After the 3 minute electric field collection and 5 minute washing steps, bright field and fluorescent images of the microelectrode pads were acquired using a CCD camera with a 10x objective, FITC filter, and a 470 nm LED excitation source. DNA with SYBR Green I from these imaged devices was not eluted or used in subsequent analysis.

4.2.4 DNA Quantification

The DNA collected using both the DEP and Qiagen protocols was quantified using Quant-iT PicoGreen (Invitrogen), a double-stranded DNA dye. Each sample was diluted and combined with the PicoGreen reagent, and the resulting fluorescence was measured with a fluorescence plate reader (Tecan).

4.2.5 PCR analysis

In order to verify that the collected DNA was from B-cells, it was amplified by PCR using Phusion High-Fidelity DNA Polymerase (New England Biolabs). The forward primers used were specific to the IGHV1, IGHV3, and IGHV4 regions, and the reverse primer was specific for the JH region. PCR thermal cycling conditions were a 5 minute initial denaturation at 98°C followed by 40 cycles of 98°C denaturation for 15 seconds, 66°C annealing for 15 seconds, and 72°C extension for 15 seconds. The PCR product was then analyzed by gel electrophoresis on a 2% agarose gel containing ethidium bromide (Life Technologies). The gels were viewed in a transilluminator and images were captured using a CCD camera. These images were analyzed in ImageJ to quantify the observed fluorescence. Remaining PCR product was cleaned up with the QIAquick PCR purification kit (Qiagen) and sequenced (Sanger sequencing).

4.3 Results

4.3.1 DEP Isolation of CFC-DNA from Blood

New DEP microarray devices (chips) as shown in Figure 4.1 allow the rapid isolation of CFC-DNA and other nanoparticulate biomarkers (CFC-RNA, exosomes, etc.) directly from a small volume of un-processed blood. As shown in Figure 4.1 (lower image C-E) a blood sample containing the CFC-DNA is put into the DEP microarray chip device and an AC electric field is then applied. At a specific AC frequency and voltage level, the CFC-DNA which is more polarizable than the surrounding media experiences positive DEP (p-DEP) which causes it to concentrate into the DEP high-field regions

over the circular microelectrode structures, while the blood cells which are less polarizable experience negative DEP (n-DEP) which causes them to move into the DEP low-field regions between the microelectrodes. After concentration of the CFC-DNA into the DEP high-field regions, which requires only 3 minutes, a fluid wash removes the blood cells and other blood components from the microarray. This is possible, because the CFC-DNA in the DEP high-field regions is held more strongly than the blood cells in the DEP low-field regions. Generally, the proteins and lower molecular weight biomolecules in the blood are not affected by the DEP fields and they are also removed by the washing procedure. The DEP field is then turned off, at which point the CFC-DNA, if fluorescently stained, can be analyzed on chip by fluorescence and then eluted for subsequent PCR and DNA sequencing analysis.

4.3.2 CFC-DNA sample preparation procedures

In this study an AC electrokinetic dielectrophoresis (DEP) device (chip) was used to isolate CFC-DNA from fifteen Chronic Lymphocytic Leukemia (CLL) patient blood samples and three normal blood samples. The study shows for the first time that a DEP device allows CFC-DNA to be isolated directly from 25 μ l of un-processed blood, on-chip fluorescent analysis of the CFC-DNA in less than five minutes, and elution of the CFC-DNA for subsequent PCR and sequencing analysis in less than ten minutes total time.

The process manipulations include addition of the blood sample into the DEP device and removal of the eluted sample upon completion of the process. Fluorescent

analysis in order to determine the concentration of CFC-DNA is also carried out after it was eluted from the DEP chip device. In order to compare the DEP process with a conventional process, a parallel study was also carried out using the Qiagen QIAamp Circulating Nucleic Acid sample preparation procedure to isolate CFC-DNA from 1 ml plasma samples from the same fifteen CLL patients and three normal individuals. The Qiagen QIAamp Circulating Nucleic Acid sample preparation is frequently used for isolation of CFC-DNA from cancer patient plasma samples. The process generally requires several hours to complete before fluorescent analysis, PCR and sequencing of the CFC-DNA can be carried out. The DNA sequencing results for both the DEP and Qiagen procedures were then compared to the CLL Lab “Gold Standard” DNA sequencing results which were previously obtained using genomic DNA isolated from the CLL patients B-lymphocytes. This process also requires several hours to complete before fluorescent analysis, PCR and DNA sequencing of the genomic DNA can be carried out.

Figure 4.2 shows a comparison of the processing time and number of manipulations required for the DEP procedure (A), the Qiagen QIAamp Circulating Nucleic Acid procedure, which includes the blood to plasma step (B), and the CLL lab procedure (C). The processing times for the Qiagen QIAamp Circulating Nucleic Acid and the CLL Lab procedure include only the actual time necessary to run a specific process step, ie. 10 minutes for centrifugation, etc. They do not include the time necessary for set-ups, carrying out transfers such as pipetting and other manipulations, which when carried out manually add at least another hour to the total time for each of the two processes.

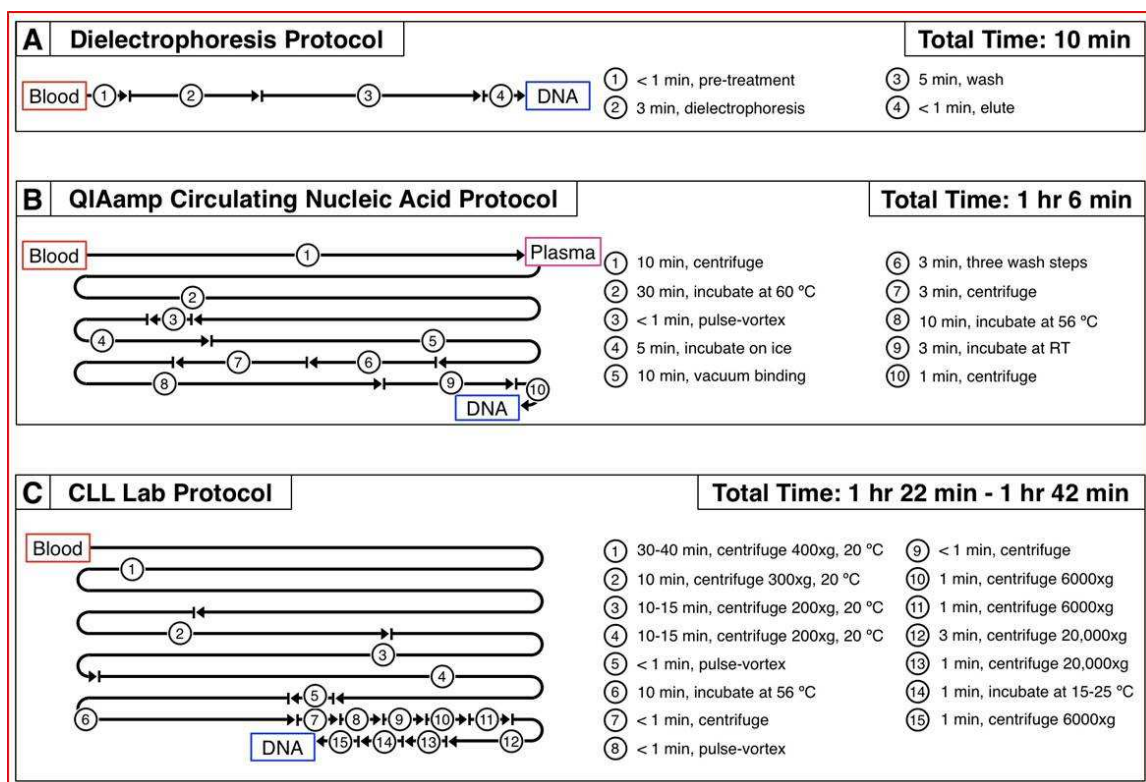


Figure 4.2: Comparison of process times and steps for the three different DNA sample preparation methods. (A) shows the DEP procedure used to isolate CFC-DNA directly from 25 μ l of CLL patient blood; (B) shows the Qiagen QIAamp Circulating Nucleic Acid procedure used to isolate CFC-DNA from 1 ml of plasma (includes blood to plasma steps); and (C) shows the procedure used to isolate genomic DNA from CLL patient B-lymphocyte cells (starting with 5 ml patient blood).

4.3.3 On-chip fluorescent detection of CFC-DNA

For on-chip fluorescent detection of the CFC-DNA SYBR Green I stain is added to the blood samples before the DEP field is applied. After DEP is carried out for three minutes and blood cells are removed by a fluidic wash, the fluorescent stained CFC-DNA which is concentrated in the DEP high-field regions (on the microelectrodes) is detected. Figure 4.3 shows the fluorescent image results for CFC-DNA isolated by DEP from one normal blood sample and from three representative CLL blood samples. On the far right are 3D fluorescent intensity images created by MATLAB which provide better visualization of the relative amounts of CFC-DNA that was isolated. Overall, the

fluorescent DNA levels were higher in most of the CLL patient samples than in the normal blood samples; and in most cases the levels were significantly higher. The fluorescence observed from the normal blood sample is more likely apoptotic DNA coming from normal degradation of cells.

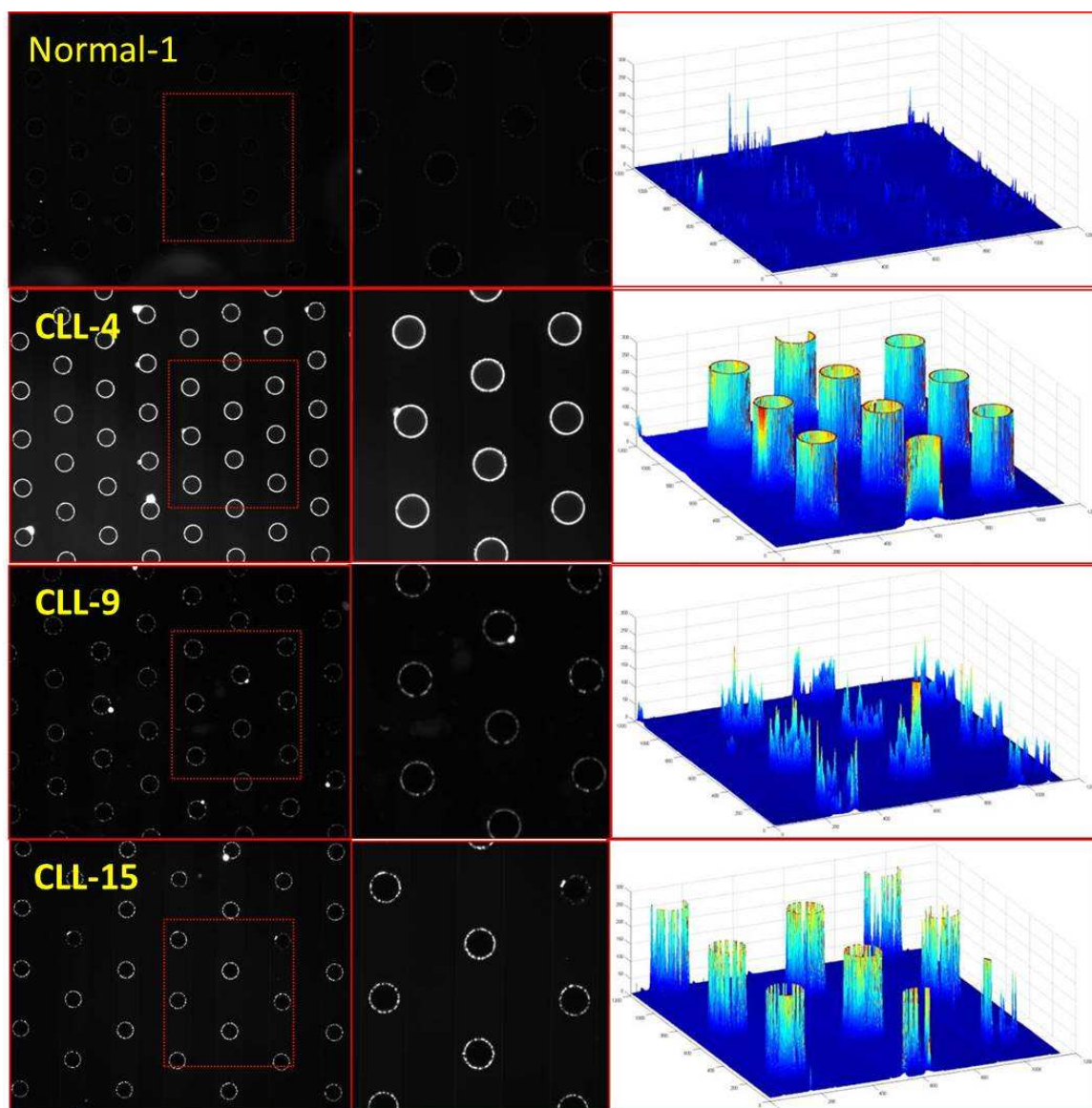


Figure 4.3: Fluorescent detection of CFC-DNA in CLL patient and normal blood samples. On-chip fluorescent imaging results from 25 μ l blood samples showing SYBR-Green stained CFC-DNA that was concentrated into the DEP high-field regions after the DEP field was applied for three minutes. (A) Shows one of the normal blood samples, and (B,C,D) show three representative CLL samples. On the far right are the 3D fluorescent intensity images created by MATLAB which provide better visualization of the relative amounts of CFC-DNA that was isolated.

4.3.4 DNA concentration in eluted samples

In addition to on-chip fluorescent detection of SYBR Green stained CFC-DNA, other experiments were carried out where the concentration of the CFC-DNA in the samples eluted after DEP were determined by PicoGreen fluorescent analysis. For these experiments, SYBR-Green was not added to the blood samples prior to DEP. PicoGreen fluorescent analysis was also carried out to determine the concentration of CFC-DNA in samples which were prepared using the Qiagen QIAamp Circulating Nucleic Acid procedure. Figure 4.4 shows the CFC-DNA concentration results for the samples eluted using the DEP process (red bars) and those from the Qiagen process (blue bars). Concentrations are given as nanograms of DNA per ml of sample used. This is to account for the dilution necessary for the picogreen assay as well as the difference between the DEP collection (25 μ l sample size, 25 μ l elution volume) and the Qiagen collection (1000 μ l sample size, 50 μ l elution volume). For the DEP procedure which started with 25 μ l of blood, the concentration of CFC-DNA in nine of the CLL samples were higher than in the highest normal blood sample (Normal-1). However, the concentration of CFC-DNA in all but one of the CLL samples (CLL-2) was higher than the concentration of DNA for the Normal blood sample 2 and sample 3. For the Qiagen procedure which started with 1 ml of plasma, the concentrations of all but two of the CLL samples (CLL-8, CLL-15) were higher than all three of the Normal samples. The concentration of DNA obtained using the DEP process was higher for all three Normal blood samples than the concentration of DNA for the three Normal plasma samples

obtained using the Qiagen procedure. There appears to be no correlation between the DEP blood results and Qiagen plasma results.

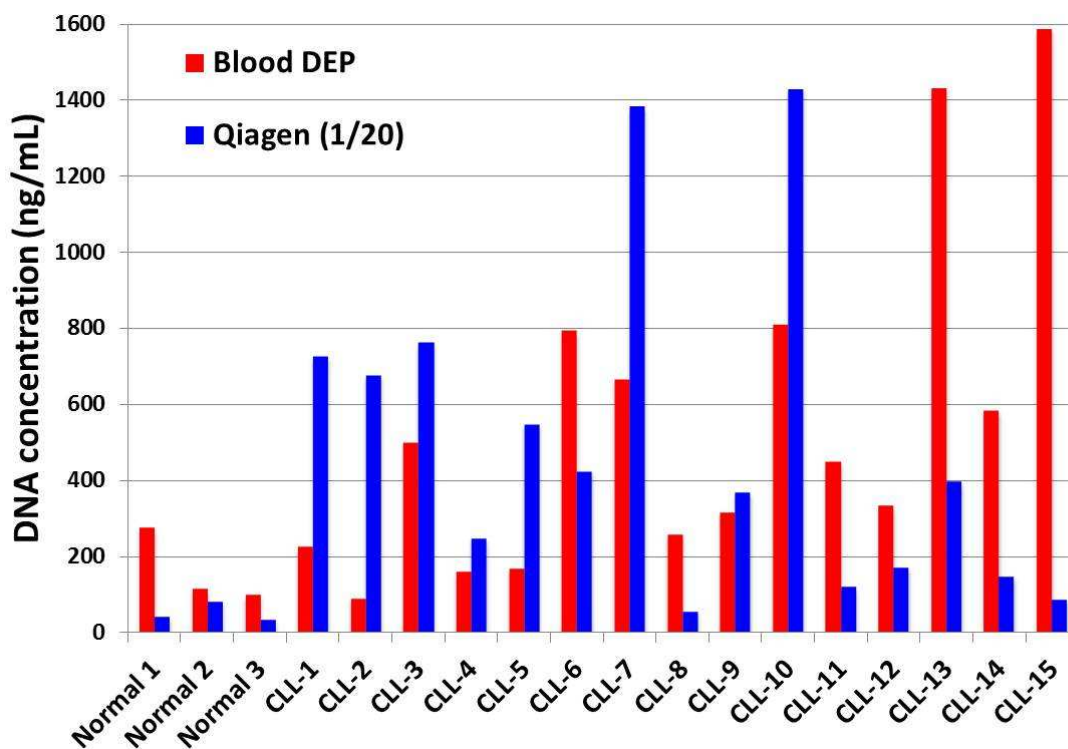


Figure 4.4: Concentration of CFC-DNA in the DEP and Qiagen eluted samples. Bar graph shows the CFC-DNA concentrations in the final eluted samples that were obtained from the DEP process (red bars) and the Qiagen process (blue bars). The DNA concentrations were determined by fluorescence analysis using Quant-iT PicoGreen (Invitrogen) assay a double-stranded DNA dye. Concentrations are given as nanograms of DNA per ml of input sample.

4.3.5 Gel Analysis of PCR results

The eluted samples for both the Qiagen extraction kits and the DEP devices were amplified using primers for the IGHV1, IGHV3, and IGHV4 regions as described previously. The agarose gels were imaged with a CCD camera in a transilluminator. The images were analyzed with ImageJ software to determine the fluorescence in the region

where the 500-550 bp target fragments appeared, regardless of whether or not a discrete band was observed. In ImageJ, the red channel was separated and used, while the blue and green channel data was discarded. The background fluorescence of the image was then removed using the “Subtract Background” tool with a radius of 50 pixels. A 40 pixel wide by 22 pixel tall region was selected around the 500-550 base pair region of each gel lane, and an “Integrate Density” measurement was taken. The resulting fluorescent measurements are shown below in Table 4.1.

Table 4.1: IGHV PCR band intensities for DEP blood and Qiagen plasma. Green cells are IGHV (1, 3, or 4) which correlate with Kipps lab database. Yellow cells do not match the IGHV in the data base but have 20% or more intensity of correct bands. For the DEP process, eluted CFC-DNA from the equivalent of just 5 μ l of the original CLL blood sample (25 μ l) was amplified using CLL-IGHV specific primers to identify the IGHV type (IGHV-1, IGHV-3, and IGHV-4). This table compares the IGHV PCR band intensity results for CFC-DNA from blood with those for the IGHV PCR results obtained from the CFC-DNA isolated from the equivalent of 100 μ l of plasma (from a total 1 ml sample volume) using Qiagen sample preparation. Correct IGHV PCR amplifications of CFC-DNA were obtained from all CLL patient samples using both DEP from blood and Qiagen from plasma. Both DEP and Qiagen also produced secondary IGHV PCR bands; eight bands for DEP and nine bands for Qiagen.

DEP				Qiagen			
Patient	VH1	VH3	VH4	Patient	VH1	VH3	VH4
TJK0064	2,114	2,522	74,524	TJK0064	7,762	3,996	88,677
TJK0115	45,238	2,170	2,039	TJK0115	89,760	3,224	24,942
TJK0973	78,850	1,779	2,426	TJK0973	86,131	2,209	2,168
TJK1094	62,004	37,353	17,529	TJK1094	5,040	61,413	2,412
TJK0528	1,442	10,874	71,157	TJK0528	4,326	4,965	90,965
TJK1044	1,934	60,509	32,171	TJK1044	2,430	60,536	2,286
TJK0334	55,069	5,153	5,036	TJK0334	87,406	1,795	1,506
TJK0613	54,462	1,864	1,419	TJK0613	50,584	3,438	19,600
TJK0762	1,883	59,795	1,311	TJK0762	6,682	59,138	11,905
TJK0847	2,244	65,427	45,746	TJK0847	2,886	30,349	20,735
TJK0248	2,140	46,385	1,355	TJK0248	2,988	53,405	2,019
TJK1024	18,377	55,487	43,869	TJK1024	19,629	64,684	1,829
TJK1206	42,101	9,242	71,089	TJK1206	38,382	2,847	79,305
TJK1217	1,903	14,531	72,242	TJK1217	1,842	27,495	79,517
TJK1262	1,916	2,241	70,315	TJK1262	30,399	26,342	75,939

The results for the IGHV PCR using material collected from normal samples is shown in Figure 4.2. It is likely that the secondary amplification observed in Table 4.1 is due to the presence of apoptotic DNA from other B-cells in the blood. This possible source for amplifiable material is supported by the amplification of material collected from the normal samples with both the DEP devices and the Qiagen kit.

Table 4.2: IGHV PCR band intensities for Normal samples. There are several samples for both the Qiagen and DEP collection that were amplified with the IGHV PCR.

DEP				Qiagen			
Patient	VH1	VH3	VH4	Patient	VH1	VH3	VH4
Normal 1	33,635	32,026	40,661	Normal 1	36,316	6,686	34,654
Normal 2	42,628	20,395	44,882	Normal 2	2,096	2,844	2,330
Normal 3	55,899	1,576	24,761	Normal 3	52,231	9,362	34,428

4.3.6 Sequencing analysis of PCR product

Once the IGHV regions for each sample were analyzed using PCR, the resulting PCR product was sequenced and compared to the result in the CLL patient database. It was important to verify with Sanger sequencing that the collected material was coming from the leukemia cell population and that the amplified IGHV regions matched what was obtained through PCR on DNA from isolated B-lymphocytes. For all 15 CLL samples, the sequences from the amplified material collected from blood with DEP matched the sequences in the database. Several of the secondary bands highlighted in yellow in Table 4.1 were also sent for sequencing. The results of these are shown below in Table 4.3. Each sequence is listed twice, as one entry is the V-GENE and allele stored in the database, and the second entry comes from the more recent sequencing of DEP isolation material. The results match in all 15 cases.

Table 4.3: Sanger sequencing results for PCR product from samples isolated from blood with DEP.

	Alternate name sequence ID	V-GENE and allele	Functionality	V-REGION identity % (nt)	J-GENE and allele	D-GENE and allele	D-Region reading frame	CDR-IMGT lengths	AA JUNCTION	JUNCTION frame
1	CLL-1 VH4cfc-DNA	Homsap IGHV4-39*01 F	Productive	95,53% (278/291 nt)	Homsap IGHJ4*02 F	Homsap IGHD3-10*01 F	2	[10.7.17]	CARVYFYGLGSSDLYFDTC	in-frame
	CLL-1 VH4CLL-DNA	Homsap IGHV4-39*01 F	Productive	95,53% (278/291 nt)	Homsap IGHJ4*02 F	Homsap IGHD3-10*01 F	2	[10.7.17]	CARVYFYGLGSSDLYFDTC	in-frame
2	CLL-2VH4cfc-DNA	Homsap IGHV1-69*01 F	Productive	100,00% (288/288 nt)	Homsap IGHJ5*02 F	Homsap IGHD2-2*01 F	1	[8.8.12]	CARRQLLFYWFDPW	in-frame
	CLL-2 VH4CLL-DNA	Homsap IGHV1-69*01 F	Productive	100,00% (288/288 nt)	Homsap IGHJ5*02 F	Homsap IGHD2-2*01 F	1	[8.8.12]	CARRQLLFYWFDPW	in-frame
3	CLL-3 VH4cfc-DNA	Homsap IGHV1-69*01 F	Productive	100,00% (288/288 nt)	Homsap IGHJ5*02 F	Homsap IGHD3-10*01 F	3	[8.8.20]	CARGTVRGVINFYLYYGMVDVW	in-frame
	CLL-3 VH4CLL-DNA	Homsap IGHV1-69*01 F	Productive	100,00% (288/288 nt)	Homsap IGHJ5*02 F	Homsap IGHD3-10*01 F	3	[8.8.20]	CARGTVRGVINFYLYYGMVDVW	in-frame
4	CLL-4 VH4cfc-DNA	Homsap IGHV3-48*03 F	Productive	98,96% (285/288 nt)	Homsap IGHJ1*01 F	Homsap IGHD3-22*01 F	2	[8.8.13]	CARGDYDNTGPTTRW	in-frame
	CLL-4 VH4CLL-DNA	Homsap IGHV3-48*03 F	Productive	98,96% (285/288 nt)	Homsap IGHJ1*01 F	Homsap IGHD3-22*01 F	2	[8.8.13]	CARGDYDNTGPTTRW	in-frame
5	CLL-5 VH4cfc-DNA	Homsap IGHV4-4*07 F	Productive	100,00% (285/285 nt)	Homsap IGHJ6*02 F	Homsap IGHD2-15*01 F	2	[8.7.19]	CARFFGGGSLYYY YYYGMDVW	in-frame
	CLL-5 VH4CLL-DNA	Homsap IGHV4-4*07 F	Productive	100,00% (285/285 nt)	Homsap IGHJ6*02 F	Homsap IGHD2-15*01 F	2	[8.7.19]	CARFFGGGSLYYY YYYGMDVW	in-frame
6	CLL-6 VH4cfc-DNA	Homsap IGHV3-64*01 F	Productive	94,79% (273/288 nt)	Homsap IGHJ4*02 F	Homsap IGHD6-13*01 F	2	[8.8.16]	CARTPQGEIAAAA PFDYW	in-frame
	CLL-6 VH4CLL-DNA	Homsap IGHV3-64*01 F	Productive	94,79% (273/288 nt)	Homsap IGHJ4*02 F	Homsap IGHD6-13*01 F	2	[8.8.16]	CARTPQGEIAAAA PFDYW	in-frame
7	CLL-7 VH4cfc-DNA	Homsap IGHV1-2*02 F	Productive	100,00% (288/288 nt)	Homsap IGHJ4*02 F	Homsap IGHD6-19*01 F	3	[8.8.13]	CARQQWLVPQRF DYW	in-frame
	CLL-7 VH4CLL-DNA	Homsap IGHV1-2*02 F	Productive	100,00% (288/288 nt)	Homsap IGHJ4*02 F	Homsap IGHD6-19*01 F	3	[8.8.13]	CARQQWLVPQRF DYW	in-frame
8	CLL-8 VH4cfc-DNA	Homsap IGHV1-8*01 F	Productive	100,00% (288/288 nt)	Homsap IGHJ4*02 F	Homsap IGHD6-19*01 F	3	[8.8.13]	CARQQWLVDLNF DYW	in-frame
	CLL-8 VH4CLL-DNA	Homsap IGHV1-8*01 F	Productive	100,00% (288/288 nt)	Homsap IGHJ4*02 F	Homsap IGHD6-19*01 F	3	[8.8.13]	CARQQWLVDLNF DYW	in-frame
9	CLL-9 VH4cfc-DNA	Homsap IGHV3-21*02 F	Productive	88,19% (254/288 nt)	Homsap IGHJ4*02 F	Homsap IGHD3-16*01 F	1	[8.8.14]	CAKGETLGMFPG FDSW	in-frame
	CLL-9 VH4CLL-DNA	Homsap IGHV3-21*02 F	Productive	88,19% (254/288 nt)	Homsap IGHJ4*02 F	Homsap IGHD3-16*01 F	1	[8.8.14]	CAKGETLGMFPG FDSW	in-frame
10	CLL-10 VH4cfc-DNA	Homsap IGHV3-33*01 F	Productive	94,10% (271/288 nt)	Homsap IGHJ6*02 F	Homsap IGHD3-16*01 F	1	[8.8.18]	CARGRSGGEGRY YYYAMDVW	in-frame
	CLL-10 VH4CLL-DNA	Homsap IGHV3-33*01 F	Productive	94,10% (271/288 nt)	Homsap IGHJ6*02 F	Homsap IGHD3-16*01 F	1	[8.8.18]	CARGRSGGEGRY YYYAMDVW	in-frame
11	CLL-11 VH4cfc-DNA	Homsap IGHV3-30*03 F	Productive	95,14% (274/288 nt)	Homsap IGHJ6*03 F	Homsap IGHD3-3*01 F	1	[8.8.14]	CAKGLRFL EAYYMDVW	in-frame
	CLL-11 VH4CLL-DNA	Homsap IGHV3-30*03 F	Productive	95,14% (274/288 nt)	Homsap IGHJ6*03 F	Homsap IGHD3-3*01 F	1	[8.8.14]	CAKGLRFL EAYYMDVW	in-frame
12	CLL-12 VH4cfc-DNA	Homsap IGHV3-53*04 F	Productive	97,19% (277/285 nt)	Homsap IGHJ3*02 F	Homsap IGHD3-10*01 F	2	[8.7.15]	CARDTSGSGGSH TFDIW	in-frame
	CLL-12 VH4CLL-DNA	Homsap IGHV3-53*04 F	Productive	97,19% (277/285 nt)	Homsap IGHJ3*02 F	Homsap IGHD3-10*01 F	2	[8.7.15]	CARDTSGSGGSH TFDIW	in-frame
13	CLL-13 VH4cfc-DNA	Homsap IGHV4-39*01 F	Productive	96,91% (282/291 nt)	Homsap IGHJ4*02 F	Homsap IGHD6-13*01 F	1	[10.7.15]	CGSQSSYSSSWY YFDYW	in-frame
	CLL-13 VH4CLL-DNA	Homsap IGHV4-39*01 F	Productive	96,91% (282/291 nt)	Homsap IGHJ4*02 F	Homsap IGHD6-13*01 F	1	[10.7.15]	CGSQSSYSSSWY YFDYW	in-frame
14	CLL-14VH4cfc-DNA	Homsap IGHV4-34*01 F	Productive	99,30% (283/285 nt)	Homsap IGHJ4*02 F	Homsap IGHD6-6*01 F	2	[8.7.21]	CARGPRGGRLA ARPTEVWMRYW	in-frame
	CLL-14 VH4CLL-DNA	Homsap IGHV4-34*01 F	Productive	99,30% (283/285 nt)	Homsap IGHJ4*02 F	Homsap IGHD6-6*01 F	2	[8.7.21]	CARGPRGGRLA ARPTEVWMRYW	in-frame
15	CLL-15 VH4cfc-DNA	Homsap IGHV4-39*01 F	Productive	100,00% (291/291 nt)	Homsap IGHJ4*02 F	Homsap IGHD5-12*01 F	1	[10.7.15]	CARRLSFGYIVAF DYW	in-frame
	CLL-15 VH4CLL-DNA	Homsap IGHV4-39*01 F	Productive	100,00% (291/291 nt)	Homsap IGHJ4*02 F	Homsap IGHD5-12*01 F	1	[10.7.15]	CARRLSFGYIVAF DYW	in-frame

4.4 Discussion

The use of cell-free circulating (CFC) DNA biomarkers for “liquid biopsy” will unquestionably be important for future cancer diagnostics and management. Unfortunately, the time and process complexity required for the isolation of CFC-DNA from plasma by conventional methods is a major limitation for developing point-of care (POC) diagnostic formats. Additionally, these processes add significant cost to the assays which will also limit their use. Likewise, the isolation of cancer related genomic DNA from transformed cells in the blood also requires relatively time consuming, complex and costly processing which may preclude viable POC diagnostics. In this study, we have shown that an AC electrokinetic DEP microarray device can be used to isolate CFC-DNA directly from CLL patient blood in less than 10 minutes. The DEP process is not only significantly faster than the conventional methods, but requires only three steps (Figure 4.2). We have also shown that DEP allows CFC-DNA to be isolated from a relatively small sample volume of only 25 μ l, which is equivalent to a drop of blood.

Before eluting the CFC-DNA from the DEP microarray, fluorescent analysis using SYBR-Green DNA staining was carried out on the CLL patient and normal patient blood samples. In almost all cases, fluorescence from the SYBR-Green DNA concentrated in the DEP high-field regions on the microelectrodes was more intense than in the normal samples; in many cases much more intense (Figure 4.3). The Mat-Lab 3-D fluorescent intensity images provide a visual comparison of the relative fluorescent intensities between the normal and the CLL samples (Figure 4.3). The ability to use

fluorescence to determine the relative amount of CFC-DNA in a clinical sample could ultimately be a very simple and rapid first phase diagnostic for monitoring disease. Other workers have now shown preliminary results correlating the level of CFC-DNA in patient plasma with survivability for lung cancer [99] and colon cancer [100]. Again, in these studies a relatively long and involved process was used to isolate the CFC-DNA from cancer patient plasma samples. For the DEP process, on-chip fluorescent analysis of CFC-DNA from blood could be carried out in less than five minutes, making it potentially useful for POC cancer monitoring.

After DEP isolation, the CFC-DNA was eluted from the microarray chip with a fluid wash (25 μ l of 1x TE buffer). The concentration of the CFC-DNA from the three normal and fifteen CLL patient samples was then determined using PicoGreen fluorescence analysis. In the parallel study, the concentration of CFC-DNA isolated by using the Qiagen CFC-DNA procedure (1 ml plasma) was also determined by PicoGreen fluorescence. Both the DEP and Qiagen methods on average show more CFC-DNA from the CLL patients than from the normal patients (Figure 4.4). For the normal samples, the Qiagen preparation from plasma shows somewhat lower concentrations of DNA (CFC-DNA/apoptotic-DNA) than the DEP method. This may be due to the fact that the DEP method involves isolation directly from blood, different elution efficiencies for removing CFC-DNA from the chip, and/or we do not have enough data points for each sample. The comparison of CLL patient CFC-DNA concentrations between the DEP process and the Qiagen process appears to be more complex. For seven of the CLL patient samples (CLL-3, 4, 6, 7, 9, 10, 12) the DEP and Qiagen concentrations were within 50% of each

other; with the Qiagen process higher for CLL-3, 4, 7, 9, 10; and the DEP process higher for CLL-6 and CLL-12. The CFC-DNA concentrations for the DEP process were significantly higher (>50%) for five of the samples (CLL-8, 11, 13, 15), while the Qiagen process CFC-DNA concentrations were significantly higher (>50%) for three of the samples (CLL-1, 2, 5). Overall the combined CFC-DNA concentrations for all fifteen CLL samples were slightly higher for the DEP process than for the Qiagen process by approximately 10%. More important than the differences in CFC-DNA concentrations, is that the CFC-DNA from the DEP process was obtained from only 25 μ l of blood in less than 10 minutes, while the CFC-DNA from the Qiagen preparation was obtained from a much larger sample (1 ml) of patient plasma and required several hours for preparation.

The primary objective of this study was to determine if the cancer related CFC-DNA that was isolated directly from a small blood sample could now be amplified by PCR for CLL IGHV analysis and DNA sequencing. For the DEP process, eluted CFC-DNA from the equivalent of just 5ul of the original CLL blood sample (25ul) was amplified using CLL-IGHV specific primers to identify the IGHV type (IGHV-1, IGHV-3, and IGHV-4). The correct IGHV PCR amplifications were obtained from all CLL patient samples for the DEP process, as well for the Qiagen process. Both DEP and Qiagen also produced secondary IGHV PCR bands; eight bands for DEP and nine bands for Qiagen. In all but one case (CLL-4 DEP Blood), the secondary bands were less intense than the correct IGHV band. In some cases, these bands may represent secondary CLL clones, or they may be coming from DNA from other non-transformed blood cells. More likely, they are PCR related in that the original IGHV PCR primers and

amplification conditions were designed for use with high concentrations of genomic DNA isolated directly from CLL patient B-lymphocytes. In the development of the IGHV PCR for use with much lower concentrations of CFC-DNA, continued optimization of the PCR conditions has helped in reducing the secondary IGHV bands. Nevertheless for this study, DNA sequencing was used to verify that CFC-DNA isolated by the DEP process was from the transformed CLL B-lymphocytes. The final DNA sequencing results for all fifteen CLL patients whose CFC-DNA was isolated by DEP were found to compare very well with the original (Gold-Standard) patient specific sequencing results. Again, the “Gold Standard” sequencing results were obtained using genomic DNA that was isolated from the CLL patients B-lymphocytes. Finally, it is important to recognize that PCR analysis and sequencing results were obtained in several cases (CLL-2, 4, 5) where the CFC-DNA concentrations were not exceptionally high.

The ability of DEP to provide rapid isolation of CFC-DNA from the equivalent of a drop of blood represents a major step forward in the quest for point of care (POC) cancer diagnostics and patient monitoring.

Chapter 4, in part, is in preparation for submission for publication as: Avery Sonnenberg, Jennifer Marciniak, Laura Rassenti, Emanuela Ghia, Elaine Skowronski, James McCanna, Sareh Manouchehri, George Widhopf, Thomas Kipps, and Michael Heller. *Isolation and Detection of Circulating Cell Free DNA Directly from Chronic Lymphocytic Leukemia Patient Blood.*

The author of this dissertation is the primary author of this manuscript.

CHAPTER FIVE:

New Electrokinetic Devices and Methods for High Conductance and High Voltage Dielectrophoresis (DEP)

5.1 Invention

This disclosure concerns novel concepts designs and ideas for high voltage DEP devices some of which are related to those disclosed in earlier disclosures and in PCT filing 2007-205-1/2009-171-1 (Ex-Vivo Multi-Dimensional System for the Separation and Isolation of Cells, Vesicles, Nano-particles and Biomarkers or Seamless Sample to Answer). More specifically this disclosure relates to new single and multi “pore based” AC/DC high voltage electrokinetic devices and improved features and methods for carrying out dielectrophoresis (DEP) under high conductance conditions. These new high voltage electrokinetic devices and methods allow rapid isolation, separation, detection and analysis of cells, bacteria, virus, cell free circulating (CFC) DNA, CFC-RNA and other cellular nanoparticulates (exosomes, etc.) as well as drug delivery and other nanoparticles to be carried out under high conductance conditions directly from blood, plasma, serum, urine and other clinical, biological and environmental samples. This invention basically eliminates or greatly reduces any sample preparation and allows “seamless sample to answer” analysis and/or diagnostics to be rapidly carried out. This can include, but is not limited to both “pre” and “post” DEP separation analysis by general and/or specific fluorescent stains (DNA, RNA, nuclei, membranes, cellular organelles (cellular nanoparticulates) and antibodies; analysis of cells, nuclei, DNA and RNA by fluorescent probe hybridization (FISH, etc.); and post analysis of cells, nuclei, DNA and RNA by PCR, sequencing and other genotyping techniques – all of which can be carried out in the same chambered compartment in which the DEP separation occurred; or the concentrated/collected materials can be transferred to a separate

container (PCR tube, etc) for subsequent analysis. The above examples do not exclude other types of detection techniques which might include radio-isotopes, colorometric, chemiluminescence, electrochemical, or other methods of biosensing for DNA, RNA, antibodies, biomolecules and cells.

5.2 Novelty

Our invention relates to very simple AC/DC high voltage electrokinetic devices and formats which allow rapid sample to answer analysis and diagnostics to be carried out using complex biological and clinical samples including blood, plasma, serum, urine etc.

5.3 Existing Art

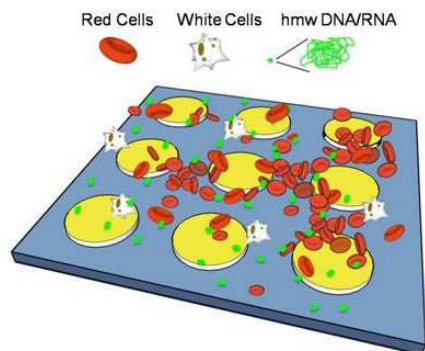
Other types of DEP devices that have been used to separate out cells from either blood or other high conductance samples, or nanoparticulates from other size particles in either blood or other high conductance buffers, require that the samples be diluted to low conductance conditions. These conventional DEP devices do not have the performance characteristics, robustness and ultimate usefulness to carry out the separation applications described in our invention. They do not provide potential for “seamless sample to answer” or point of care diagnostics.

5.4 Method of Operation

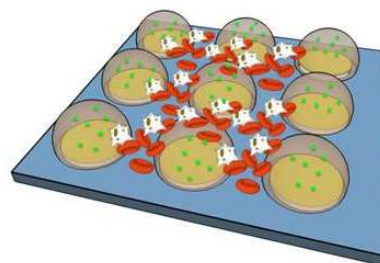
5.4.1 Previous Device Design

We have demonstrated the isolation and detection of high molecular weight DNA (HMW-DNA), cell free circulating (CFC-DNA) and nanoparticles from whole blood using these new AC/DC electrokinetic dielectrophoretic (DEP) devices and methods. Both fluorescent nanoparticles and fluorescent-stained HMW DNA in undiluted whole blood samples were separated and held in DEP high field regions and then detected after the blood cells were removed by a fluidic wash. In buffy coat blood, with reduced cell numbers, nanoparticles concentrated into the DEP high field regions while the blood cells concentrated into the DEP low field regions. A fluidic wash then selectively removed the cells while the nanoparticles remained trapped. More importantly, we have now also demonstrated that unlabeled HMW DNA could also be isolated into the high field regions, and then stained with a fluorescent dye for subsequent detection, demonstrating an intrinsic DEP advantage of separating unlabeled analytes. Overall, DEP can now be developed as a “seamless” sample to answer tool which can be used with complex biological samples (blood, plasma, etc.) for a variety of research and diagnostic applications.

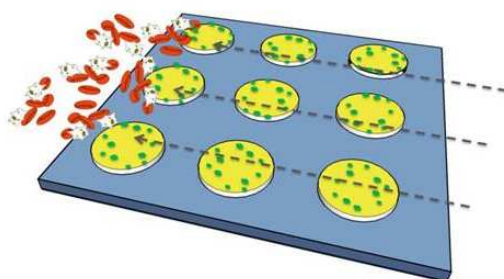
Step 1 - Blood Sample with Cell Free Circulating hmw DNA/RNA is Applied to the DEP Device



Step 2 - The DEP Field is Applied



Step 3 - Fluidic Wash is Applied to Remove Cells



Step 4 - Add Fluorescent DNA/RNA Stain and Wash

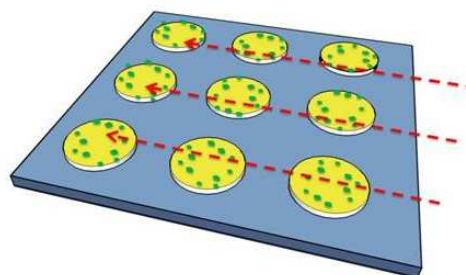


Figure 5.1: Original concept/scheme for the DEP separation of DNA/Nanoparticles from blood and other high conductance samples (Steps 1-4). Step 1 - the first step in sample to answer diagnostics where DEP is used to carry out separation of high molecular weight DNA in whole blood (This has been demonstrated). Step 2 - Shows second step in sample to answer diagnostics where DEP is used to carry out separation of high molecular weight DNA in whole blood (This has been demonstrated). Step 3 - Shows third step in sample to answer diagnostics where DEP is used to carry out separation of high molecular weight DNA in whole blood (This has been demonstrated). Step 4 - Shows fourth step in sample to answer diagnostics where DEP is used to carry out separation of high molecular weight DNA in whole blood (This has been demonstrated).

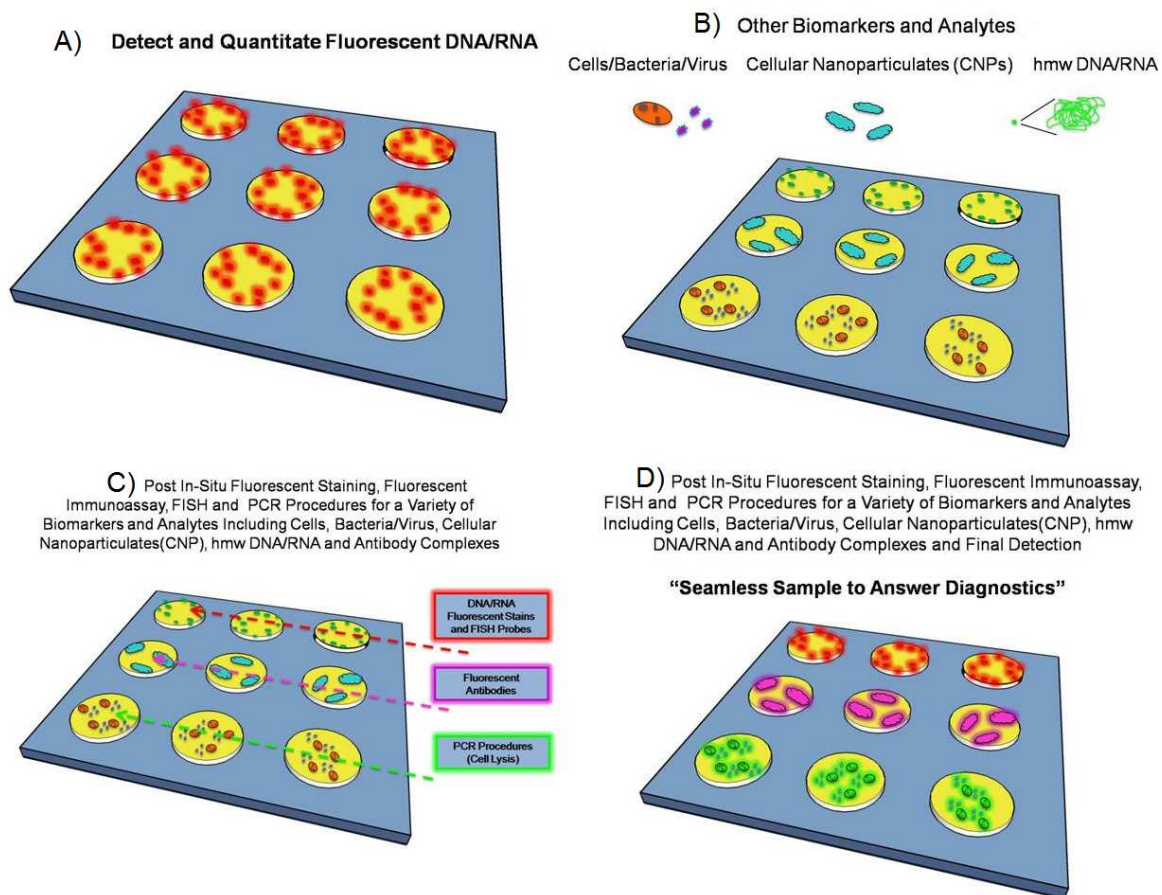


Figure 5.2: Seamless Sample to Answer Diagnostics. A) Shows fluorescent quantification of DNA/RNA after DEP is used to carry out separation of high molecular weight DNA in whole blood (This has been demonstrated). B) Shows where DEP is used to carry out separation of bacteria, virus, cellular nanoparticulates or CNPs (which can include cellular membrane, nuclei, vacuoles, endoplasmic reticulum, mitochondria, etc.), antibody complexes and other biomarkers from whole blood. C) Shows the post fluorescent staining, fluorescent immunoassay, FISH, and PCR procedures which can be used in-situ (in the same compartment) to carry out analysis of cells, bacteria, virus, CNPs and antibody complexes (This has been demonstrated). D) Shows the final detection of cells, bacteria, virus, CNPs and antibody complexes.

5.4.2 Basic design of earlier three chambered multi-pore electrokinetic DEP devices for the separation of DNA/Nanoparticles from blood and other high conductance samples

Figure 5.3 and Figure 5.4 show the basic design for a three chambered multi-pore electrokinetic DEP device in which the electrodes are placed into separate chambers and positive DEP regions and negative DEP regions are created within an inner sample chamber by passage of the AC DEP field through pore or hole structures. (These devices were disclosed earlier and are in the PCT filing 2007-205-1/2009-171-1 Ex-Vivo Multi-Dimensional System for the Separation and Isolation of Cells, Vesicles, Nanoparticles and Biomarkers or Seamless Sample to Answer). Various geometries can be used to form the desired positive DEP (high field) regions and DEP negative (low field) regions for carrying cell, nanoparticle and biomarker separations with the sample chamber. Such pore or hole structures can be filled with a porous material (agarose or polyacrylamide hydrogels) or be covered with porous membrane type structures (paper, cellulose, nylon, etc). Such porous membrane overlaying structures can have thicknesses from one micron to one millimeter, but more preferably from 10 microns to 100 microns; and pore sizes that range from 100 nanometer to 10 mm, but more preferably from 10 microns to 1000 microns. By segregating the electrodes into separate chambers, these unique DEP devices basically eliminate any electrochemistry effects, heating or chaotic fluidic movement from influencing the analyte separations that are occurring in the inner sample chamber during the DEP process. These chambered devices can be operated at very high AC voltages (> 100 volts pk-pk), and in addition to DEP they could also be used to carry out

DC electrophoretic transport and electrophoresis in sample chamber. In general these devices and systems can be operated in the AC frequency range of from 1000 Hz to 100 mHz, at voltages which could range from 1 volt to 2000 volts pt-pt; and DC voltages from 1 volt to 1000 volts, at flow rates of from 1 microliters per minute to 10 milliliter per minute and in temperature ranges from 1 °C to 100 °C . The chambered devices are shown in Figure 5.3 and Figure 5.4. Such devices can be created with a variety of pore and/or hole structures (nanoscale, microscale and even macroscale) and may contain membranes, gels or filtering materials which can control, confine or prevent cells, nanoparticles or other entities from diffusing or being transported into the inner chambers. However, the AC/DC electric fields, solute molecules, buffer and other small molecules can pass through the chambers. Figure 5.3 and Figure 5.4 represents a most basic version of these devices and a variety of forms are envisioned by this invention. These include but are not limited to multiplexed electrode and chambered devices, devices that allow reconfigurable electric field patterns to be created, devices that combine DC electrophoretic and fluidic processes; sample preparation devices, sample preparation/diagnostic devices that include subsequent detection and analysis, lab-on-chip devices, point of care and other clinical diagnostic systems or versions.

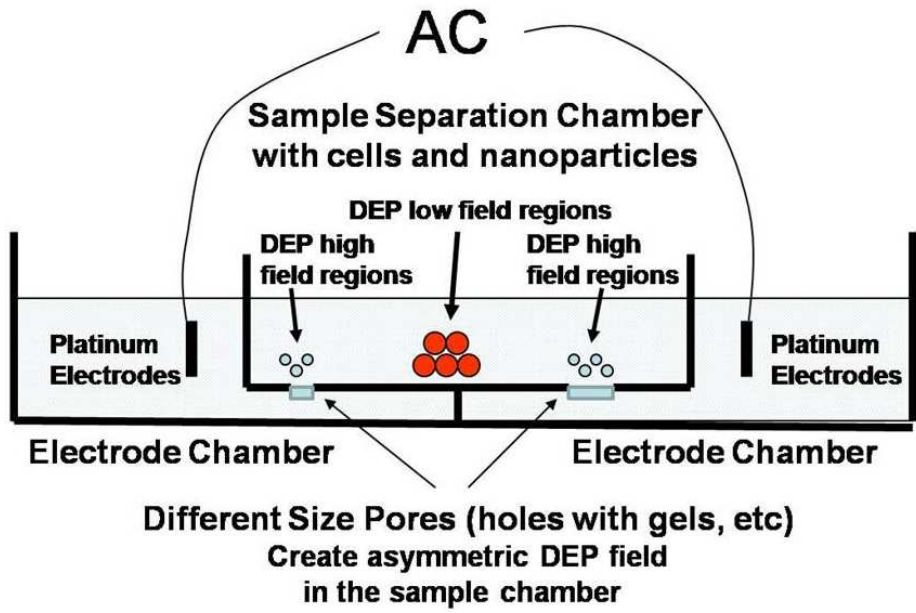


Figure 5.3: Multiple chamber high conductance DEP Device.

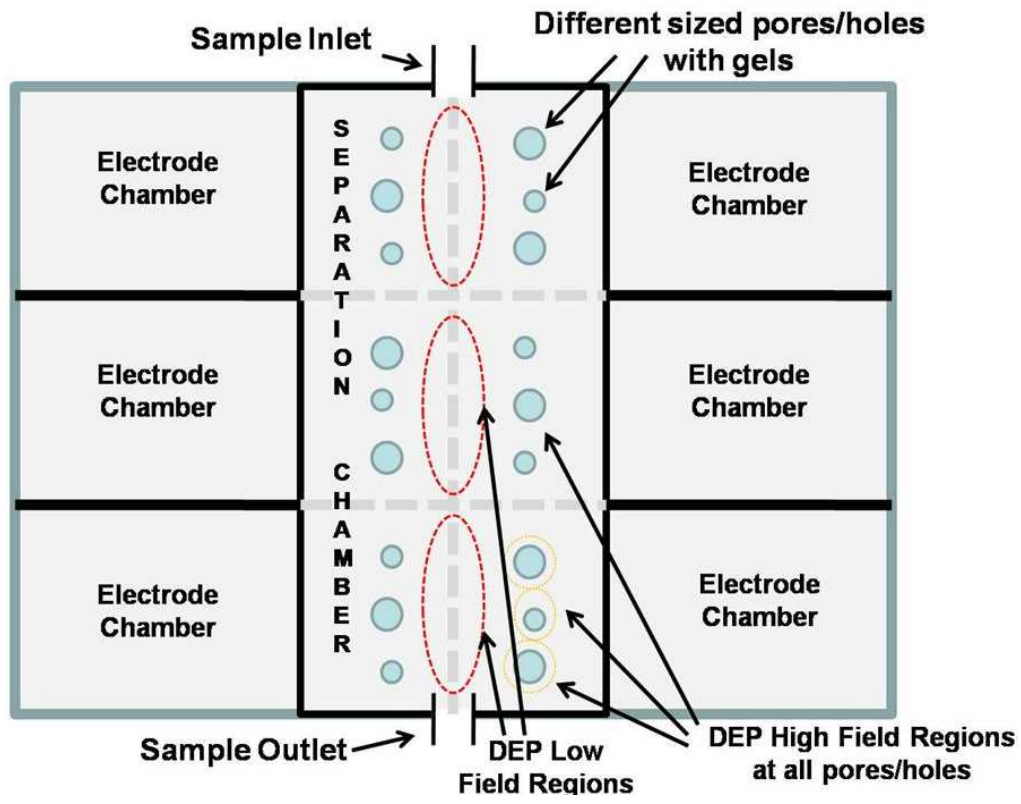


Figure 5.4: Top view of multiple chamber high conductance DEP device

5.4.3 Description of New Devices, Designs and Concepts for even simpler two chambered and single pore electrokinetic DEP devices for the rapid separation of cells, CFC-DNA /RNA or nanoparticles from blood and other high conductance samples.

Figure 5.5 shows the basic design diagram for a very simple high voltage Single Pore Two Chamber DEP Device which can be constructed from very simple plastic, glass, paper membrane, sponge, porous gel and other materials. The figure shows the DEP separation of nanoparticles from micron size particles, where the red nanoparticles are concentrated around the high field region, which occurs at the edge of the pore structure (small hole in the plastic base); and micron size green particles in the low field regions radiating out to the platinum ring electrode (inner sample chamber). The DEP high field region occurs around the edges of the pore structure because this is where the DEP field between the outer buffer chamber and inner chamber is most constricted. It is also in the scope of this invention to (1) incorporate more than one pore structure, and/or other types of pore structures, hole or slit structures; (2) design pore or hole structures/geometries so that the DEP high field (analyte concentration) regions occur on one side or the other side of the pore or inside the pore or hole structure; (3) to separate the sample chamber electrode into a third chamber connected via conductance channel (membrane, gel, etc) back to the sample chamber; (4) to incorporate input and out flow channels for both introducing and extracting samples and/or collecting analytes (cells, DNA, nanoparticles, etc.); (5) to use a DC (electrophoretic) duty cycles along with AC DEP to better collect (concentrate) analytes in a preferred region of the pore or inner

device structure; and (6) to design more linear flow devices with parallel electrodes and pores which move blood cells to low field regions while CFC-DNA and nanoparticles are collected in the high field pore structures. It is also anticipated that these devices can be used for sample preparation as well as for seamless sample to answer applications.

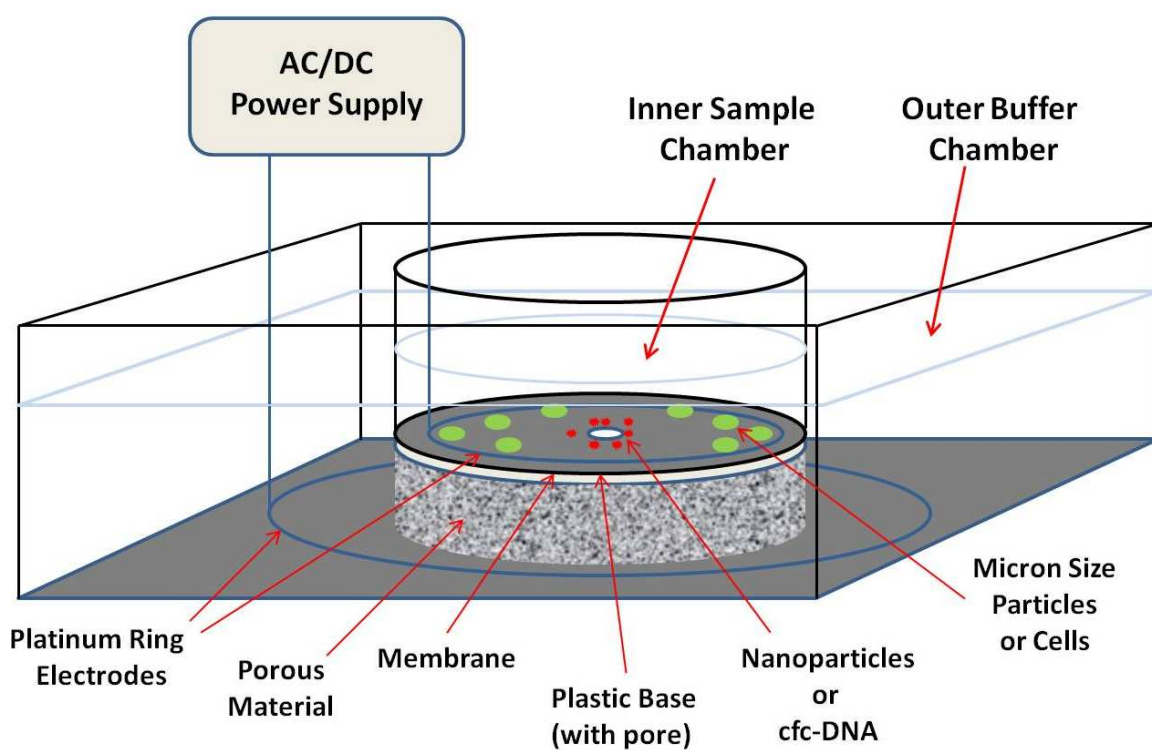


Figure 5.5: Basic Diagram of the new Single Pore Two Chamber DEP Device. Showing red nanoparticles concentrated around the high field regions (which occur at the edge of the pore structure) and micron size green particles in the low field regions.

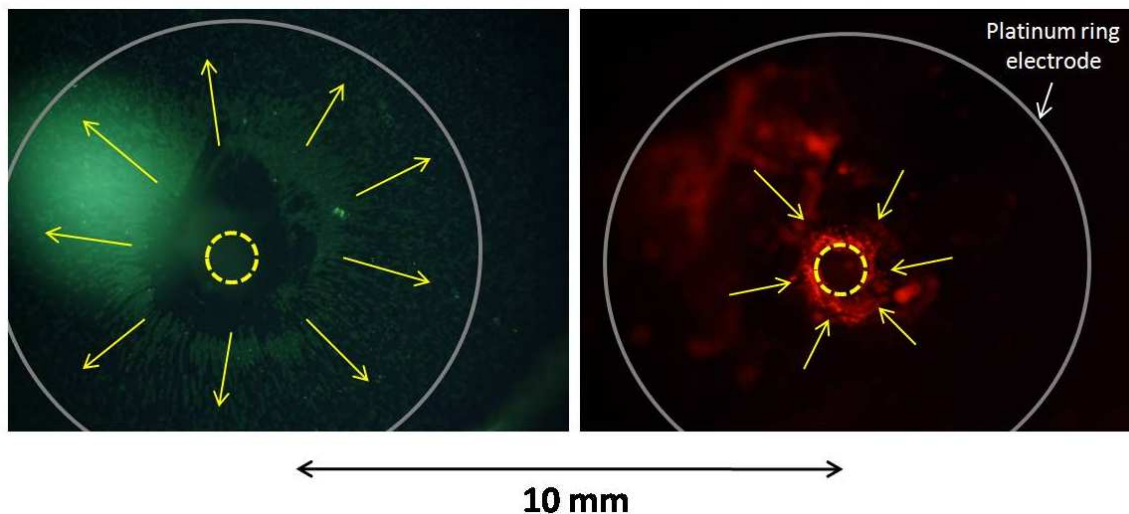


Figure 5.6: Results for using a two chamber single pore device. The DEP separation of 10 micron beads and 40 nm fluorescent nanoparticles in 1xTBE buffer on a two chamber single pore (~800 um diameter) device at 160 volts pk-pk. Left side shows 10 micron beads moving to low field regions, right side shows red fluorescent nanobeads concentrating in the high field regions at the edge of the pore (yellow circle).

Figure 5.7 shows the basic design diagram for a very novel and simple *Pipette Tip DEP Device* which can be constructed from commonly used plastic/glass pipette tips, plastic/glass capillary tubes, plastic tubing, glass/plastic slides, platinum electrode, agarose gel (or other porous gel membrane materials) and PDMS or other plastic, rubber or glass construction materials. The figure shows the DEP separation of nanoparticles from micron size particles, where the red nanoparticles are concentrated around the high field region, which occurs at the edge of the pipette tip hole structure; and micron size green particles in the low field regions radiating out to the platinum ring electrode (sample chamber). The DEP high field region occurs around the edges of the pipette tip hole structure because this is where the DEP field between the outer sample chamber and inner chamber (inside the pipette) is most constricted. It is also in the scope of this invention to (1) utilize multiple pipette tip arrangements for automated sample

preparation; (2) design pore or hole structures/geometries so that the DEP high field (analyte concentration) regions occur on one side or the other side of the hole or inside the pore or hole structure; (3) to design the device so that analytes concentrated inside the device can analyzed in-situ by PCR, immunoassay, etc., providing a seamless sample to answer version of the technology; and (5) to use a DC (electrophoretic) duty cycles along with AC DEP to better collect (concentrate) analytes in a preferred region of the hole or inner device structure.

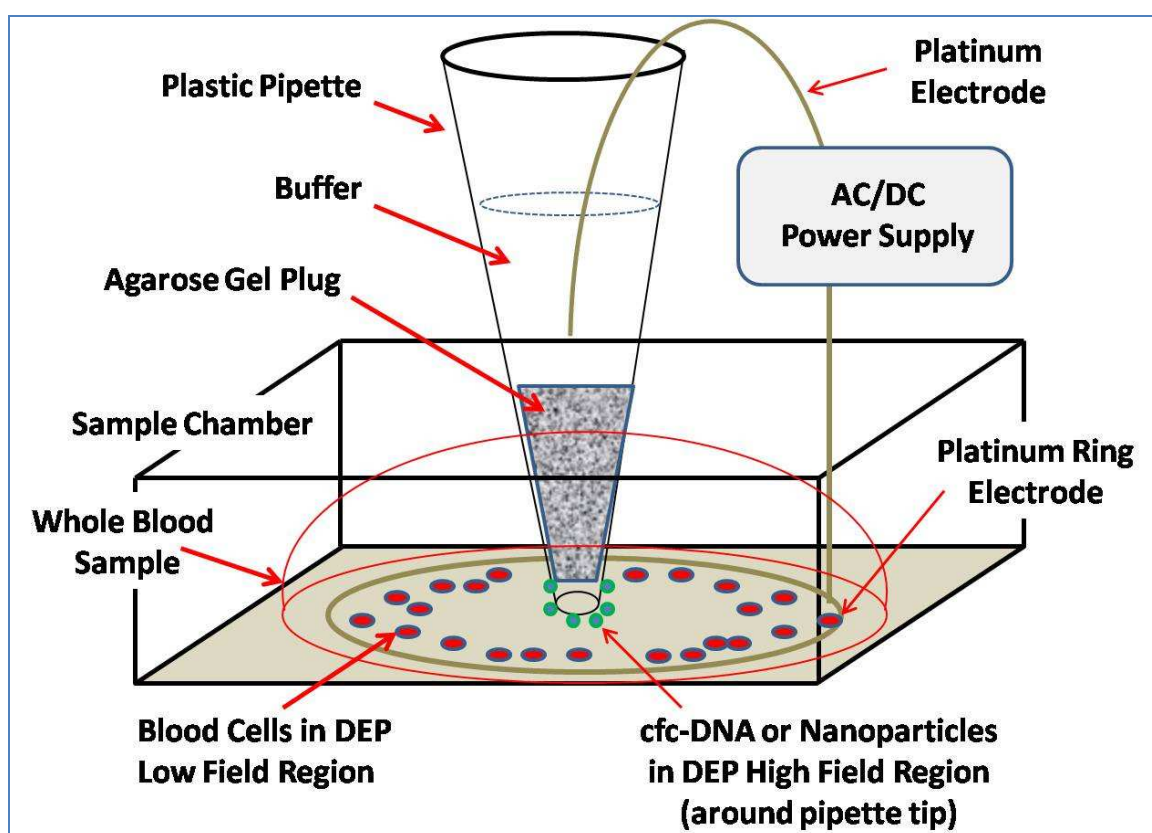


Figure 5.7: Basic design diagram for a very novel and simple Pipette Tip DEP Device which can be constructed from commonly used materials.

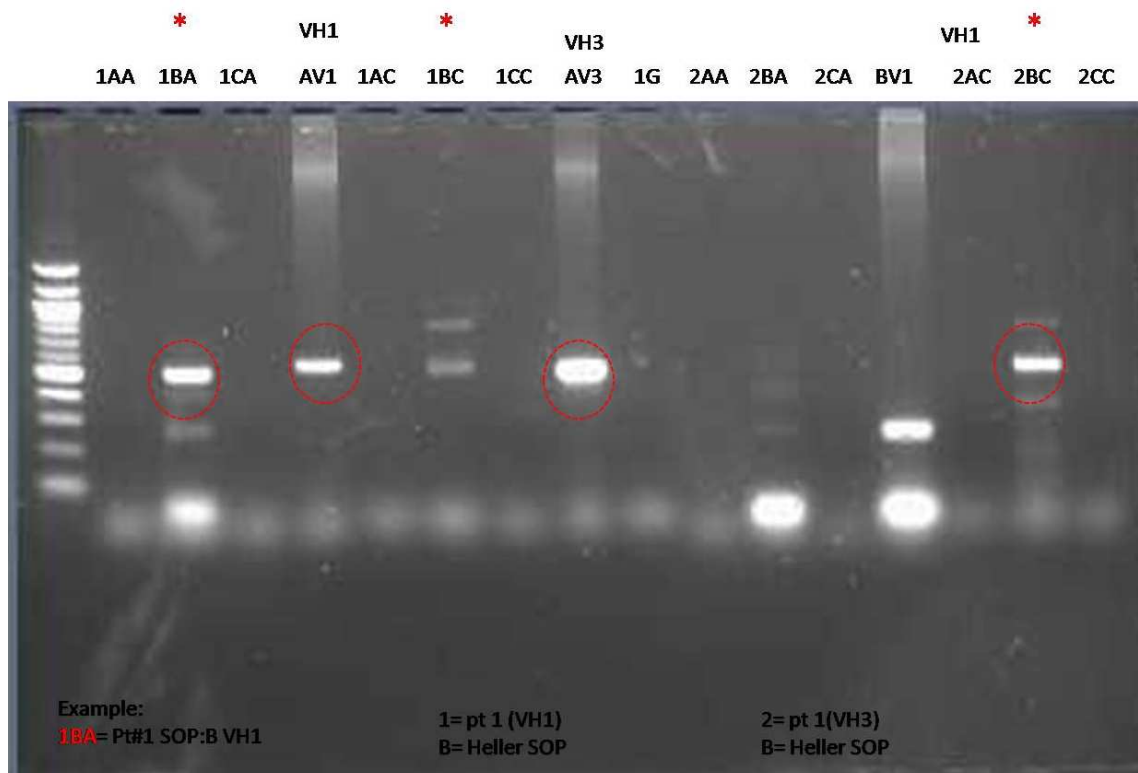


Figure 5.8 : PCR results from CFC-DNA extracted from CLL cancer patient blood samples. A pipette tip device was used to isolate CFC-DNA from about 25ul of CLL cancer patient whole blood samples, by applying 200 volts pk-pk at about 5-10 kHz AC for 5 minutes. The pipette tip was removed from the blood sample and the collected CFC-DNA deposited into a PCR tube (with PCR buffer) and PCR was then carried out. The results show the PCR detection of patient specific IGHV-L immunoglobulin rearrangements. Blood to PCR could be carried out in about five minutes.

5.5 Stage of development of the invention

We have demonstrated new devices for the rapid isolation and detection of nanoparticles, high molecular weight DNA (HMW-DNA) and CFC-DNA from whole blood (including CLL a cancer patients). Overall, these new DEP devices can now be developed for sample preparation applications, as well as a “seamless” sample to answer tool which can be used with complex biological samples (blood, plasma, etc.) for a variety of research and diagnostic applications.

5.6 Potential commercial applications of the invention

In addition to sample preparation for CFC-DNA/RNA and seamless sample to answer cancer diagnostic applications, we envision a variety of separation and isolation applications which include rare cell detection for adult stem cell isolation from blood, other bodily fluids or any buffers, e.g. hematopoietic progenitors; gross separation between cells and low molecular weight DNA from blood, other bodily fluids or any buffers for the purposes of cancer detection and other diagnostics; cancer cell isolation from blood, other bodily fluids or any buffers for both diagnostic as well as therapeutic purposes; and protein isolation from blood, other bodily fluids or any buffers for the purposes of diagnostics or therapeutics.

Chapter 5 is a reprint of the following provisional patent application: Michael Heller, Rajaram Krishnan, Avery Sonnenberg. *New Electrokinetic Devices and Methods for High Conductance and High Voltage Dielectrophoresis (DEP)*. Patent Pending. Provisional Patent # 61/413,306.

The author of this dissertation is an inventor on this patent application.

CHAPTER SIX:

Summary and future work

6.1 Summary and conclusions

Realization of the concept of personalized medicine will require a significant increase in the amount of information that must be collected from each patient in order to make decisions informed by all of the aspects that make that patient's pathology unique. To do this in a cost-effective way, there will undoubtedly be a need for improvement in the understanding of particular disease states and how they vary over a population as well as advances in the technology available to collect this information from the variety of samples that are clinically available. A variety of DNA, RNA, protein, and other biomarkers will be used to inform these decisions, and the equipment to rapidly and inexpensively extract them from the available samples in a point-of-care environment has yet to be developed. Every avenue to differentiate these analytes must be pursued, and it is likely that a combination of new technological developments and refinements of current techniques will ultimately be responsible for the reduction in cost and complexity that is necessary for widespread adoption.

In this work, we have developed a method to harness the dielectric properties of DNA to separate it quickly from blood and other high conductivity samples in a low-complexity system that is inherently integratable with other molecular analysis tools and workflows. The versatility to be adopted as a front-end sample processing technology for a number of different molecular diagnostics will be a key factor in the pursuit of continued development of this technique. We have focused on demonstrating that this method can replace the much more complex and time-consuming conventional sample preparation that is used to isolate CFC-DNA from blood samples. We successfully visualized the

captured material with fluorescent DNA dye and proposed a possible model for this material by mechanically disrupting blood cells and showing similar imaging results. We went on to demonstrate the versatility of the method by isolating DNA, virus, and mitochondria from blood and storage buffer that were considered to be outside the range of possible application of dielectrophoresis due to the high electrical conductivity of these samples. To demonstrate that the collected DNA was not altered in any way that prevented conventional fluorescent and PCR analysis and was collected in sufficient quantity, we focused on a set of 15 Chronic Lymphocytic Leukemia samples. We showed that the DNA that we were able to isolate from the blood of these patients provided the same genetic information that was obtained directly from the B-lymphocytes using a conventional sample preparation workflow. The amounts collected, as indicated by bulk fluorescent analysis using a plate reader, were very similar on average to those collected with the adsorption columns commonly used in CFC-DNA studies.

While this work demonstrates a significant improvement in terms of speed and complexity of DNA isolation compared to current methods, it has also illuminated some of the limitations of the use of dielectrophoresis as a sample preparation technology. There have also been a number of new areas of interest related to this technology that could be pursued in future projects.

6.2 Limitations

6.2.1 Limitations of current DEP device

The most recent iteration of the DEP device, manufactured by Biological Dynamics, is hard-wired to the specific electrode geometry detailed in Chapter 5. This is the most useful single geometry, but an individually addressable array similar to the one made by Nanogen and detailed in Chapter 2, provides more flexibility for research purposes. In addition, both the Nanogen and Biological Dynamics devices are not designed with high-frequency signals in mind. The traces are not sufficiently shielded from one another and the silicon dioxide layer is not of sufficient thickness to prevent the parasitic capacitive coupling of the signals with neighboring traces and the sample itself. As we were conducting our experiments at 10 kHz for this work, we did not need to worry about this effect. Figure 6.1 (D) below demonstrates the poor isolation of the traces when an electric field is applied at 1 MHz in a sample containing *E. coli*. The bacteria gather on the edges of the circular electrodes, as is expected, but they also are concentrated along the traces between electrodes, which are covered with silicon dioxide. While the device is not prevented in this case from concentrating bacteria into the high-field regions, the formation of high field regions is much different than at 10 kHz, an experiment which is shown in Figure 6.1 (C). This frequency-dependent leakage of signal must be reduced or at least accounted for if the device is intended to operate at frequencies at or above 1 MHz.

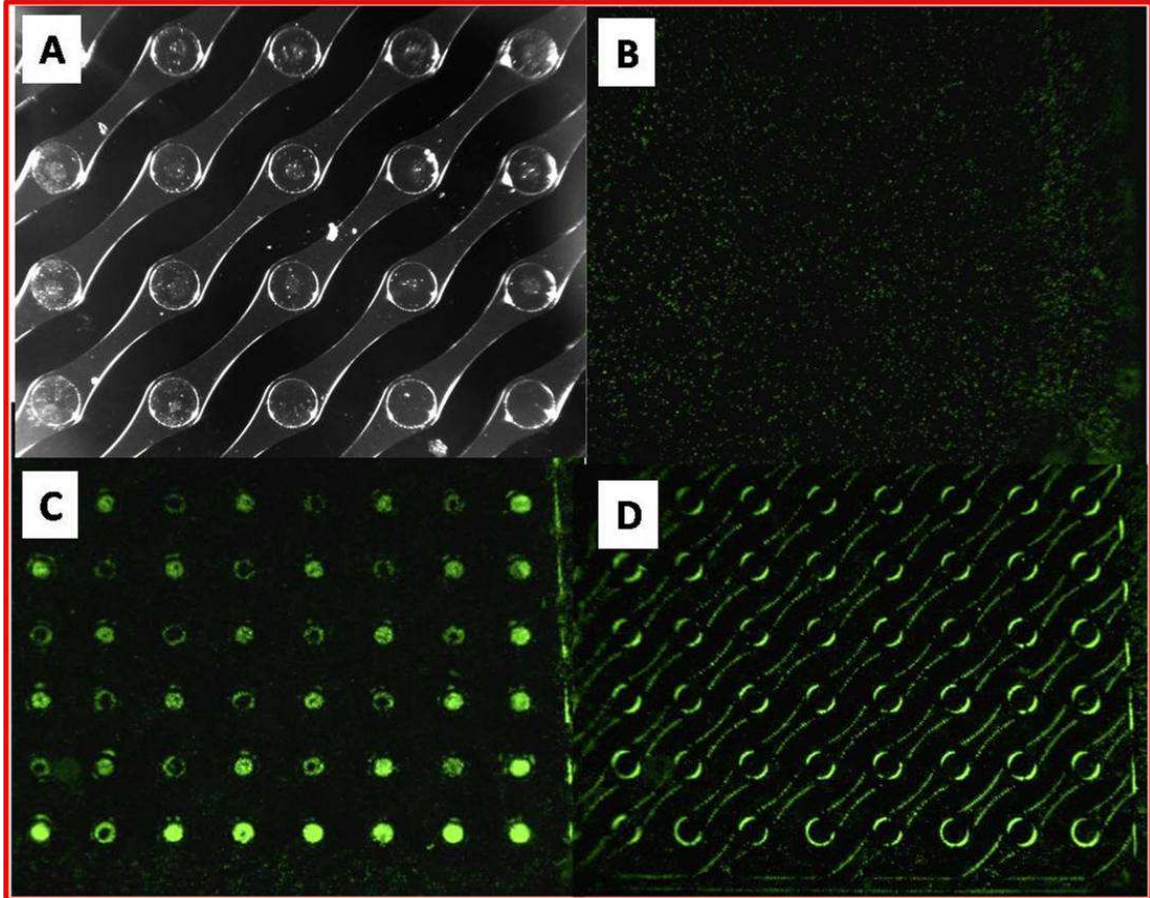


Figure 6.1: DEP separation of E. coli at high and low frequency. (A) shows a section of the first generation BioDyn microchip array DEP device in bright field (circular microelectrodes are 80 micron in diameter). (B) shows the BioDyn microchip array under green fluorescence after a solution containing green fluorescent E. coli have been added. (C) shows BioDyn microchip array after 5 minutes of DEP at 20 volts AC at 10kHz, the green fluorescent E. coli have concentrated on in the DEP high field regions (on the microelectrodes). (D) shows BioDyn microchip array after 5 minutes of DEP at 20 volts AC at 1 MHz, the green fluorescent E. coli have concentrated on in the DEP high field regions (on the edges of the microelectrode and on the microwire leads).

6.2.2 Limitations of comparison to Qiagen extraction kit

When using the picogreen fluorescent DNA quantification kit, a correlation was not seen between the levels collected using the Qiagen adsorption kits and the DEP method for individual patients. Some patients had very high levels of DNA recovered when using the Qiagen kits, but low levels with the DEP method, and vice versa. There

are many variables at play in this result. First of all, the Qiagen kit used plasma, whereas the DEP method worked with blood. This difference does not account for all of the variation however, as the same plasma (frozen and thawed) used for the Qiagen kit was also run on another set of DEP devices (data not shown). The DNA level eluted from these devices, when measured with the picogreen kit, did not correlate with either the Qiagen collection results or the DEP from blood results. The lack of any trend here was due to the fact that not only are blood and plasma very different in terms of the types of particles that remain or have been removed through centrifugation, but the separation methods rely on very different properties of the DNA. A very thorough examination of the capture efficiency of varied size ranges and concentrations for both methods would help to clear up this issue. A potential pitfall is that in blood or plasma, the DNA is often complexed to proteins, which will cause the results of such a study to differ from characterization of DNA spiked into similar samples. It is quite possible also that DNA complexed to proteins tends to spin out more than completely free DNA from the plasma samples, and is thus present in lower relative quantities in the samples eluted from the Qiagen collection method.

6.2.3 Limitations of biomarkers and rate of adoption

While we have demonstrated the ability to isolate and analyze DNA from blood samples, we cannot control the adoption or rejection of any specific biomarker or the validation or increased use of biomarker presence or absence in clinical diagnostics. The need to remove time and complexity from the sample preparation steps remains,

regardless, and it is important to continue development of research tools and methods such as those contained within this dissertation.

6.3 Future Work

6.3.1 Integration of DEP array with on-chip downstream analysis

The most impactful advancement to this work would come in the integration of the current DEP biomarker collection technique with downstream analysis on a single device. While the work in this thesis has demonstrated that a DEP device can be used to significantly reduce the amount of sample preparation necessary to separate DNA biomarkers from blood samples, fluorescent analysis, PCR, and gel electrophoresis were all done off-chip after the collected material was eluted. As a research tool, it is important that the material can be eluted to eliminate any restrictions on the type of analysis that is performed. As a diagnostic technique in a point-of-care device, analysis would need to be integrated into the same microfluidic device. To demonstrate that the device is fundamentally amenable to such use, we filled the device with a control PCR reaction, sealed it with epoxy, and subjected it to a standard PCR thermal cycling regime. Figure 6.2 below shows that when the fluorescence was measured through the viewing window, an increase in SYBR Green I fluorescence was observed, consistent with exponential amplification of the target region of DNA. The product length was validated by gel electrophoresis. The materials in the chip do not necessarily inhibit the PCR, but the polyHEMA hydrogel has a strong tendency to interact with proteins [101], including DNA polymerase. Addition of BSA into the PCR reaction solved this issue.

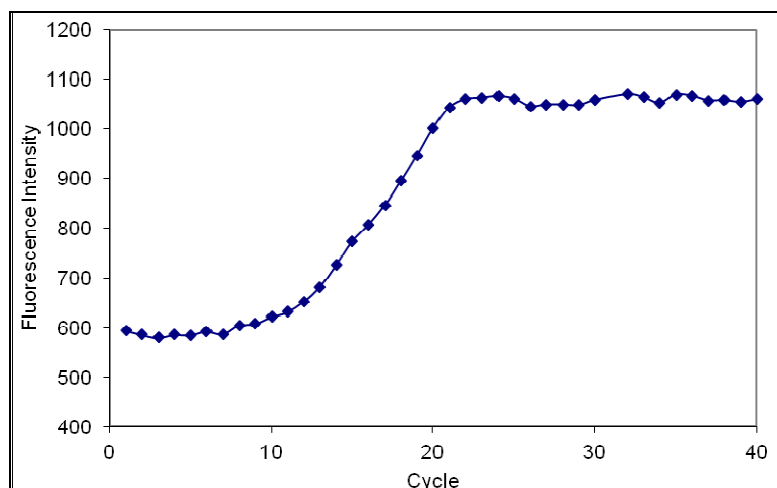


Figure 6.2: On-chip PCR. A control reaction was applied to the DEP device, which was sealed and subject to thermal cycles as used in conventional PCR.

6.3.2 Use of DEP to collect other types of biomarkers

6.3.2.1 RNA collected from blood samples

Collection of DNA from biological samples can provide valuable information about a cell population that may be useful as a biomarker, but there is no information as to the level of expression of that particular gene of interest. Beyond abnormal genetic sequences that are known to be associated with or provide information about a disease state, the level of expression of a gene can have prognostic and diagnostic value in some cases. Analysis of RNA within biological samples such as blood would give insight into gene expression levels, as well as provide additional information that could allow the source of the necrotic cell death to be localized to a particular tissue type. RNA is significantly less stable and more easily degraded when compared to DNA, so it may seem that it would not last in circulation as a cell-free molecule. The likelihood is that both the DNA and RNA within the bloodstream are bound to histones, other proteins, and

cellular fragments and components. We have achieved some preliminary success with completing reverse transcription and PCR on material collected from Chronic Lymphocytic Leukemia samples, demonstrating that this type of material can be collected and analyzed.

6.3.2.2 Extracellular Vesicle collection

A new area of biomarker investigation is extracellular vesicles, sometimes called exosomes. These particles in the 30-120 nm size range and the vesicle structure prevents degradation of the contents that are contained within. It is thought that the DNA, protein, and especially RNA contained within these vesicles could be used for diagnostic and prognostic goals, and research is ongoing into the role of extracellular vesicles in cell-cell signaling pathways. Because of their size, separating them via centrifugation from plasma and cerebral spinal fluid is possible but takes many hours. If they are to be used as a biomarker in a clinical setting, new extraction and analysis techniques must be developed to speed this process up and obviate the need for a large centrifuge. In initial exploratory work, we have been able to isolate these particles from cell culture media. Figure 6.3 below is a green fluorescent image of fluorescently-stained extracellular vesicle trapped on a DEP device.

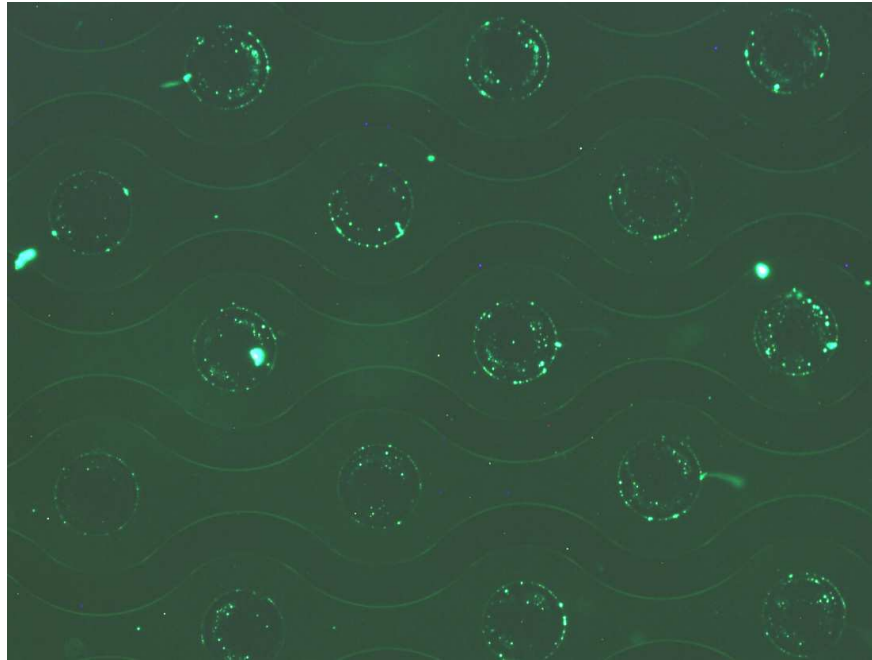


Figure 6.3: Fluorescent extracellular vesicles trapped on a DEP Device

The vesicles from this device were eluted and the RNA that was known to exist within the vesicles was collected and analyzed via RT-PCR. This work is very preliminary, but provides encouragement that DEP could be leveraged to aid in collection of this interesting biomarker.

6.3.2.3 Collection of pathogens from environmental samples

Because DEP relies on the dielectric properties of a target and the solution in which it is suspended, it is useful for complex and varied solutions such as those that might be encountered when dealing with environmental samples. As long as the DEP response of the target is known over a range of sample conditions, measurements can easily be made with embedding sensing elements in the device design. Adjustments based on electrical conductivity of the solution could be made in the software of a device,

choosing the applied electric field voltage and frequency accordingly. In this way, DEP is a much more adaptable technique than those that rely more heavily on solution conditions being favorable to a particular reaction. One application of this is for separation and detection of pathogens from environmental samples. This has implications for use in food safety and defense against biological attacks. We have shown that *E. coli* can be separated from samples with up to a 1:6 dilution of human plasma. Above this conductivity, the bacteria will not move toward the high field region at frequencies that are capable of being transmitted on the device used for these experiments. Higher frequencies could be used in the future to potentially find a higher crossover frequency. The advantage of collection the devices used for this work is that once collected, the bacteria can be electrically lysed with a short DC pulse, and the DNA can then be captured using a much lower frequency. This allows the sample to be washed while the DNA is held in the high-field regions on the electrodes.

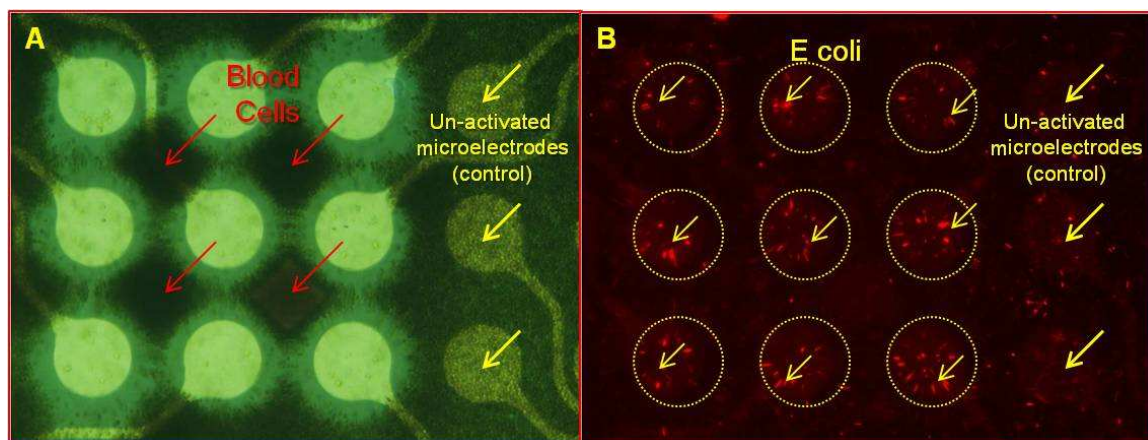


Figure 6.4: Shows the DEP separation of red fluorescent *E. coli* (1×10^6 organisms per ml) from 1/6 diluted Buffy Coat blood containing ~1% blood cells, using our DEP microarray device (microelectrode diameter 80 μm). DEP was carried out at 20 volts AC at 850kHz for 15 minutes. Nine microelectrodes were activated and three (on right) were not activated and serve as a control region for the experiment. (A) Shows the DEP separation results in white light. In the DEP activated region, blood cells are concentrated in the low field areas between the microelectrodes (red arrows). In the un-activated region, blood cells can still be seen scattered over the region. (B) Now shows the DEP microarray in red fluorescence. The red fluorescent *E. coli* can be seen concentrated in clusters within the nine activated microelectrode high field regions. The *E. coli* remain scattered over the un-activated region.

6.3.2.4 Protein collection

Most of this thesis, as well as the suggestions for future exploration, focus on analysis of DNA and RNA that can be collected from biological solutions such as blood, plasma, and cerebral spinal fluid. The protein content in these solutions is so high that finding rare proteins that may have significant value as biomarkers becomes a challenge. The levels of DEP force used in this thesis are too small to overcome the Brownian motion experienced by proteins and any particles under about 20 nm in effective radius. This is because the DEP force is proportional to the volume of the particle. In the future it may be possible to use a multi-stage separation to fractionate a biological sample with DEP and use much higher electric field gradients to isolate proteins from the massive protein content in these solutions. Significant development in devices and some dilution

may be necessary to generate the necessary force on these proteins in high-conductivity solutions while preventing the rapid degradation of the electrode structures. Removing the electrodes from the high field regions, as is done in the pore devices detailed in Chapter 5 of this thesis, is one approach that could be pursued. Despite the difficulty, the ability to utilize DEP for protein collection or subdivision would provide an extra dimension by which to separate protein biomarkers from biological solutions.

6.3.3 DEP theory for nanoscale entities in high conductance

One of the biggest areas for improvement that this work has helped to reveal is in the modeling of nanoscale entities in high conductivity buffers in order to predict their dielectrophoretic response. The simplification of the Clausius-Mossotti Factor from the initial derivation to the equation shown in Chapter 1 makes some assumptions about the particle that begin to fall apart under the conditions used in the experiments described in this thesis. This is the reason that we have refrained from making theoretical and/or simulation-based claims on the exact particle behavior over various frequency ranges. For cells and particles larger than 1 μm , it is reasonable in some cases to ignore the surface parameters of the particle, as the surface area to volume ratio is small. At the nanoscale, when dealing with virus, DNA particles, cellular nanoparticulates, and extracellular vesicles, the surface area to volume ratio is much higher. In addition, the high conductivities of the buffers and biological samples used in this work mean that the electric double layer surrounding the particles is much thinner than it would be in lower electrical conductivity buffers. The combination of these factors means that the

conventional CMF equation is not adequate to describe the motion of small particles in high conductivity buffers. This issue was briefly addressed in Chapter 1, but it is important to reiterate it here, as there is a need for development and extensive experimental validation in this area.

6.3.4 Manipulation of dielectric properties of medium or target

6.3.4.1 Manipulation of target biomarker or analyte properties

Manipulation of the dielectric properties of a biomarker or analyte is a potentially useful approach to easing its recovery from a complex solution. An example of this would be to complex an antibody or other binding moiety to an insulating, conducting, or semiconductor particle. Depending on the properties of the target and the complexed particle, the targets DEP response could be enhanced, altered, or reversed. This technique could be as simple as using an antibody alone to increase the size of a target so that the target-antibody complex would experience a larger DEP force due to the increased volume vs. the target alone.

6.3.4.2 Manipulation of buffer properties

It is possible that adding molecules to a solution would significantly alter the DEP response of some or all of the particles within that solution beyond just the effect of this substance on the electrical conductivity and permittivity of the medium. The size, mobility, and charge of the molecules could have a significant effect on the region immediately surrounding a target particle in terms of the formation of the electric double

layer. Substances for addition could also be chosen based on their known interactions with the most prevalent ionic species within the solution or other factors. A key factor to development of the understanding necessary to choosing materials will be the advanced modeling of the microenvironment around each particle as described above.

REFERENCES

1. Siegel, R., D. Naishadham, and A. Jemal, *Cancer statistics, 2012*. CA: A Cancer Journal for Clinicians, 2012. **62**(1): p. 10-29.
2. Moschos, S.A., *Genomic biomarkers for patient selection and stratification: the cancer paradigm*. Bioanalysis, 2012. **4**(20): p. 2499-511.
3. McLeod, H.L., *Cancer Pharmacogenomics: Early Promise, But Concerted Effort Needed*. Science, 2013. **339**(6127): p. 1563-1566.
4. Vogelstein, B., et al., *Genetic alterations during colorectal-tumor development*. N Engl J Med, 1988. **319**(9): p. 525-32.
5. Alix-Panabieres, C., H. Schwarzenbach, and K. Pantel, *Circulating tumor cells and circulating tumor DNA*. Annu Rev Med, 2012. **63**: p. 199-215.
6. Stroun, M., et al., *Isolation and characterization of DNA from the plasma of cancer patients*. Eur J Cancer Clin Oncol, 1987. **23**(6): p. 707-12.
7. van Hoesel, A.Q., et al., *Assessment of DNA methylation status in early stages of breast cancer development*. Br J Cancer, 2013.
8. de Maat, M.F.G., et al., *Assessment of Methylation Events during Colorectal Tumor Progression by Absolute Quantitative Analysis of Methylated Alleles*. Molecular Cancer Research, 2007. **5**(5): p. 461-471.
9. Board, R.E., et al., *DNA methylation in circulating tumour DNA as a biomarker for cancer*. Biomark Insights, 2008. **2**: p. 307-19.
10. Tan, H.T., Y.H. Lee, and M.C.M. Chung, *Cancer proteomics*. Mass Spectrometry Reviews, 2012. **31**(5): p. 583-605.
11. Welsh, J.B., et al., *Large-scale delineation of secreted protein biomarkers overexpressed in cancer tissue and serum*. Proc Natl Acad Sci U S A, 2003. **100**(6): p. 3410-5.
12. Verma, M., et al., *Proteomic approaches within the NCI early detection research network for the discovery and identification of cancer biomarkers*. Ann N Y Acad Sci, 2001. **945**: p. 103-15.
13. Sawyers, C.L., *The cancer biomarker problem*. Nature, 2008. **452**(7187): p. 548-552.

14. Mishra, A. and M. Verma, *Cancer Biomarkers: Are We Ready for the Prime Time?* *Cancers*, 2010. **2**(1): p. 190-208.
15. Winter, J.M., C.J. Yeo, and J.R. Brody, *Diagnostic, prognostic, and predictive biomarkers in pancreatic cancer*. *Journal of Surgical Oncology*, 2013. **107**(1): p. 15-22.
16. Levine, A.J., *p53, the cellular gatekeeper for growth and division*. *Cell*, 1997. **88**(3): p. 323-31.
17. Nigro, J.M., et al., *Mutations in the p53 gene occur in diverse human tumour types*. *Nature*, 1989. **342**(6250): p. 705-8.
18. Brennan, J.A., et al., *Molecular assessment of histopathological staging in squamous-cell carcinoma of the head and neck*. *N Engl J Med*, 1995. **332**(7): p. 429-35.
19. Kobayashi, S., et al., *EGFR mutation and resistance of non-small-cell lung cancer to gefitinib*. *N Engl J Med*, 2005. **352**(8): p. 786-92.
20. Schwarzenbach, H., D.S. Hoon, and K. Pantel, *Cell-free nucleic acids as biomarkers in cancer patients*. *Nat Rev Cancer*, 2011. **11**(6): p. 426-37.
21. Fleischhacker, M. and B. Schmidt, *Circulating nucleic acids (CNAs) and cancer-- a survey*. *Biochim Biophys Acta*, 2007. **1775**(1): p. 181-232.
22. Ziegler, A., U. Zangemeister-Wittke, and R.A. Stahel, *Circulating DNA: a new diagnostic gold mine?* *Cancer Treat Rev*, 2002. **28**(5): p. 255-71.
23. Sozzi, G., et al., *Quantification of free circulating DNA as a diagnostic marker in lung cancer*. *J Clin Oncol*, 2003. **21**(21): p. 3902-8.
24. Sozzi, G., et al., *Analysis of circulating tumor DNA in plasma at diagnosis and during follow-up of lung cancer patients*. *Cancer Res*, 2001. **61**(12): p. 4675-8.
25. Gautschi, O., et al., *Circulating deoxyribonucleic Acid as prognostic marker in non-small-cell lung cancer patients undergoing chemotherapy*. *J Clin Oncol*, 2004. **22**(20): p. 4157-64.
26. Wu, T.L., et al., *Cell-free DNA: measurement in various carcinomas and establishment of normal reference range*. *Clin Chim Acta*, 2002. **321**(1-2): p. 77-87.
27. Gormally, E., et al., *Circulating free DNA in plasma or serum as biomarker of carcinogenesis: practical aspects and biological significance*. *Mutat Res*, 2007. **635**(2-3): p. 105-17.

28. Jen, J., L. Wu, and D. Sidransky, *An overview on the isolation and analysis of circulating tumor DNA in plasma and serum*. Ann N Y Acad Sci, 2000. **906**: p. 8-12.
29. *Healthy Challenges*. Nat. Nanotechnol., 2007. **2**(8): p. 451.
30. Irvine, D.J., *Drug delivery: One nanoparticle, one kill*. Nat Mater, 2011. **10**(5): p. 342-3.
31. Nishiyama, N., *Nanomedicine: nanocarriers shape up for long life*. Nat Nanotechnol, 2007. **2**(4): p. 203-4.
32. Ferrari, M., *Cancer nanotechnology: opportunities and challenges*. Nat Rev Cancer, 2005. **5**(3): p. 161-71.
33. Nishiyama, N. and K. Kataoka, *Current state, achievements, and future prospects of polymeric micelles as nanocarriers for drug and gene delivery*. Pharmacol Ther, 2006. **112**(3): p. 630-48.
34. Diehl, F., et al., *Detection and quantification of mutations in the plasma of patients with colorectal tumors*. Proc Natl Acad Sci U S A, 2005. **102**(45): p. 16368-73.
35. Albrecht, D.R., et al., *Probing the role of multicellular organization in three-dimensional microenvironments*. Nat Methods, 2006. **3**(5): p. 369-75.
36. Becker, F.F., et al., *Separation of human breast cancer cells from blood by differential dielectric affinity*. Proc Natl Acad Sci U S A, 1995. **92**(3): p. 860-4.
37. Stephens, M., et al., *The dielectrophoresis enrichment of CD34+ cells from peripheral blood stem cell harvests*. Bone Marrow Transplant, 1996. **18**(4): p. 777-82.
38. Asbury, C.L. and G. van den Engh, *Trapping of DNA in nonuniform oscillating electric fields*. Biophys J, 1998. **74**(2 Pt 1): p. 1024-30.
39. Hughes, M.P., *Nanoparticle Manipulation by Electrostatic Forces*, in *Handbook of Nanoscience, Engineering, and Technology, Second Edition*, W.A. Goddard, et al., Editors. 2007, CRC Press: Boca Raton, Florida, USA. p. 1-32.
40. Cheng, J., et al., *Preparation and hybridization analysis of DNA/RNA from E. coli on microfabricated bioelectronic chips*. Nat Biotechnol, 1998. **16**(6): p. 541-6.
41. Cheng, J., et al., *Isolation of cultured cervical carcinoma cells mixed with peripheral blood cells on a bioelectronic chip*. Anal Chem, 1998. **70**(11): p. 2321-6.

42. Cummings, E.B. and A.K. Singh, *Dielectrophoresis in microchips containing arrays of insulating posts: theoretical and experimental results*. Anal Chem, 2003. **75**(18): p. 4724-31.
43. Lapizco-Encinas, B.H., et al., *Insulator-based dielectrophoresis for the selective concentration and separation of live bacteria in water*. Electrophoresis, 2004. **25**(10-11): p. 1695-704.
44. O'Brien, R.W., *The high-frequency dielectric dispersion of a colloid*. J. Colloid Interface Sci., 1986. **113**: p. 81-93.
45. Saville, D.A., et al., *An extended Maxwell–Wagner theory for the electric birefringence of charged colloids*. J. Chem. Phys., 2000. **16**: p. 6974-6983.
46. Zhao, H. and H.H. Bau, *Effect of double-layer polarization on the forces that act on a nanosized cylindrical particle in an ac electrical field*. Langmuir, 2008. **24**(12): p. 6050-9.
47. Burt, J.P.H., T.A.K. Al-Ameen, and R. Pethid, *An optical dielectrophoresis spectrometer for low-frequency measurements on colloidal suspensions*. J. Phys. E: Sci. Instrum., 1989. **22**(11): p. 952-957.
48. Gascoyne, P.R., et al., *Membrane changes accompanying the induced differentiation of Friend murine erythroleukemia cells studied by dielectrophoresis*. Biochim Biophys Acta, 1993. **1149**(1): p. 119-26.
49. Zhao, H., *Double-layer polarization of a non-conducting particle in an alternating current field with applications to dielectrophoresis*. Electrophoresis, 2011. **32**(17): p. 2232-44.
50. Alazzam, A., et al., *Interdigitated comb-like electrodes for continuous separation of malignant cells from blood using dielectrophoresis*. Electrophoresis, 2011. **32**(11): p. 1327-36.
51. Jaramillo Mdel, C., et al., *On-line separation of bacterial cells by carbon-electrode dielectrophoresis*. Electrophoresis, 2010. **31**(17): p. 2921-8.
52. Ermolina, I., J. Milner, and H. Morgan, *Dielectrophoretic investigation of plant virus particles: Cow Pea Mosaic Virus and Tobacco Mosaic Virus*. Electrophoresis, 2006. **27**(20): p. 3939-48.
53. Ramos, A., et al., *Ac electrokinetics: a review of forces in microelectrode structures*. J. Phys. D: Appl. Phys., 1998. **31**: p. 2338-2353.
54. Green, N.G., A. Ramos, and H. Morgan, *Ac electrokinetics: a survey of sub-micrometre particle dynamics*. J. Phys. D: Appl. Phys., 2000. **33**: p. 632-641.

55. Cui, L., D. Holmes, and H. Morgan, *The dielectrophoretic levitation and separation of latex beads in microchips*. *Electrophoresis*, 2001. **22**(18): p. 3893-901.
56. Morgan, H., M.P. Hughes, and N.G. Green, *Separation of submicron bioparticles by dielectrophoresis*. *Biophys J*, 1999. **77**(1): p. 516-25.
57. Ermolina, I. and H. Morgan, *The electrokinetic properties of latex particles: comparison of electrophoresis and dielectrophoresis*. *J Colloid Interface Sci*, 2005. **285**(1): p. 419-28.
58. Asbury, C.L., A.H. Diercks, and G. van den Engh, *Trapping of DNA by dielectrophoresis*. *Electrophoresis*, 2002. **23**(16): p. 2658-66.
59. Washizu, M., et al., *Applications of electrostatic stretch-and-position of DNA*. *IEEE T. Ind. Appl.*, 1995. **31**(3): p. 447-456.
60. Gagnon, Z., S. Senapati, and H.C. Chang, *Optimized DNA hybridization detection on nanocolloidal particles by dielectrophoresis*. *Electrophoresis*, 2010. **31**(4): p. 666-71.
61. Asokan, S.B., et al., *Two-dimensional manipulation and orientation of actin-myosin systems with dielectrophoresis*. *Nano Lett.*, 2003. **3**(4): p. 431-437.
62. Holzel, R., et al., *Trapping single molecules by dielectrophoresis*. *Phys Rev Lett*, 2005. **95**(12): p. 128102.
63. Han, K.H. and A.B. Frazier, *Lateral-driven continuous dielectrophoretic microseparators for blood cells suspended in a highly conductive medium*. *Lab Chip*, 2008. **8**(7): p. 1079-86.
64. Gao, J., et al., *Hybrid electrokinetic manipulation in high-conductivity media*. *Lab Chip*, 2011. **11**(10): p. 1770-5.
65. Pratt, E.D., et al., *Rare Cell Capture in Microfluidic Devices*. *Chem Eng Sci*, 2011. **66**(7): p. 1508-1522.
66. Srivastava, S.K., A. Artemiou, and A.R. Minerick, *Direct current insulator-based dielectrophoretic characterization of erythrocytes: ABO-Rh human blood typing*. *Electrophoresis*, 2011. **32**(18): p. 2530-40.
67. Kuczynski, R.S., H.C. Chang, and A. Revzin, *Dielectrophoretic microfluidic device for the continuous sorting of Escherichia coli from blood cells*. *Biomicrofluidics*, 2011. **5**(3): p. 32005-3200515.

68. Krishnan, R., et al., *Alternating current electrokinetic separation and detection of DNA nanoparticles in high-conductance solutions*. Electrophoresis, 2008. **29**(9): p. 1765-74.
69. Krishnan, R. and M.J. Heller, *An AC electrokinetic method for enhanced detection of DNA nanoparticles*. J Biophotonics, 2009. **2**(4): p. 253-61.
70. Krishnan, R., et al., *Interaction of Nanoparticles at the DEP Microelectrode Interface under High Conductance Conditions*. Electrochem commun, 2009. **11**(8): p. 1661-1666.
71. Sosnowski, R.G., et al., *Rapid determination of single base mismatch mutations in DNA hybrids by direct electric field control*. Proc Natl Acad Sci U S A, 1997. **94**(4): p. 1119-23.
72. Leonard, K.M. and A.R. Minerick, *Explorations of ABO-Rh antigen expressions on erythrocyte dielectrophoresis: changes in cross-over frequency*. Electrophoresis, 2011. **32**(18): p. 2512-22.
73. Sano, M.B., et al., *Contactless dielectrophoretic spectroscopy: examination of the dielectric properties of cells found in blood*. Electrophoresis, 2011. **32**(22): p. 3164-71.
74. Khoshmanesh, K., et al., *Dielectrophoretic platforms for bio-microfluidic systems*. Biosens Bioelectron, 2011. **26**(5): p. 1800-14.
75. Khoshmanesh, K., et al., *Dynamic analysis of drug-induced cytotoxicity using chip-based dielectrophoretic cell immobilization technology*. Anal Chem, 2011. **83**(6): p. 2133-44.
76. Wei, C.L., et al., *Does conductance catheter measurement system give consistent and reliable pressure-volume relations in rats?* IEEE Trans Biomed Eng, 2011. **58**(6): p. 1804-13.
77. Hirsch, F.G., et al., *The electrical conductivity of blood. I: Relationship to erythrocyte concentration*. Blood, 1950. **5**(11): p. 1017-35.
78. Visser, K.R., *Electric conductivity of stationary and flowing human blood at low frequencies*. Med Biol Eng Comput, 1992. **30**(6): p. 636-40.
79. Green, M.R., et al., *Abraxane, a novel Cremophor-free, albumin-bound particle form of paclitaxel for the treatment of advanced non-small-cell lung cancer*. Ann Oncol, 2006. **17**(8): p. 1263-8.
80. Krishnan, R. and M.J. Heller. *Rapid Isolation and Detection of Cell Free Circulating DNA and Other Disease Biomarkers Directly from Whole Blood*. in

Proceedings of the 6th international conference on circulating nucleic acids in plasma and serum held on 9-11 November 2009 in Hong Kong. 2009. Hong Kong: Springer.

81. Heller, M.J., R. Krishnan, and A. Sonnenberg. *Rapid Isolation and Detection of Cell Free Circulating DNA and Other Disease Biomarkers Directly from Whole Blood.* in *TechConnect World presents Nanotech Conference & Expo 2010.* 2010. Anaheim, California, USA.
82. Jahr, S., et al., *DNA fragments in the blood plasma of cancer patients: quantitations and evidence for their origin from apoptotic and necrotic cells.* *Cancer Res*, 2001. **61**(4): p. 1659-65.
83. Lasser, C., M. Eldh, and J. Lotvall, *Isolation and characterization of RNA-containing exosomes.* *J Vis Exp*, 2012(59): p. e3037.
84. Mathivanan, S., H. Ji, and R.J. Simpson, *Exosomes: extracellular organelles important in intercellular communication.* *J Proteomics*, 2010. **73**(10): p. 1907-20.
85. Jiang, Y. and X. Wang, *Comparative mitochondrial proteomics: perspective in human diseases.* *J Hematol Oncol*, 2012. **5**: p. 11.
86. Prati, D., *Transmission of hepatitis C virus by blood transfusions and other medical procedures: a global review.* *J Hepatol*, 2006. **45**(4): p. 607-16.
87. Sonnenberg, A., et al., *Dielectrophoretic isolation of DNA and nanoparticles from blood.* *Electrophoresis*, 2012. **33**(16): p. 2482-90.
88. Chiorazzi, N., K.R. Rai, and M. Ferrarini, *Chronic lymphocytic leukemia.* *N Engl J Med*, 2005. **352**(8): p. 804-15.
89. Lin, K.I., et al., *Relevance of the immunoglobulin VH somatic mutation status in patients with chronic lymphocytic leukemia treated with fludarabine, cyclophosphamide, and rituximab (FCR) or related chemoimmunotherapy regimens.* *Blood*, 2009. **113**(14): p. 3168-71.
90. Hamblin, T.J., et al., *Unmutated Ig V(H) genes are associated with a more aggressive form of chronic lymphocytic leukemia.* *Blood*, 1999. **94**(6): p. 1848-54.
91. Damle, R.N., et al., *Ig V gene mutation status and CD38 expression as novel prognostic indicators in chronic lymphocytic leukemia.* *Blood*, 1999. **94**(6): p. 1840-7.

92. Rassenti, L.Z., et al., *ZAP-70 compared with immunoglobulin heavy-chain gene mutation status as a predictor of disease progression in chronic lymphocytic leukemia*. N Engl J Med, 2004. **351**(9): p. 893-901.
93. Ghia, E.M., et al., *Use of IGHV3-21 in chronic lymphocytic leukemia is associated with high-risk disease and reflects antigen-driven, post-germinal center leukemogenic selection*. Blood, 2008. **111**(10): p. 5101-8.
94. Gao, Y.J., et al., *Increased integrity of circulating cell-free DNA in plasma of patients with acute leukemia*. Clin Chem Lab Med, 2010. **48**(11): p. 1651-6.
95. Hohaus, S., et al., *Cell-free circulating DNA in Hodgkin's and non-Hodgkin's lymphomas*. Annals of Oncology, 2009. **20**(8): p. 1408-1413.
96. Fais, F., et al., *Chronic lymphocytic leukemia B cells express restricted sets of mutated and unmutated antigen receptors*. J Clin Invest, 1998. **102**(8): p. 1515-25.
97. Rassenti, L.Z., et al., *Relative value of ZAP-70, CD38, and immunoglobulin mutation status in predicting aggressive disease in chronic lymphocytic leukemia*. Blood, 2008. **112**(5): p. 1923-30.
98. Sonnenberg, A., et al., *Dielectrophoretic isolation and detection of cfc-DNA nanoparticulate biomarkers and virus from blood*. Electrophoresis, 2013. **34**(7): p. 1076-84.
99. van der Drift, M.A., et al., *Circulating DNA is a non-invasive prognostic factor for survival in non-small cell lung cancer*. Lung Cancer, 2010. **68**(2): p. 283-7.
100. Guadalajara, H., et al., *The concentration of deoxyribonucleic acid in plasma from 73 patients with colorectal cancer and apparent clinical correlations*. Cancer Detect Prev, 2008. **32**(1): p. 39-44.
101. Lord, M.S., et al., *The effect of charged groups on protein interactions with poly(HEMA) hydrogels*. Biomaterials, 2006. **27**(4): p. 567-75.